2011

Development of Quantitative LC-MS/MS Methods for the Pharmacological Studies of Anti-Cancer Drugs

Lan Li
Cleveland State University

DEVELOPMENT OF QUANTITATIVE LC-MS/MS METHODS FOR THE PHARMACOLOGICAL STUDIES OF ANTI-CANCER DRUGS

LAN LI

Bachelor of Science in Cellular and Molecular Biology

University of Science and Technology of China

July 2003

submitted in partial fulfillment of requirements for the degree

DOCTOR OF PHILOSOPHY IN CLINICAL-BIOANALYTICAL CHEMISTRY

at

CLEVELAND STATE UNIVERSITY

FEBRUARY 2011

This dissertation has been approved

for the Department of CHEMISTRY

and the College of Graduate Studies by

_____

Dissertation Chairperson, Yan Xu
Department of CHEMISTRY

_____

Date

_____

Baochuan Guo
Department of CHEMISTRY

_____

Date

_____

Lili Liu
Department of CHEMISTRY

_____

Date

_____

Xue-Long Sun
Department of CHEMISTRY

_____

Date

_____

Aimin Zhou
Department of CHEMISTRY

_____

Date

DEVELOPMENT OF QUANTITATIVE LC-MS/MS METHODS FOR THE PHARMACOLOGICAL STUDIES OF ANTI-CANCER DRUGS

LAN LI

ABSTRACT

In the development of anti-cancer drugs, it is essential to study the pharmacological profiles of the drugs. Among the analytical tools utilized in the pharmacological studies, LC-MS/MS has gained increased popularity due to its unequivocal sensitivity and specificity, as well as the ability of handling a wide variety of compounds with relatively simple sample preparation procedures.

In this work, a brief review on the method rational, instrumentations, analytical method validation, and work flow of the method development was included. The processes of LC-MS/MS method development for the pharmacological studies of three anti-cancer drugs (*i.e.*, methoxyamine, fludarabine, and 6-benzylthioinosine) were illustrated. To be more specific, a tetra-enzyme cocktail utilized for DNA adducts release was introduced. LC-MS/MS methods for the analysis of methoxyamine modified DNA abasic sites and fludarabine incorporated in DNA were developed toward the DNA adducts released from DNA with the enzyme cocktail. The methods were applied to the drug effect and drug mechanism studies. Another two LC-MS/MS method was developed for the quantification of 2-fluoroadenine released from the fludarabine incorporated DNA and free 6-benzylthioinosine drug molecule in mouse and human plasma. The first method helped to provide direct evidence to a newly proposed drug resistance mechanism

toward fludarabine through DNA base excision repair; while the second method realized the pharmacokinetic studies of the drug.

The results in this work not only demonstrated the capability of LC-MS/MS in solving sophisticated pharmacological puzzles, but will provide useful information guiding the preclinical studies and clinical therapy development of the anti-cancer drugs listed above.

TABLE OF CONTENTS

LIST OF TABLES

LIST OF FIGURES

CHAPTER I

INTRODUCTION TO PHARMACOLOGICAL STUDY OF DRUGS AND ANALYTICAL METHOD DEVELOPMENT

1.1. Pharmacological studies of anti-cancer drugs

1.1.1. General introduction

Cancer has become one of the biggest threats to human health and life. In 2010, there were over 1.5 million new cancer cases diagnosed in United States, and the number of deaths from cancer were estimated at over 0.5 million [1]. Among all of the anti-cancer treatments available to date, chemotherapy, along with surgery and radiotherapy

are the most common approaches. The key of establishing effective chemotherapy strategies lies in the development of anti-cancer drugs. In National Cancer Institute along, during the past two decades, more than 80,000 compounds were screened as anti-cancer drug candidates, and there are over 1,500 clinical trials undergoing [2]. As the majority of the anti-cancer drugs are extremely heterogeneous chemical entities, in the drug discovery and therapy development, it is essential to understand the pharmacological properties of the drugs [3].

The pharmacological study of the drugs consists of two major components, pharmacokinetic studies and pharmacodynamic studies.

Pharmacokinetic (PK) study includes liberation, adsorption, distribution, metabolism, and excretion of the pharmaceutical substance administered to the living organism. Among these studies, liberation study discovers the process of drug releasing from specific formulations; absorption and distribution studies illustrate the process of the drug entering the circulation of the living organisms and the dissemination of the drug in the living organisms, respectively; metabolism study focus on the irreversible chemical transformations from the drug to its metabolites; excretion studies elucidates the process in which the drug and/or its metabolites are eliminated from the living organism. This study scheme is often referred as LADME [4].

Differing from PK studies that discovers “what the body does to the drug”, pharmacodynamic (PD) studies aims “what the drug does to the body” [5]. To be more

specific, PD studies evaluate the physiological impacts of the pharmaceutical substance to the living organisms. It has a focus of understanding the functioning mechanisms of the drug and usually involves three major objects: receptor binding, postreceptor effects, and chemical interactions [6]. The major goal of PD study is to establish the dose-response profile, thus PD study is often carried out together with the PK study.

1.1.2. Three anti-cancer drugs

In this work, in order to facilitate the pharmacokinetics and/or pharmacodynamics of three anti-cancer drugs, methoxyamine (MX), fludarabine (F-ara-A), and 6-benzylthioinosine (6BT), LC-MS/MS methods were developed and applied to the studies. The major aims in LC-MS/MS facilitated pharmacological studies of these drugs can be described as the following:

MX (figure 1.1 A) is a small molecule that is reactive to DNA apurinic/apyrimidinic (AP) sites. The blockage of the AP sites by MX is able to invalidate the enzymatic recognition and repair of the AP sites through DNA base excision repair (BER), and thus reverse the BER related drug resistance to some methylating agents and anti-metabolites [7, 8]. MX is currently under phase I clinical studies and the PK profile of the drug is analyzed with an LC-MS/MS method developed by our group [9]. In the drug effect analysis of MX, a part of PD studies of the drug, the

blocking efficiency of MX toward the AP sites must be evaluated. In another word, methods are needed in quantification of MX modified AP (MX-AP) sites and free AP sites. The significance of the drug effect study lies in its ability of providing better understand on the drug functioning mechanisms and potential in guiding the clinical trials.

F-ara-A (figure 1.1 B) is a purine analogue effective in the treatment of hematological malignancies [10]. The monophosphate form of the drug has been approved by United States Food and Drug Administration (FDA) to treat refractory B-cell chronic lymphocytic leukemia (CLL), and the pharmacological properties of the drug have been intensively studied [11]. As F-ara-A inhibits multiple enzymes involved in DNA synthesis, it was generally accepted as a DNA chain terminator [12, 13]. However, recent studies indicated that F-ara-A may also be incorporated in the middle of a DNA strand, and BER can be one of the mechanisms contributing to the drug resistance [8]. To have a better understand of the drug functioning and resistance mechanisms, methods have to be developed to quantify the drug incorporation in DNA and to analyze the drug moiety released during BER (*i.e.*, the 2-fluoroadenine or F-Ade). The former study can be considered as a part of the PD study; while the later, as a metabolism study, belongs to the category of PK studies.

6BT (figure 1.1 C) is another purine analogue that has shown great potential in the treatment of acute myeloid leukemia (AML). As it induces differentiation or highly specific cytotoxicity to the malignant cells from multiple subtypes of AML, it may provide cure to the cancers without introducing serious side effects. Although the

mechanisms of differentiation inducement remain unclear, the specific cytotoxicity of 6BT to the AML cells may be attributed to its specific entry into the malignant cells. To better understand the functioning mechanisms and PK profile of the drug, methods must be developed to analyze the free drug from biological matrices. The results will, for sure, benefit both the preclinical and clinical studies of the drug.

A

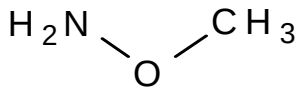

Methoxyamine (MX)

M.W. = 47

B

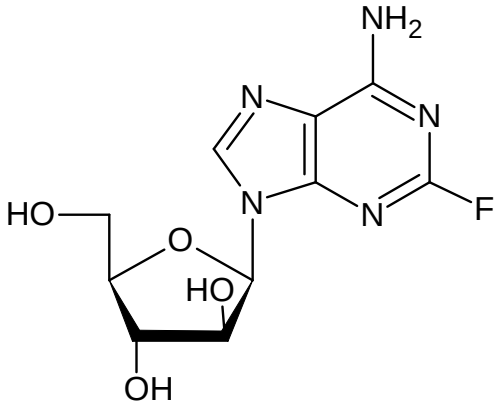

Fludarabine (F-ara-A)

M.W. = 285

C

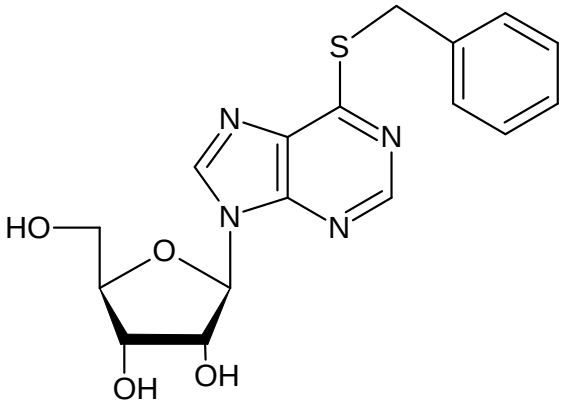

6-Benzylthioinosine (6BT)

M.W. = 374

Figure 1.1, Three anti-cancer drugs: methoxyamine (A), fludarabine (B), and 6-benzylthioinosine (C).

1.1.3. LC-MS/MS and pharmacological studies

Among the wide variety of tools utilized in the pharmacological studies, LC-MS/MS has gained more and more popularity due to its high sensitivity and specificity. In this work, LC-MS/MS has demonstrated its problem solving abilities in all the research projects proposed in the above section:

In the evaluation of the blocking efficiency of MX to the AP sites, the MX-AP adducts were quantified with an LC-MS/MS method. In this method, the DNA was first hydrolyzed enzymatically, so that the MX-AP adducts could be released from DNA backbone as free small molecules, MX-deoxyribose (MX-dR). Then, LC-MS/MS method was developed toward the released small molecule, and the quantification of MX-AP adducts was realized. By applying the developed method into the drug effect studies, dose- and time- effect profiles were obtained from an *in vitro* cell study; while another time-effect profile was obtained from an *in vivo* study carried out on a patient enrolled in the phase I clinical studies. With the LC-MS/MS evaluation of the free AP sites already achieved by Roberts *et al.* [14], future combination of the methods will provide a even better view to the blocking efficiency of MX to the AP sites.

Similar strategies have been applied into the incorporation analysis of F-ara-A: the incorporated drug was first release with enzymatic hydrolysis, and then analyzed with LC-MS/MS. The method has been utilized in a dose-effect study of F-ara-A on a

leukemia cell line, HL60. Quantitative evaluation of the drug incorporation with validated methods may also provide insight in drug functioning mechanism elucidation.

In the assessment of the drug resistance effects on the incorporated F-ara-A through uracil DNA glycosylase (UDG), an LC-MS/MS method was developed for the analysis of F-Ade, a molecule released by UDG from the incorporated drug. The positive results shown in the detection of F-Ade from *in vitro* UDG digestion on F-ara-A incorporated DNA 40-mer and cellular DNA provided direct evidences to the effect of BER on the incorporated drug. Measurement of F-Ade from the cell lysates obtained from F-ara-A treated cells also served as *in vivo* support for the mechanism.

Quantification of 6BT from mouse and human plasma with LC-MS/MS method we developed enabled the PK study of the drug. In fact, a preliminary PK study has already been performed on mice, and the PK parameters were calculated after PK modeling. Meanwhile, the semi-quantitative analysis of 6BT from different types of cells also illustrated the enhanced entry of 6BT into leukemia cell lines. The results explain the specific cytotoxicity of 6BT to the leukemia cells.

1.2. Quantitative LC-MS/MS method development

In order to provide accurate and reliable data for the PK and PD studies, a quantitative LC-MS/MS method usually includes four elements: liquid chromatography

(LC) separation of the analyte(s) from other interferences compounds, biological sample extraction in order to exclude matrix effects, mass spectrometry detection of the analyte(s), and analytical method validation or method performance evaluation. All four elements are described in more details in the flowing sections.

1.2.1. Liquid chromatography

Although the high detection specificity of mass spectrometers allows effective analyte detection from relative complicated sample matrix, too much interference, however, will attenuate the detection sensitivity. The interference compounds can compete with the analyte during the ionization process, decreasing the ionization efficiency of the analyte, and thus hurt the detection sensitivity. To avoid this situation, liquid chromatography (LC) is often needed to separate the analyte from the sample matrix.

The principle of LC can be simply described as the following: first, carried by the mobile phase, the sample (*i.e.*, a mixture of analyte, matrix substances, and solvents) is introduced to the column; as the mobile phase keeps flowing, all of the compounds are also moved forward by the mobile phase; however, the compounds that have stronger interactions with the stationary phase move slower, and tend to stay longer on the column; by this means, the compounds in the mixture can be separated based on their different

affinities to the stationary phase, and finally eluted out from the column in an order of time (figure 1.2).

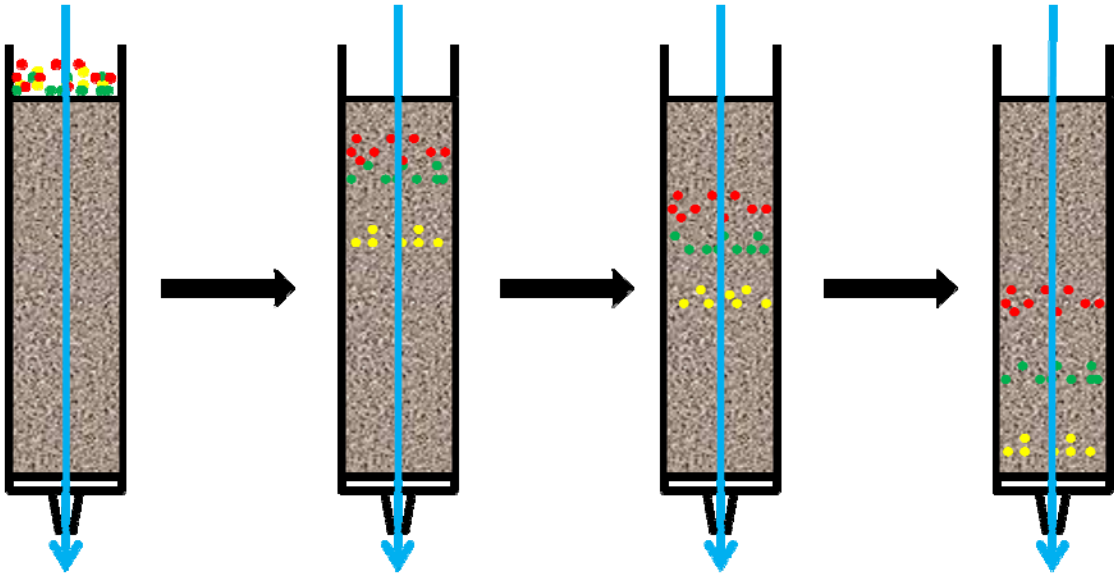

Figure 1.2, Illustration of liquid chromatography.

Currently, the most typical separation mechanisms utilized in LC-MS/MS include: normal phase/ reverse phase, ion-pairing, and ion-exchange LC [15].

Normal phase LC utilizes the polarity of the compounds in the separation. Normal phase LC is realized through a polar stationary phase, typically silica or polar organic functional groups (*e.g.*, cyano and amino), and a non-polar mobile phase (*e.g.*, hexane and heptanes). Based on the principle of like-dissolves-like, polar compounds will have stronger interactions with the stationary phase and be eluted out later than those relatively non-polar compounds. Slightly polar solvent, such as isopropanol, ethyl acetate, and chloroform are often mixed with the non-polar mobile phase to increase the elution power toward the extremely polar compounds [15].

Reverse phase LC, opposite to the normal phase LC, utilizes non-polar stationary phase, typically alkyl hydrocarbons (*e.g.*, octadecyl, octyl, and butyl), combined with polar water miscible organic solvents (*e.g.*, methanol, acetonitrile, and tetrahydrofuran) as the mobile phase. Reverse phase LC retains non-polar compounds on the columns longer than the polar ones. Strong elusion power in reverse phase LC can be achieved by increase the percentage of organic solvents in the mobile phases [15]. Comparing to the normal phase LC, reverse phase LC is more commonly used in LC-MS/MS analysis.

Aqueous normal-phase LC, a newly developed LC mechanism, has started to get popular in the separation of polar compounds. It utilizes the reverse phase columns with polar surface modification as the stationary phase. The mobile phase is usually composed of high percentage of relatively polar organic solvent *(e.g.*, methanol and

acetonitrile) with the addition of a small portion of water. As the polarity of the stationary phase is still higher than the mobile phase, polar compounds can be retained on the column, yet non-polar compounds and inorganic salts are eluted out with no or little retention [15].

Ion-pairing LC can be performed on both normal and reverse phase column, yet it is more commonly carried out on a reverse phase column. When the analyte is relatively polar and hard to be retained on the reverse phase column, a "counter-ion", namely the ion-pairing agent, of opposite charge to the analyte is added into the mobile phase. This ion-pairing agent often possesses a relative non-polar moiety that can have stronger interaction with the stationary phase. After the column is fully equilibrated with the mobile phase, the stationary phase is kinetically coated with the ion-pairing agent. As the ion-pairing agent is able to interact with the analyte ions through electrostatic attraction, the analyte can also be retained on the column temporarily. When the ion-pairing agent is eluted out, the analyte is eluted out with it. Examples of the most commonly used ion-pairing agents that are compatible with MS detection are trifluoroacetic acid (TFA) (anionic), pentafluoroproprionic acid (PFPA) (anionic), heptafluorobutyric acid (HFBA) (anionic), and triethylamine (cationic) [15, 16].

Ion-exchange LC utilizes stationary phases presenting ionizable groups that attract ions with opposite charge. To retain the analyte, the pH of the mobile phase must be adjusted to a specific value, under which the analyte can be attracted by the stationary phase through electrostatic interaction. During the elusion process, the pH of the mobile

phase can be changed to a value that prevent or minimize the interaction between the analyte and the stationary phase. Comparing to the reverse phase LC and ion-pairing LC, ion-exchange LC is less commonly used in LC-MS/MS because of the large amount of buffer salts it introduces often suppresses the ionization [15].

1.2.2. Biological sample extraction

As the analysis of anti-cancer drugs often involves complicated biological samples (*e.g.*, plasma, tissue, urine, *in vitro* enzymatic reaction products, *etc.*), interferences (*e.g.*, proteins, lipids, fatty acids, organic salts, glycerol, *etc*.) in these samples are often hard to be completely eliminated by LC along. If not removed before the LC-MS/MS analysis, they can easily contaminate the LC column and invalid the analysis. To insure the successful of the analysis, and make the methods robust for repeating analysis, certain sample extraction procedures must be carried out to clean up the sample matrix before the LC-MS/MS analysis.

Three major sample extraction strategies are commonly utilized for biological samples: protein precipitation, liquid-liquid extraction, and solid-phase extraction.

Protein precipitation Protein is one of the most common matrix interference often exists in large amount in some biological samples (*e.g.*, plasma and tissue). If not being eliminated before LC, it may precipitate when encountered the organic solvents in

the LC process and clog the LC system. The best way to avoid this situation is to precipitate it out before the LC-MS/MS analysis. The structure of a protein is held by three major kinds of weak interactions: hydrophobic interactions, hydrogen bonds, and electrostatic interactions. Thus disturbing one or more of these interactions is the most effective way to precipitate the protein. Addition of organic solvents, such as methanol and acetonitrile, is able to interrupt the hydrophobic interaction; while introducing extremes of pH disrupts the electrostatic interactions [17]. As a result, the protein precipitation is often realized by mixing the biological samples together with organic solvents and volatile acids or bases. After a short vortex, the mixture can be centrifuged and the supernatant is taken out. This supernatant can either be dried and then reconstituted before analysis, or directly injected into the LC-MS/MS system.

Protein precipitation is the simplest and fastest strategy in biological sample extraction. However, it is not effective in removing other interferences, such as lipids and salts. When there are needs for cleaner samples, other extraction strategies must be considered.

Liquid-liquid extraction (LLE) utilizes the distribution ratio of a certain compound in two immiscible solvents to extract the compound [18]. To be more specific, after mixing the two immiscible solvents completely, any compound dissolved in these two phases will reaches an equilibration. At this moment, the ratio of the concentrations of this compound in the two solvents, $[\text{compound}]_{\text{solvent 1}}$ / $[\text{compound}]_{\text{solvent 2}}$, becomes a constant. Given the volumes of the two solvents are the same, the one in which the

compound has higher solubility tends to retain more mass of the compound. In another word, the solvent that dissolves the compound more easily, namely the extraction solvent, is able to "absorb" the compound from the other solvent. In real extraction procedure, the extraction solvent is often utilized in a larger volume to ensure high recovery.

As most of the biological samples are already in aqueous solution, organic solvents are often applied to extract the compounds from the aqueous phase. Based on the polarity of the analyte, extraction solvents ranged from different polarities can be chosen for the best extraction efficiency. Extremely hydrophobic analyte can be extract more efficiently with non-polar solvents, such as hexane and carbon tetrachloride. For polar analytes, polar solvents, such as chloroform and ethyl acetate, can be the effective extraction solvents. When extracting extremely polar compounds, adjusting pH, mixing the extraction solvent with small portion of water miscible solvents (*e.g.*, isopropanol), and/or salting out can also be applied to increase extraction efficiency [18].

Besides polarity, another rule of extraction solvents selection is the boiling points. Solvents with low boiling points are often preferred, as they can be dried by evaporation easily during the sample concentration process [18].

Comparing to protein precipitation, LLE is more complicated and harder to be optimized. Nevertheless, it is more effective in removing salts from biological samples comparing to protein precipitation. Meanwhile, due to the introducing of organic solvents, LLE can also precipitate and remove proteins efficiently.

Solid-phase extraction (SPE) is the most complicated extraction method in the three, yet it is also the one that provides the cleanest sample after extraction. Unlike the LLE utilizing liquid as the extraction material, SPE use solid sorbent as the extraction material. The extraction mechanisms are very similar to those of LC. Normal/reverse phase, ion-pairing, and ion-exchange are, again, the major extraction mechanisms. However, instead of pumping mobile phase continuously through the solid phase and eluting the analyte gradually from the sorbent with a gradient or isocratic method, the extraction can be clearly divided into a loading stage and an elusion stage.

Generally speaking, the SPE can be achieved through the following process. First, the solid sorbent is equilibrated with a buffered solution called loading buffer. This loading buffer usually provides weaker interaction to the analyte comparing the sorbent. Then, the sample dissolved in or diluted with the loading buffer is added onto the sorbent. Because the analyte has stronger interaction with the sorbent than it has with the loading buffer, the analyte can be temporarily retained by the sorbent. Other interference compounds that do not interact with the sorbent will pass through the sorbent, and sometimes, be further cleaned up by a wash step. Finally, another buffered solution that dissolves the analyte better than the sorbent, namely the elusion buffer, is applied to wash off the analyte from the sorbent. At this moment, the analyte will be dissociated from the sorbent, while the interferences that interact with the sorbent more strongly may still stay on the sorbent. By this means, the analyte can be effectively purified from the biological samples (figure 1.3) [19].

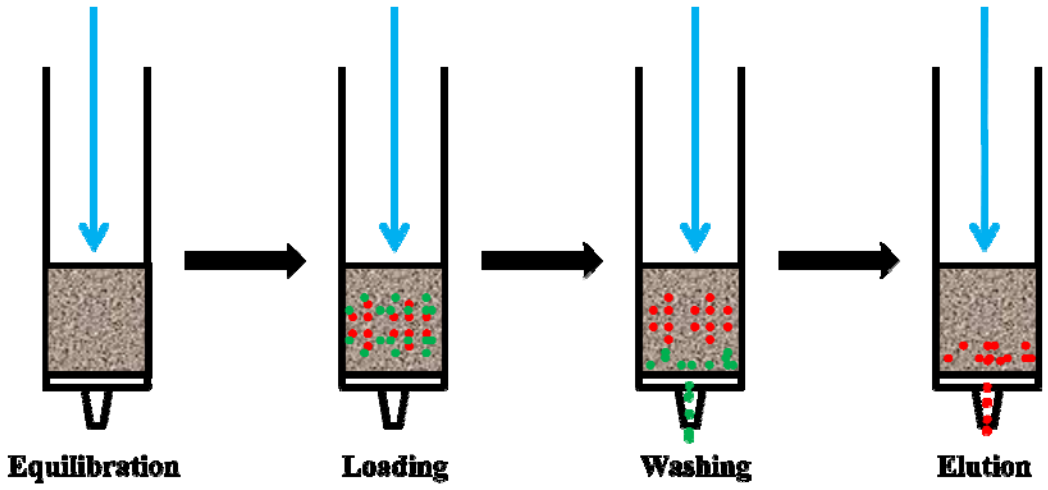

Figure 1.3, Illustration of off-line SPE.

In fact, SPE can happen either off-line or on-line. In an off-line SPE, the cartridges packed with specific sorbent are equilibrated, loaded with samples, washed, and striped with elusion buffer in separated steps. In an on-line SPE, however, the cartridge is connected into an LC system, and pre-equilibrated with a continuous flow of loading solution. After the sample has been injected onto the cartridge, the mobile phase can be switched to the elusion buffer that flows to the opposite direction (figure 1.4). When the elusion buffer reaches to the cartridge, it is able to dissociate the analyte from the sorbent in a narrow the elusion band.

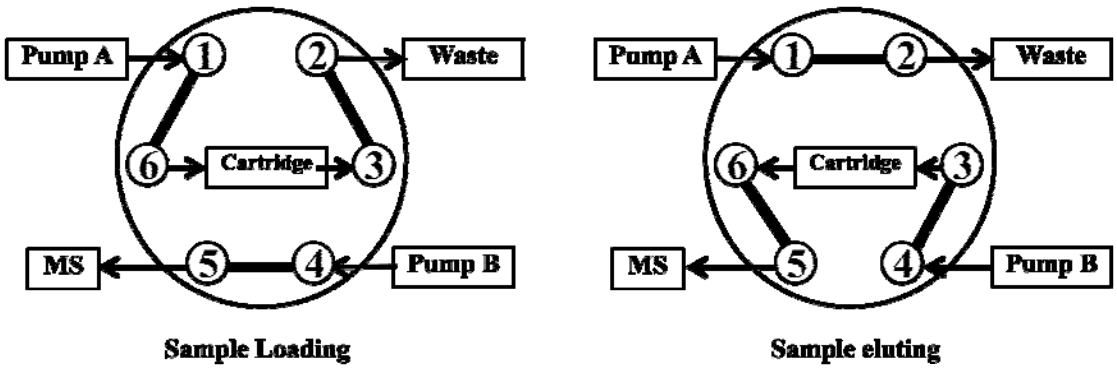

Figure 1.4, Illustration of on-line SPE.

1.2.3. Mass spectrometry

Mass spectrometry is a technique that identifies the molecules through their mass to charge (*m/z*) ratio. The basic working procedure of a mass spectrometer includes several steps. First, the sample containing the analyte is vaporized in the ion source. Then, the vaporized analyte particles together with the vaporized particles of other species in the sample are ionized in the gas phase through a certain ionization mechanism. Afterward, these ions enter into an electromagnetic field, the mass analyzer, and get separated based on their *m/z* ratios. Finally, the separated ions can be amplified by the detector, and the collection of ion signals composes the mass spectrum [20]. To increase the specificity of the analysis, the ionized analyte is often picked out by adjusting the electromagnetic field. Then the selected analyte ion will be further broken down to a batch of specific fragments. By picking a proper fragment of the analyte ion for the analyte monitoring and analysis, the analyte can be identified and measured with both high specificity and sensitivity.

To achieve this procedure, the mass spectrometer must possess several elements: the ion source, the mass analyzer, and the detector.

Ion Sources The most commonly used ionization methods coupled with liquid chromatography are electrospray ionization (ESI), atmospheric pressure chemical ionization (APCI), and atmospheric pressure photoionization (APPI) [21].

In *ESI*, the sample solution is passed through a capillary tube. With the help of a high electric potential, either positive or negative, added at the end of the capillary tubing, the solution can be sprayed into a jet of charged droplets. Meanwhile, a flow of nebulizer gas along the same direction with the spray helps disperse the droplets and increases the spray efficiency. The small dimensions of the droplets significantly increase their surface areas, and enable the solvent to evaporate quickly. At the same moment, a heated drying gas is applied to these droplets to avoid condensation and accelerate evaporation. During the process of evaporation, the decreased dimension of the droplet keeps increasing the charge density on its surface. Eventually, the repulsion between the like charges breaks up the droplets and releases single ions and neutral molecules (figure 1.5). ESI is a gentle ionization technique that especially efficient for polar compounds that is already ionized in solution through protonation or deprotonation. It is especially valuable in the ionization of large molecules, such as proteins and oligonucleotides, as it reduces the chances of fragmentation during ionization [22].

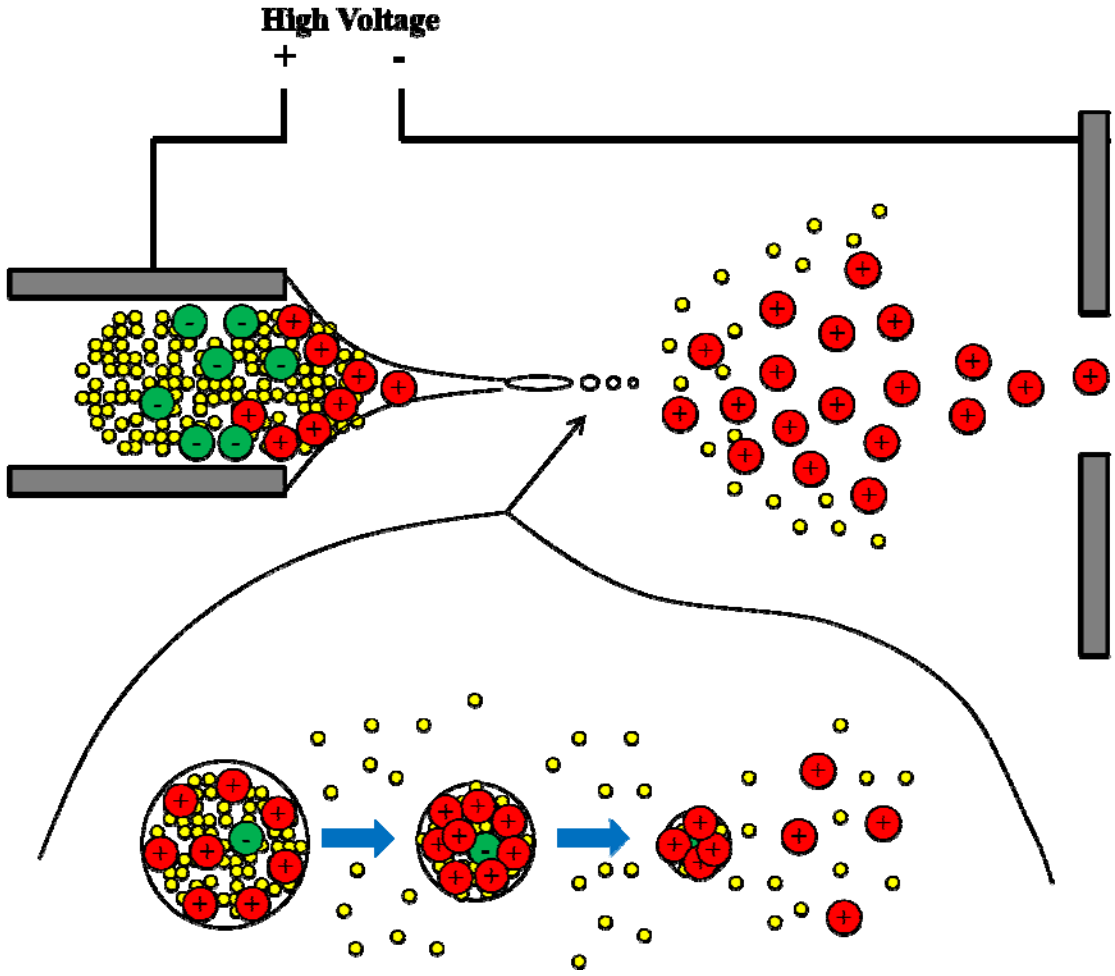

Figure 1.5, Illustration of ESI.

APCI is a form of chemical ionization, and is often realized on a modified ESI source. However, unlike ESI that the majority of the ionization happens in solution, in APCI, the ionization takes place after the solution is fully gasified. To be more specific, after the sample solution is sprayed through a capillary tube with the help of the nebulizer gas, the liquid droplets are evaporated in the source and form neutral aerosol cloud. Once the aerosol cloud is formed, nitrogen or oxygen ionized by the corona discharge is able to pass their charges to the solvent molecules, and then the solutes. The advantage of APCI comparing to ESI lies in its ability to ionize less polar compounds. Yet it is not as gentle as ESI, and tends to generate more fragments during ionization [23].

APPI Unlike ESI and APCI that depend on compound polarity during ionization, APPI ionizes molecules according to their ionization energy. In APPI, after the aerosol cloud is formed by the spray, the photons generated by the Krypton discharge lamp can interact with the molecules in the gas phase and pass their energy to the molecules. Then the neutral molecules utilize this energy as the ionization energy and get ionized. Nowadays, to improve the ionization efficiency, a dopant is often added to the ionization chamber. In this case, the photos generated by the Krypton discharge lamp first ionize the dopant. Then, the dopant passes the charges to the compounds of interest. This kind of ionization mechanism is also named as dopant-assisted APPI (DA-APPI). The advantage of this technique lies in its ability of ionizing extremely non-polar compounds. Nevertheless, as this technique requires heating the sample solution up to 250-350 ℃, its application is only limited to compounds with good thermal stability [21, 24].

As all compounds studied in this work were polar compounds, ESI was utilized throughout this work.

Mass analyzers Currently, the most commonly used mass analyzers in LC-MS/MS are triple-quadruple (QqQ), ion-trap (IT-MS), and quadruple-time-of-flight (Q-TOF) mass spectrometers.

QqQ This type of mass spectrometer consists two quadrupole mass filters (Q1 and Q3) in series and a non mass-resolving quadruple (Q2) in between. Thus QqQ works as a tandem mass spectrometer (MS/MS) that is able to give two dimensions of mass separation. Each quadrupole consists of four parallel metal electrodes. For Q1 and Q3, among the four electrodes, each pair of electrodes opposite to each other are connected and applied with the same radio frequency voltage. By applying another direct current onto the radio frequency voltages, a specific electromagnetic field is formed between the electrodes. This magnetic field only allows ions with certain *m/z* to have stable trajectories. And thus only these specific ions can pass through the field without hitting the electrodes; while all the other undesired ions are filtered out. Unlike Q1 and Q3, Q2 is the collision center that accommodates the collision-induced dissociation (CID). In this chamber, neutral gas molecules, such as helium, nitrogen, and argon, are accelerated. When these molecules collide with the ions traveled through Q1, the high kinetic energy carried by these molecules can be passed to the ions and break these ions into fragments. Although Q2 does not have mass-resolving power, the quadruple design is able to focus the fragments and pass them to Q3 (figure 1.6). Because LC-MS/MS realized through

QqQ is able to provide a wide linear calibration range for the compounds, it is most commonly utilized in the quantitative analysis of pharmaceutical compounds and their metabolites [25, 26]. In this work, all LC-MS/MS was performed exclusively with this type of mass spectrometers.

IT-MS Similar to the quadrupoles in QqQ, IT-MS is also composed of four electrodes added with radio frequency voltages, and generates a specific electromagnetic field. However, instead of letting the ions passing through, IT-MS traps the ions of interest first, and then exports these ions for detection. When MS/MS applies, IT-MS first traps the molecular ions with *m/z* of interest. Then, in the same trap chamber, the trapped ions are broken down with CID. Finally, IT-MS exports the fragments to the detector and generates a spectrum of the fragments. The advantage of IT-MS lies in its high sensitivity in the full scan mode. Besides, by its intrinsic design, IT-MS is able to handle more than one degree of fragmentation. After the first CID, the trap is able to pick out a specific fragment of the analyte, namely the daughter ion, and carry out another CID toward this daughter ion to obtain granddaughter ion. This property is especially useful in unknown specie identification. However, as the linear calibration range of compounds on IT-MS is usually much narrower comparing to QqQ, it only has very limited application in the quantification works [27].

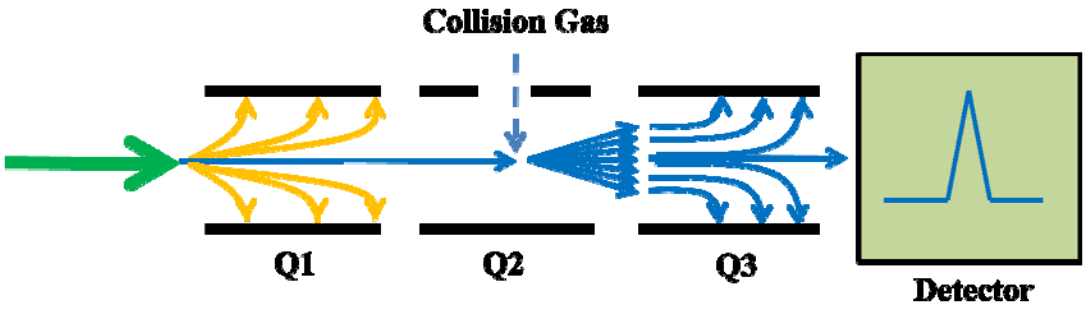

Figure 1.6, Illustration of QqQ mass analyzer.

Q-TOF With the only difference of Q3 substituted by a time-of-flight (TOF) mass analyzer, Q-TOF has very similar configuration as QqQ. The basic working mechanism of TOF can be explained as the following: all the ions are accelerated by a certain electric field to gain kinetic energy. The higher the charge, the more kinetic energy the ion will gain. For the ions with the same charge, the kinetic energy they gained would be the same. Then these ions are exported to a high vacuum space free of electromagnetic field, so that they can fly freely toward the detector. As when the kinetic energy is the same, the ions weight less fly faster, ions with different *m/z* will reach the detector at different time and get resolved. In this instrumentation, Q1 can serve as a pre-filter for the molecular ions, and Q2 remains to be the collision center. The fragments generated by CID can then be further resolved and analyzed by the TOF. Under some occasions, when intact molecules are the objects of the analysis, TOF can be operated along. In another word, all the ions entered into the mass spectrometer can bypass the Q1 and Q2, and directly enter TOF for analysis. The advantages of Q-TOF lie in its high mass resolution and the wide *m/z* analysis range. Thus, it is often utilized in unknown compound identification and large molecule (*e.g.*, peptides, proteins, oligonucleotides, *etc.*) analysis. [28, 29].

Detector When the ions finally travel to the detector of the mass spectrometer, the detector amplifies and records either the charges or the currents produced by these ions. The signals are then passed to the data analysis system and get presented as certain spectrum. Although there are multiple types of detectors (*e.g.*, Microchannel plate

detector, Faraday cup, ion-to-photon detector, *etc.*), electron multiplier is the most typically used detector for the previously mentioned instrumentations.

During the working cycle of the electron multiplier, the ions reach to the detector can be amplified by secondary emission. To be more specific, the single electron can be accelerated by an electric field and then collide with the secondary emissive material coated on the surface of the electron multiplier tube. This kind of collision induces the emission of another 1-3 electrons. When the secondary emission is repeated for several cycles, the one electron reached the detector can be amplified to a beam of electrons (figure 1.7). Finally, this beam of electron is collected by a metal anode and demonstrated as a detectable pulse [30].

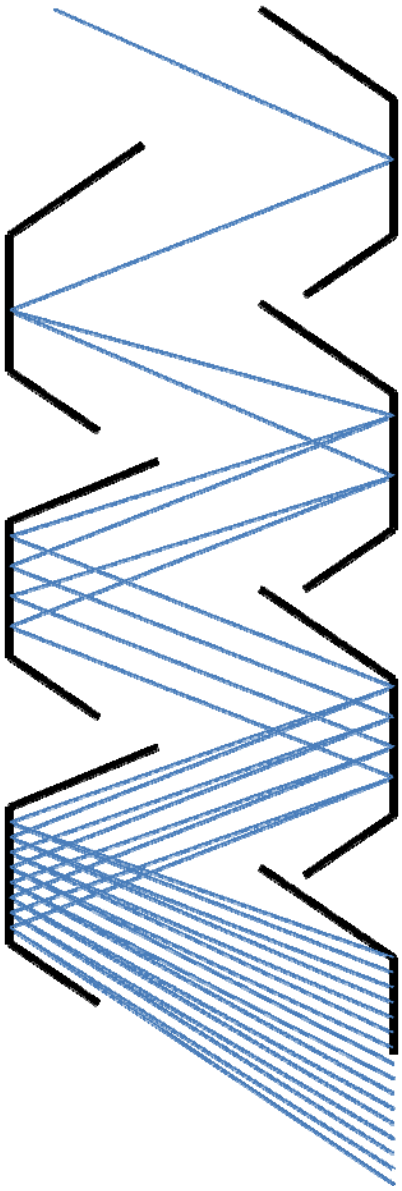

Figure 1.7, Illustration of electron multiplier.

1.2.4. Method validation

Once an LC-MS/MS method (including the proper sample extraction method) has been developed, it is necessary to evaluate the performance of the method, especially when the developed method will be utilized for quantitative purposes.

Although there are many different standards for method validation, the most commonly accepted one in the pharmaceutical industry in United States is the "Guidance for Industry Bioanalytical Method Validation" proposed by FDA [31]. According to FDA, several factors about the method and the analyte have to be considered when validating a bioanalytical method. These factors include selectivity, recovery, calibration curve, accuracy, precision, and stability. Besides, as the matrix of the biological samples, even the matrix of the post-extract samples, may affect the signal of the analyte, evaluation of matrix effect has also become a must in the method validation.

Selectivity studies how specific the bioanalytical method is toward the analyte. The interferences coming from same type of blank biological samples, yet from at least six different sources have to be tested. The signal of the interference caused by non-specific responses should be evaluated at the level of lower limit of quantification (LLOQ). In another word, the non-specific response of the detector should not affect the accurate quantification of the LLOQ.

Recovery is an evaluation of the effectiveness of the extraction methods. It can be obtained by comparing the signals of the analyte in the extracted sample and in the pure

authentic analyte solution spiked in the post-extraction blank matrix. To determine the recovery of the extraction method accurately, at least three concentration levels (*i.e.*, a low, a medium, and a high) throughout the calibration range should be evaluated. At each concentration level, three replicates of the samples should be prepared. The mean value and the standard deviation of the measurements should be recorded and reported.

Matrix effect is an evaluation of the effectiveness of both the extraction methods and LC methods, because if the extraction method or LC failed to provide enough separation between the analyte and the interferences, the signal of the analyte may be significantly suppressed or, sometimes, enhanced. Matrix effect is usually calculated by comparing the signals of the analyte in the pure authentic solution spiked in the post-extraction blank matrix with that in the pure authentic solution along. Like the determination of recovery, at least three concentration levels are needed, and three replicates are required for each concentration level. The mean and standard deviation of the measurements should be recorded and reported.

Calibration curve The calibrators must be prepared in the same biological matrix as the real samples. Usually, the calibrators should be prepared by spiking know amount of analyte into the biological matrix. For a linear calibration curve, at least six non-zero calibrators should be included in the curve. A double-blank sample with no addition of analyte or the internal standard (IS) should be included. Besides, a zero sample, with no addition of analyte, yet containing same concentration of IS as all the non-zero calibrators, should also be included. The accuracy and precision of each calibrator should be

evaluated. The accuracy of each calibrator is determined by the percent error of the calculated concentration (equation 1.1).

$$Accuracy = \frac{(Analyte)_{meas.} - (Analyte)_{nomi.}}{(Analyte)_{nomi.}} \times 100\% \quad (1.1)$$

Here $(Analyte)_{meas.}$ represents the measured concentration of the analyte from the calibration curve. $(Analyte)_{nomi.}$ indicates the nominal concentration of the analyte.

The inter-assay precision of each calibrator is determined by the coefficient of variation (CV%) from several measurements toward the same calibrator (equation 1.2).

$$CV\% = \frac{Standard\ Deviation}{Average} \times 100\% \quad (1.2)$$

Sometimes, the same calibration curve is repeated for several times on different days, so that the inter-assay precision of the calibrators can be determined. By dividing the standard deviation of the calculated values with the average of the calculated values, the inter-assay precision can be obtained.

For any point on the calibration curve, except the LLOQ, the accuracy and precision should be within ±15%. For LLOQ, the values should not exceed ±20%.

Accuracy and Precision The calculations of the accuracy and precision are the same with those described above. However, to evaluate the accuracy and precision of a method, a set of quality control (QC) samples are needed. These QC samples usually include at least three concentration levels (low, medium, and high). For each

concentration level, five parallel replicates should be prepared. Since the accuracy and precision at the LLOQ should also be evaluated, if the low concentration QC samples (LQCs) are not the same with the LLOQ, another five replicates of LLOQ should be prepared.

During real sample analysis, there is possibility that some of the real samples possess concentrations either higher or lower than the upper or lower limit of quantification. In these occasions, diluted or concentrated quality control samples are also need for the accuracy and precision studies.

The acceptable criteria of accuracy and precision for the QC samples are, again, within ±15%, except at LLOQ as ±20%.

Stability The stability studies provide important information on sample handling and storage. The most common stability studies include the following categories: short-term stability, long-term stability, freeze and thaw stability, post-preparative stability, and stock solution stability. The short-term, long-term, and freeze and thaw stabilities illustrate the stability of the analyte in the biological matrix. The post-preparative stability analyzes the stability of the analyte in the post-extraction sample matrix. The stock solution stability measures the stability of the analyte in high concentration pure stock solutions. For each stability study, at least two concentration levels, a low and a high, are needed. At each concentration level, three parallel replicates should be prepared. The signals of the analyte in the samples after incubation will be compared with those

freshly made samples. The degradation of the analyte can then be clearly indicated by the signal loss.

Short-term stability studies are usually carried out under room temperature. The biological matrix spiked with known concentrations of analyte will be left on bench top or in a place that away from direct light exposure. The samples are usually kept under this condition for 4 to 24 h. However, the study time can be adjusted accordingly based on the actual need in the real sample analysis.

Long-term stability In this type of studies, the spiked samples should be kept in a desired storage place, such as a refrigerator (4 ℃) or in a freezer (-20 or -80 ℃). The total study time should be longer than the time span between the collection time of the first sample and the analysis time of the last sample. The most common time span is from 1 to 6 months.

Freeze and thaw stability At least three freeze and thaw cycles should be carried out for this type of studies. For each cycle, the samples should be frozen in the desired storage temperature (*e.g.*, -20 or -80 ℃) for 12-24 h. Then, the samples should be thawed under room temperature without assistance.

Post-preparative stability After the samples are processed, they usually will be kept in an autosampler, waiting for analysis. Therefore, the stability of the analyte and the internal standard in the processed samples should also be evaluated. The study time should not be shorter than the total running time of a whole batch of sample.

Stock solution stability For the stock solutions, at least two kinds of stabilities must be studied: short-term stability at room temperature, as well as freeze and thaw stability. At least 6 hours storage at room temperature should be included in the short-term stability studies; at least three freeze-and-thaw cycles should be carried out in the freeze and thaw stability studies.

1.2.5. A general work flow of quantitative LC-MS/MS method development

A quantitative LC-MS/MS method can be developed in the following work flow (figure 1.8):

First, the analyte is infused into the mass spectrometer for mass identification and characterization. In this step, the mass spectrum of the analyte is obtained, so that the molecule ion(s) can be identified. Under most of the occasions, to further improve the detection specificity, CID is also introduced, fragmenting the selected molecular ion into a batch of specific product ions. By scanning these product ions, the predominant product ion is often picked out for analyte identification and quantification. Then the mass spectrometer can monitor the analyte through specific mass transition channel. Meanwhile, a suitable internal standard (IS) is also selected to increase the accuracy and precision of the analysis. Mass identification and characterization will be carried out to this IS as well.

Then, an LC method will be developed toward the analyte and the IS. The LC method must be able to provide sufficient separation between the analyte and the possible interferences existing in the sample matrix. For accurate peak integration, the analyte signal peak eluted from the column must be symmetrical, and the retention time must be repeatable.

Afterward, an effective extraction method can be developed to further eliminate the interferences in the sample matrix. A preliminary recovery and matrix effect study can be carried out to evaluate the effectiveness of the extraction method.

Then, repeat injections toward a post-extraction biological sample can be carried out on the LC-MS/MS system with the developed LC-MS/MS method. If the signal does not vary significantly *(i.e.*, CV% less than 15%) between each injection and the signal of the analyte or the IS does not decrease significantly with the repeated analysis, both the extraction and the LC method can be kept.

Next, the ESI and MS/MS parameters can be fine tuned to provide the maximum detection sensitivity.

Finally, the whole method can be validated with the FDA guidance. When all of the validation criteria are met, the method becomes an analytical method, and can be applied to real pharmacological studies.

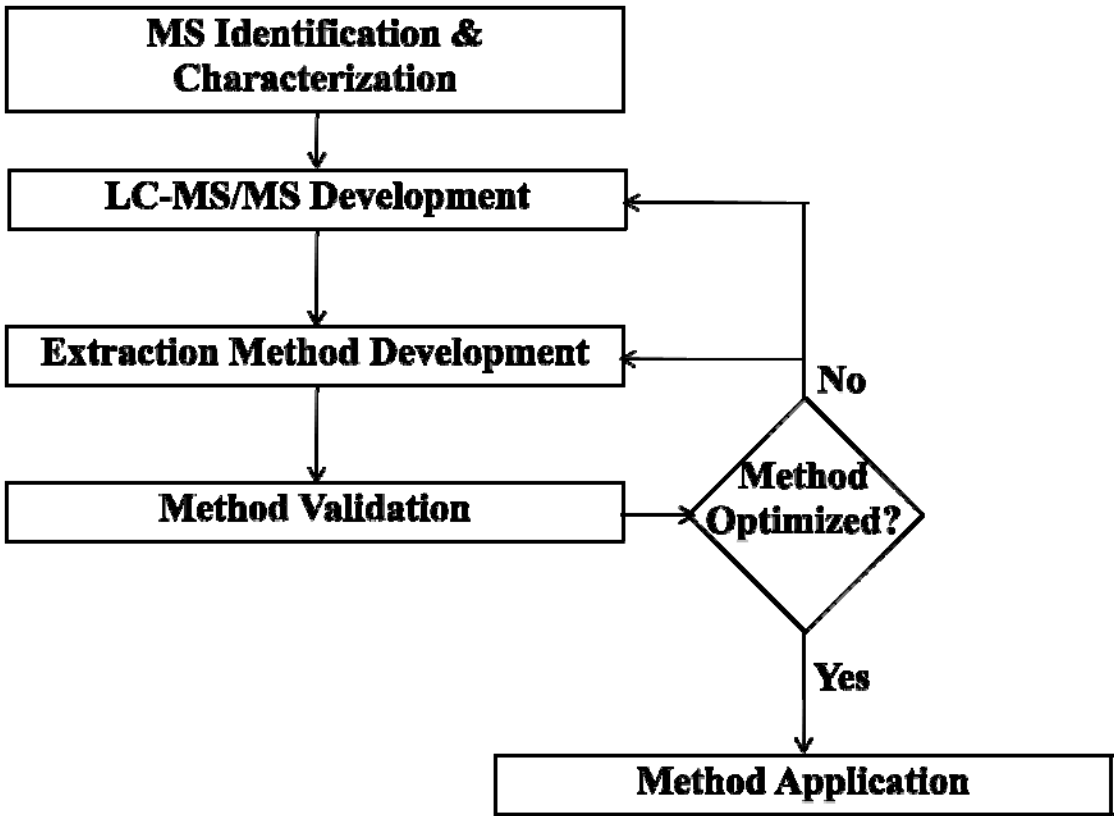

Figure 1.8, Workflow of bioanalytical LC-MS/MS method development.

1.3. Conclusion

In this chapter, a brief discussion has been made on the importance of pharmacological studies, including pharmacokinetics and pharmacodynamics studies, in the process of anti-cancer drug development. Then three anti-cancer drugs with different unsolved problems in their pharmacological studies were introduced; LC-MS/MS methodologies on how to solve these problems were proposed. To emphasize the problem solving ability of LC-MS/MS in the pharmacological studies of the anti-cancer drugs, the mechanisms and techniques of LC, biological sample extraction, mass spectrometry, and bioanalytical method validation has been reviewed briefly. A general workflow of bioanalytical LC-MS/MS method development has also been laid out at the end of the chapter. By following the workflow, pharmacological studies involving similar problems can be achieved with LC-MS/MS methods.

1.4. References

1. A. Jemal, R. Siegel, J. Xu, E. Ward. CA Cancer. J. Clin. 60 (2010) 277.

2. National Cancer Institute. Drug Discovery at the NCI: Fact Sheet. Available at http://www.cancer.gov/cancertopics/factsheet/nci/drugdiscovery, 2006

3. Edited by: W.D. Figg, H.L. McLeod. Handbook of Anticancr Pharmacokinetics and Pharmacodynamics, Humana Press Inc., NJ, 2004.

4. M.E. Winter. Basic clinical pharmacokinetics, Lippincott Williams & Wilkins Health, PA, 2010.

5. L.Z. Benet. Pharmacokinetics: Basic Principles and Its Use as a Tool in Drug Metabolism, in: Drug Metabolism and Drug Toxicity, J.R. Mitchell, M.G. Horning (eds.), Raven Press, NY, 1984.

6. M. Rowland, T.N. Tozer. Clinical pharmacokinetics and pharmacodynamics : concepts and applications, Lippincott William & Wilkins, PA, 2011.

7. L. Liu, L. Yan, J.R. Donze, S.L. Gerson. Mol. Cancer Ther. 2 (2003) 1061.

8. A.D. Bulgar, M. Snell, J.R. Donze, E.B. Kirkland, L. Li, S. Yang, Y. Xu, S.L. Gerson, L. Liu. Leukemia. 24 (2010) 1795.

9. S. Yang, L. Liu, S.L. Gerson, Y. Xu. J. Chromatogr. B. 795 (2003) 295.

10. A.M. Tsimberidou, M.J. Keating. Cancer. 115 (2009) 2824.

11. V. Gandhi, W. Plunkett. Clin. Pharmacokinet. 41 (2002) 93.

12. K. Kamiya, P. Huang, W. Plunkett. J. Biol. Chem. 271 (1996) 19428.

13. P. Huang, S. Chubb, W. Plunkett. J. Biol. Chem. 265 (1990) 16617.

14. K.P. Roberts, J.A. Sobrino, J. Payton, L.B. Mason, R.J. Turesky. Chem. Res. Toxicol. 19 (2006) 300.

15. L.R. Snyder, J.J. Kirkland. Introduction to Modern Liquid Chromatography, 2nd Edition, John Wiley & Sons, Inc., Canada, 1979.

16. T. Cecchi. Ion-pair Chromatography and Related Techniques, CRC Press, FL, 2010.

17. D.L. Nelson, M.M. Cox. Lehninger Principles of Biochemistry, fourth edition, W. H. Freeman and Company, NY, 2005.

18. Science and Practice of Liquid-Liquid Extraction, Edited by J.D. Thornton, Oxford University Press, NY, 1992.

19. Solid-phase Extraction : Principles, Techniques, and Applications, Edited by N.J.K. Simpson, Marcel Dekker, NY, 2000.

20. O.D. Sparkman. Mass Spectrometry Desk Reference, Global View Pub., PA, 2000.

21. T. Kauppila, Atmospheric Pressure Photoionization-Mass Spectrometry. Academic dissertation, Finland, 2004.

22. C.G. Herbert, R.A.W. Johnstone. Mass spectrometry basics, CRC Press, FL, 2003.

23. A.E. Ashcroft. Ionization methods in organic mass spectrometry, Royal Society of Chemistry, UK, 1997.

24. National High Magnetic Field Laboratory Education Home. Atmospheric Pressure Photoionization (APPI). Available at http://www.magnet.fsu.edu/education/tutorials/tools/ionization-appi.html, 2010.

25. E. de Hoffmann. V. Stroobant. Mass Spectrometry: Principles and Applications, John Wiley & Sons Ltd., Canada, 2003.

26. E. de Hoffmann. J. Mass. Spectrom. 31 (1996) 129.

27. R.E. March, J.F.J. Todd. Quadrupole ion trap mass spectrometry, Wiley-Interscience, NJ, 2005.

28. I.V. Chernushevich, A.V. Loboda, B.A. Thomson. J. Mass Spectrom. 36 (2001) 849.

29. R.J. Cotter. Time-of-flight mass spectrometry : instrumentation and applications in biological research, American Chemical Society, DC, 1997

30. J.S. Allen. Rev. Sci. Instrum. 18 (1947) 739.

31. U.S. Food and Drug Administration (FDA) & Center for Drug Evaluation and Research (CDER), Guidance for Industry: Bioanalytical Method Validation, available at http://www.fda.gov/cder/guidance/4252fnl.htm, 2001.

CHAPTER II

ENZYMATIC RELEASE OF DNA ADDUCTS FROM DNA BACKBONE

2.1. Introduction

When DNA is under the stress of certain anti-cancer drugs or some cancerogenic agents, abnormities will be introduced into DNA bases, or even the entire nucleotide residue [1-4]. To evaluate the effects of these anti-cancer drugs or cancerogenic agents on DNA, the resulted DNA adducts are often quantified. DNA adducts with strong and unique fluorescent or UV absorption can be directly measured with a fluorescent or UV spectrometer. However, for most of the adducts that do not give strong and specific signals on fluorescent or UV detectors, mass spectrometry remains one of the most

effective tools for DNA adduct quantification. Meanwhile, to facilitate the DNA adduct quantification with mass spectrometry, the adducts are often released from the DNA backbone with enzymatic hydrolysis procedures. The typical end products of this type of hydrolysis are mononucleotide monophosphates or nucleosides, and the released adducts.

The most commonly utilized enzymes include bovine pancreatic deoxyribonuclease I (DNase I), micrococcal nuclease (MN) from *Staphylococcus aureus*, nuclease P1 (NP1) from *Penicillium citrinum*, phosphodiesterase I (PDE I) from snake venom, phosphodiesterase II (PDE II) from spleen, and calf intestinal or shrimp alkaline phosphatase (ALP).

Deoxyribonuclease I is an endonuclease splitting phosphodiester bonds preferentially adjacent to pyrimidine nucleotides and typically yields tetranucleotides with a free 3'-end hydroxyl group and a free 5'-end phosphate group [5]. DNase I is able to take both single and double strand DNA as digestion substrates. However, the activity of DNase I can be inhibited by histones when digesting chromatin [6]. The optimized pH for DNase I is 7.8. To achieve best digestion efficiency, DNase I can be activated with bivalent metal ions, such as Mg^{2+} and Ca^{2+}. In another word, chelating agents such as EDTA can deactivate the enzyme by depleting the metal ions needed for the enzyme activity [7]. The activity of DNase I can also be inhibited by detergent, such as sodium dodecyl sulfate (SDS) [8].

Micrococcal nuclease is an endo-exonuclease that can hydrolyze both DNA and RNA. Although it is relatively non-specific, it does have a preference of cleaving at sites

rich in adenylate, deoxyadenylate or thymidylate. The typical products of MN digestion are mono- or di- nucleotides [9]. Yet unlike DNase I that generates 5'-phophonucleotides, MN releases 3'-phosphonucleotides. MN functions better under slightly basic pH (*i.e.*, pH 7.0-10.0), with the optimized pH of 9.2. Again, Ca^{2+} is important for the activation of the enzyme; while the enzyme can be inhibited by chelating agents or nucleoside 5'-phosphates or deoxyribonucleoside 5'-phosphates [9, 10].

Nuclease P1 is a 5' to 3' exonuclease. The common substrate for this enzyme is RNA and single strand DNA. The completely hydrolyzed product is single nucleotides with a phosphate group on the 5' position [11]. Double strand DNA is not an effective substrate of NP1 especially under the existence of high concentrations (*i.e.*, higher than 400 mM) of NaCl. NP1 has higher specificity to the nucleotides located on the 5' end of the phosphodiester bonds comparing to those located on the 3' end of the phosphodiester bonds [12]. The best pH for NP1 functioning is 5.4, and the optimized digestion temperature is 70 ℃. The enzyme can be activated by a variety of metal ions, such as Cu^{2+}, Co^{2+}, Mn^{2+}, Fe^{2+}, Ba^{2+}, and Zn^{2+}. The enzyme's activity can be significantly suppressed (*c.a.* 50%) with the existence of 0.1-0.2% SDS (w/v) [11].

Phosphodiesterase I is a 3' to 5' exonuclease. It can successively hydrolyze DNA or RNA from 5' end to 3' end to single nucleotide level. Same to NP1, PDE I releases single nucleotides with 5'-phosphate as the typical digestion product [13]. It is even more non-specific comparing to nuclease P1, and it is only sensitive to the configuration of the phosphate in the phosphodiester bond [14]. Optimized digestion

efficiency of PDE I can be achieved by adjusting the pH to 8.9 under the existence of Mg^{2+} [15]. EDTA as well as reducing agents, such as glutathione, cysteine, and ascorbic acids, are effective inhibitors for PDE I. The enzyme can also be partially inhibited by ATP, ADP, and AMP [15].

Phosphodiesterase II is a 5' to 3' exonuclease. The action of PDE II on DNA requires prior removal of the 5'-end phosphate group and the generation of a free hydroxyl group. Then it successively hydrolyzes DNA or RNA and releases single nucleotides with 3'-phosphate. The enzyme acts the most efficiently at pH 5.5 in a succinate or phosphate buffer. Similar enzyme activity can also be achieved in acetate buffer between pH 6.0 and 7.0 [16].

Alkaline phosphatase is a hydrolase removes phosphate groups from a wide variety of molecules, such as protein and nucleotides. As its name suggested, ALP hydrolyzes the phosphate groups most efficiently under alkaline conditions. For example, the optimized pH for bovine intestinal ALP is pH 9.8 [17, 18].

When a DNA adduct needs to be released from the DNA backbone, either one of two enzyme combinations are the most commonly selected: DNase plus NP1 and/or PDE I [19-23], or MN plus PDE II [24-26]. Both enzyme combinations are sufficient to completely hydrolyze DNA into single nucleotide level, and thus release the DNA adduct as free small molecule. However, ALP is also added into the digestion system sometimes, because the removal of the phosphate group can, sometimes, simplify the LC method development. In our study, we mixed together DNase I, NP1, PDE I, and ALP as an

enzyme cocktail. By utilizing MX-AP DNA as a model, the components and digestion time of the enzyme cocktail have been optimized. However, for different DNA adduct, the digestion efficiency of each enzyme may vary. To achieve best digestion effect for a specific DNA adduct, the enzyme system will need to be optimized individually.

2.2. Material and methods

2.2.1. Chemicals and solutions

MX·HCl, BisTris, Calf Thymus DNA, *O*-(4-Nitrobenzyl) hydroxylamine, ethanol, sodium citrate, DNase I, NP1, and ALP (bovine intestinal) were obtained from Sigma-Aldrich (St. Louis, MO). NaH_2PO_4, NaCl, and $ZnCl_2$ were purchased from Fisher Scientific (Fair Lawn, NJ). Tris base was from Bio-Rad Laboratories (Hercules, CA). Hydrochloric acid was from EMD Chemicals (Gibbstown, NJ). PDE I was obtained from Worthington Biochemical Corporation (Lakewood, NJ). Deionized water was prepared by the Barnstead NANOpure® water purification system (Thermo Scientific, Waltham, MA, USA).

2.2.2. MX-AP DNA preparation

To obtain the MX-AP DNA, AP-DNA was first prepared following a procedure modified from an existing method [27]. To be more specific, 5.0 mg of lyophilized calf thymus DNA was resuspended in 4.0 mL of 10 mM Tris-HCl (pH 7.0). Then, the pre-existing AP sites on the CT-DNA were blocked by mixing the DNA solution with 1 mL of 10 mM *O*-(4-Nitrobenzyl) hydroxylamine (NBHA, dissolved in 10 mM Tris-HCl and adjusted to pH 7.0 with HCl). After incubation at 37 ℃ for 2 h, the pre-existing AP sites were considered as been blocked completely. Then, the DNA solution was transferred into clean 1.5 mL centrifuge tubes as 250 μL per aliquot. In each tube, DNA was precipitated with 1.0 mL of pre-chilled (-20 ℃) ethanol and was left at -20 ℃ for 30 min. DNA pellets were recovered by centrifugation at 4 ℃, 10000 × g for 15 min. Then the pellet in each tube was washed with pre-cold (4 ℃) 70% ethanol for 3 times. For each wash, the DNA pellet was mixed with 1 mL of 70% ethanol by 1 min vortex, followed by centrifugation at 10000 × g for 5 min. After washing, the DNA pellets were dried by leaving the centrifuge tubes uncapped in a fume hood for 30 min at room temperature. The dried DNA pellet in each centrifuge tube was resuspended in 250 μL of 10 mM sodium citrate buffer (containing 10 mM sodium citrate, 10 mM NaH_2PO_4, and 10 mM NaCl, adjusted to pH 5.0 with HCl). AP sites were generated by heating the DNA solution at 70 ℃ on a heat block (VWR International, Radnor, PA) for 30 min, and the reaction was stopped by chilling the DNA samples on ice immediately after heating.

Then, DNA was precipitated out, washed, and dried again with the methods described above. By resuspending the DNA pellets in 10 mM Tris-HCl (pH 7.0), the pellets in the 1.5 mL centrifuge tubes were combined and the concentration of DNA was adjusted to 2 mg/mL by its UV absorption at 260 nm (*i.e.*, 1 OD is equivalent to 50 μg/mL DNA). At this step, AP-DNA is obtained.

For each 2.5 mL of AP-DNA solution, after addition of 2.5 mL of 20 mM MX (dissolved in 30 mM of BisTris, pH 7.0) the mixture was incubated in 37 ℃ for 2 h. Next, the DNA was precipitated out, washed for three times according to the methods described above, and then dried with the same method yet for 1 h. Finally, the dried DNA pellet was resuspended in 5 mM BisTris (pH 7.0) to a concentration of 1 mg/mL (based on UV absorption at 260 nm).

2.2.3. Enzymatic hydrolysis condition optimization

Several different digestion methods were tried for the optimized digestion condition. MX-AP DNA (1 mg/mL in 5 mM BisTris, pH 7.0) prepared in section 2.7 was utilized in the tests. Digestion samples were prepared as triplets for each digestion method. The enzyme working solutions were prepared as the following: DNase I was dissolved with 0.9% NaCl to 10 mg/mL (*ca.* 20000 unit/mL); NP1 was dissolved with 1 mM $ZnCl_2$ to 1 mg/mL (*ca.* 200 unit/mL); PDE I was dissolved with deionized water to

100 unit/mL. Each 0.5 μL (12.5 units) of ALP was mixed with 40 μL of PDE right before the addition of PDE I.

Method 1: each 40 μL of MX-AP DNA was incubated with 0.4 μL of DNase I at 37 ℃ for 1.5 h. Then, 0.6 μL of NP1 was added and incubated with the DNA at 37 ℃ for another 3 h. Finally, a 1.6 μL of PDE I and ALP mixture was added and incubated with the DNA at 37 ℃ for 12.5 h.

Method 2: An enzyme cocktail was prepared by mixing 10 μL DNase I, 15 μL NP1, 40 μL PDE I, and 0.5 μL of ALP. For each 40 μL of MX-AP DNA, 2.6 μL of the enzyme cocktail was added and mixed well with the DNA sample. The incubation was then kept at 37 ℃ for 17 h.

Method 3: An enzyme cocktail was prepared by mixing 10 μL 0.9% NaCl, 15 μL NP1, 40 μL PDE I, and 0.5 μL of ALP. For each 40 μL of MX-AP DNA, 2.6 μL of the enzyme cocktail was added and mixed well with the DNA sample. The incubation was then kept at 37 ℃ for 17 h.

Method 4: An enzyme cocktail was prepared by mixing 10 μL DNase I, 15 μL 1 mM $ZnCl_2$, 40 μL PDE I, and 0.5 μL of ALP. For each 40 μL of MX-AP DNA, 2.6 μL of the enzyme cocktail was added and mixed well with the DNA sample. The incubation was then kept at 37 ℃ for 17 h.

Method 5: An enzyme cocktail was prepared by mixing 10 μL DNase I, 15 μL NP1, 40 μL deionized water, and 0.5 μL of ALP. For each 40 μL of MX-AP DNA, 2.6

μL of the enzyme cocktail was added and mixed well with the DNA sample. The incubation was then kept at 37 ℃ for 17 h.

Method 6-10: An enzyme cocktail was prepared by mixing 10 μL DNase I, 15 μL NP1, 40 μL PDE I, and 0.5 μL of ALP. For each 40 μL of MX-AP DNA, 2.6 μL of the enzyme cocktail was added and mixed well with the DNA sample. The incubation was then kept at 37 ℃ for 5, 10, 15, 20, and 25 h, respectively.

2.2.4. Digestion efficiency determination

The mean peak area of the triplicate samples digested with the same method was obtained and compared with that of the triplicate samples digested with the other methods. In the same set of experiments (method 1-5, or method 6-10), the highest mean peak area obtained from a certain digestion method was arbitrarily assigned as 100%. The percentiles of the mean peak areas of the other samples in the set were calculated with equation 2.1. The digestion efficiencies of different methods were compared through these percentiles.

$$Percentile = \frac{\bar{A}}{\bar{A}_{max}} \times 100\% \quad (2.1)$$

2.3. Results and discussions

2.3.1. Comparison between sequential digestion and enzyme cocktail

By referring to the work of Yamazoe *et al.* and Lin *et al.*, the quaternary enzyme system consisting of DNase I, NP1, PDE I, and ALP was chosen [28, 29]. In this system, DNase I is thought to increase the digestion speed of NP1 and PDE I by generating free ends on the DNA. In addition, the oligonucleotide generated by DNase I weakens the hydrogen bonds between the double strand, and releases single strand DNA, a better substrate for NP1 [11]. When the first three enzymes work together to hydrolyze the DNA, single strand or double strand, into deoxyribonucleotides (dNMPs), ALP works at the same time to remove the phosphate groups from the dNMPs, resulting deoxyribonucleosides (dNs). Although the four enzymes work in a sequential mechanism, according to some previous work in DNA adduct release [19-23], DNaseI, NP1 or PDE I, and ALP are often mixed together as an enzyme cocktail, and the digestion can be achieved in one step instead of through a multi-step sequential digestion process. As comparing to the one-step cocktail digestion, when there is no automatic liquid handling system available, the procedure is much more complicated. Besides, when the sample size is small, handling of small volume (less than 0.5 μL) of enzyme solution is also involved. Without automation techniques, the accuracy and reproducibility of this kind of sample handling can be relatively low. Diluting the enzyme solution into larger volumes

may reduce the errors caused by pipetting, but the large sample size may introduce more complicity and waste of solvent in sample extraction. Based on these considerations, the releasing efficiencies of the tetra-enzyme system on MX-AP adducts through sequential digestion and through cocktail digestion were compared. In the digestion method 1 and 2, the amount of each enzyme and the total digestion time were controlled to be the same. The digestion efficiency was measured with the method described in section 2.2.4.

Figure 2.1 A (column 1 and 2) indicated that although the cocktail digestion released slightly lower amount of MX-dR comparing to the sequential digestion, the difference is not significant ($p < 0.05$). When taking the advantages it can bring about, the cocktail digestion will have more value in practice.

2.3.2. Significance of DNase I, NP1, and PDE I in the digestion

After the cocktail digestion has been chosen as the preferred digestion strategy, the significances of each enzyme in the release of MX-AP were evaluated. Although ALP is not necessary in enzymatic release of MX-AP from the DNA backbone, it is the only enzyme that removes the phosphate group. It has to be included in the system as long as the non-phosphorylated digestion products are preferred. In this work, developing LC method for the non-phosphorylated products is relatively straightforward comparing to the phosphorylated products, thus ALP was kept in the enzyme cocktail. For the other

three enzymes, three different enzyme combinations (digestion method 3 to 5), each with one enzyme missing, were experimented. The amounts of all the other enzymes and the digestion time were kept the same in each experiment.

According to column 3 to 5 in figure 2.1 A, elimination of any one of the enzymes (DNase I, NP1, or PDE I) led to digestion efficiency losses at different extents. However, DNase I seemed to play the least important role in the digestion process. This result is also consistent with the digestion mechanism of DNase I, as it is an enzyme that only increases the efficiency of the other two enzymes. The data also indicated that NP1 was the key enzyme in the release of MX-AP; while the maximum digestion efficiency, however, was only achieved with the synergy of PDE I.

2.3.3. Enzyme kinetics

After the optimization of digestion process and enzyme cocktail composition, the best digestion time was experimented. By digesting the MX-AP DNA with the enzyme cocktail for 5, 10, 15, 20, and 25 h, a kinetic curve was obtained (figure 2.1 B). From the curve, the optimized digestion time was between 15 and 20 h. As a result, a total digestion time of 17 h was adopted due to its best fit to an 8 h working schedule.

A

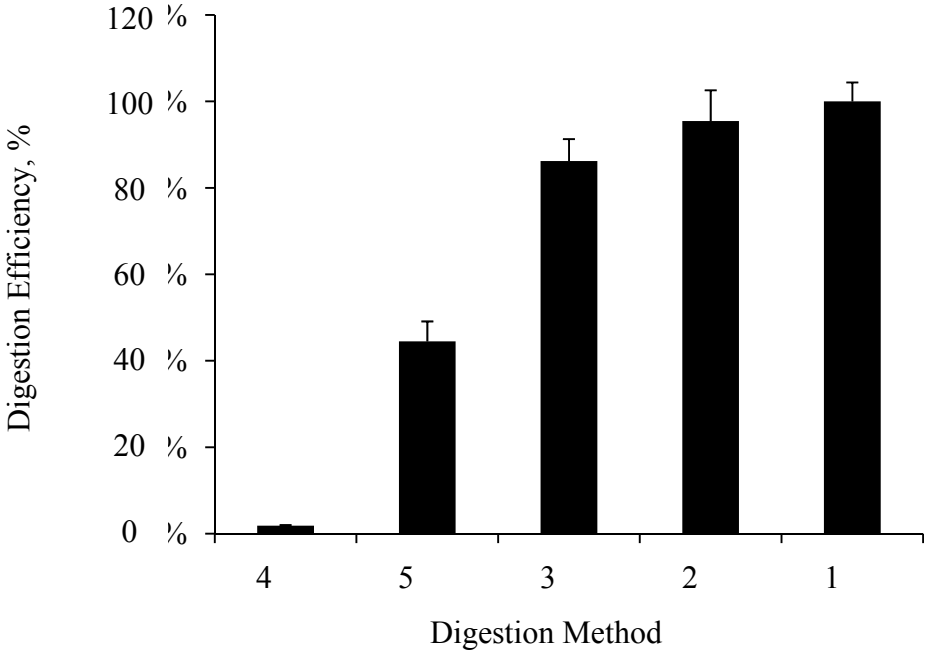

B

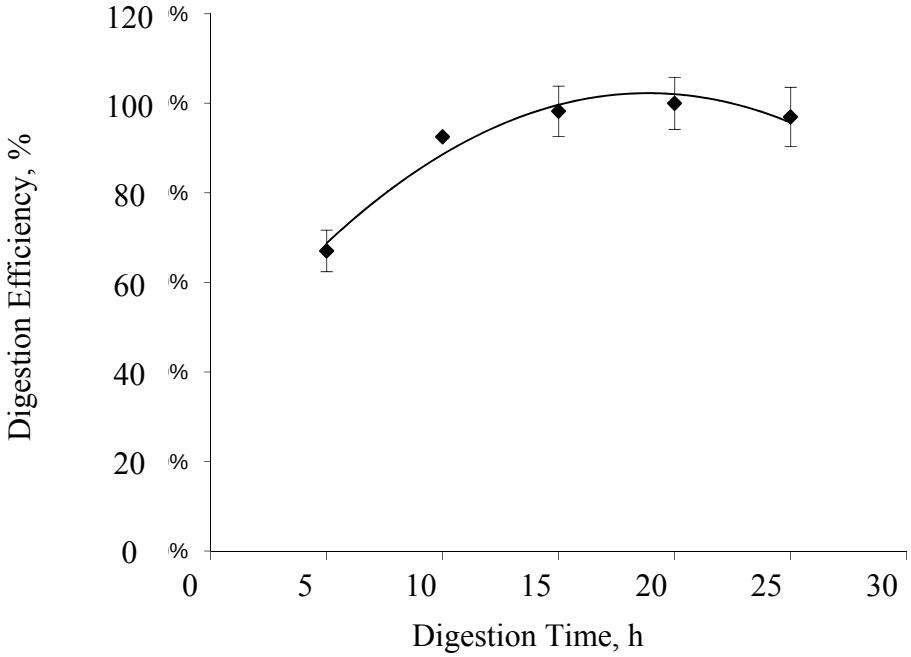

Figure 2.1, Enzyme digestion efficiency comparison. (A) The MX-AP DNA was digested with 5 different methods (the number below each column represent the number of the digestion method); and (B) the kinetics profile of the enzyme cocktail from 5 h to 25 h.

2.3.4. DNA concentration determination through the released dNs

Although DNA concentration is most frequently determined by the UV absorption of the DNA samples at 260 nm (OD_{260}), with the interferences caused by impurities, such as protein and RNA, the accuracy of the measurement can be seriously affected. Evaluation of OD_{260}/OD_{280} or OD_{260}/OD_{230} may provide some idea on the purity of the DNA samples, but the results are still qualitative instead of quantitative.

During the enzymatic release of DNA adducts, however, all the normal DNA units are released as dNs (or dNMPs when ALP is not added). The released dNs can serve as perfect indicators for DNA quantification without introducing complicated procedures. Another advantage of utilizing dNs released from enzyme digestion as the standard for DNA quantification lies in that it can, at same time, reflect the digestion efficiency of the enzymes on a specific DNA sample. During the DNA extraction, some of the impurities introduced during the extraction process, such as SDS and protease K, may hurt the efficiency of the enzymes and lead to lower DNA adduct release. In another word, even when two samples contain exactly the same concentrations of DNA, impurities in one sample may lead to much less DNA adduct release for the sample contaminated with SDS or protease K comparing to the sample with higher purity. DNA concentration determination with dNs can also normalize the digestion efficiency and make the results more reliable.

In this work, commercially available calf-thymus DNA (CT-DNA) was utilized as pure DNA standard. We assume that the concentration of the CT-DNA standards can be accurately determined by its OD_{260} due to its high purity. The concentrations of the CT-DNA standard and the real samples were first roughly normalized to 1 mg/mL according to their OD_{260}. Then, both the standard and the real samples were digested with the method 2 described in section 2.2.3. After enzyme digestion and IS addition, yet prior to the sample extraction, 1 μL of the digestion product was taken out from each real sample and the standard, and diluted with deionized water for 1000 times. Next, the diluted digestion samples were injected into an LC-MS/MS system and analyzed with a newly developed LC-MS/MS method (figure 2.2). The peak areas of the dNs of the real samples were integrated, and compared with the CT-DNA standard. The peak area of each type of dN (*i.e.*, dA, dC, dG, or dT) of the standard was assigned as 100%. The percentile of a specific dN in a real sample was determined with equation 2.2:

$$dN\% = \frac{A_N}{A_{N,Std}} \times 100\% \tag{2.2}$$

Here A_N indicates the peak area of a specific dN in the real sample; while $A_{N,Std}$ indicates the peak area of a specific dN in the digested CT-DNA standard. N can be substituted with A, C, G, or T.

Then the concentration of a certain DNA sample can be calculated more accurately with equation 2.3.

$$[DNA]_{meas.} = [DNA]_{Std} \times \frac{dA\% + dC\% + dG\% + dT\%}{4} \quad (2.3)$$

Here $[DNA]_{meas.}$ means the measured DNA concentration of a real sample; while $[DNA]_{Std.}$ indicates the DNA concentration of the CT-DNA standard (*i.e.*, 1 mg/mL in this work). In this equation, dA%, dC%, dG%, and dT% are the percentiles of dA, dC, dG, and dT, respectively.

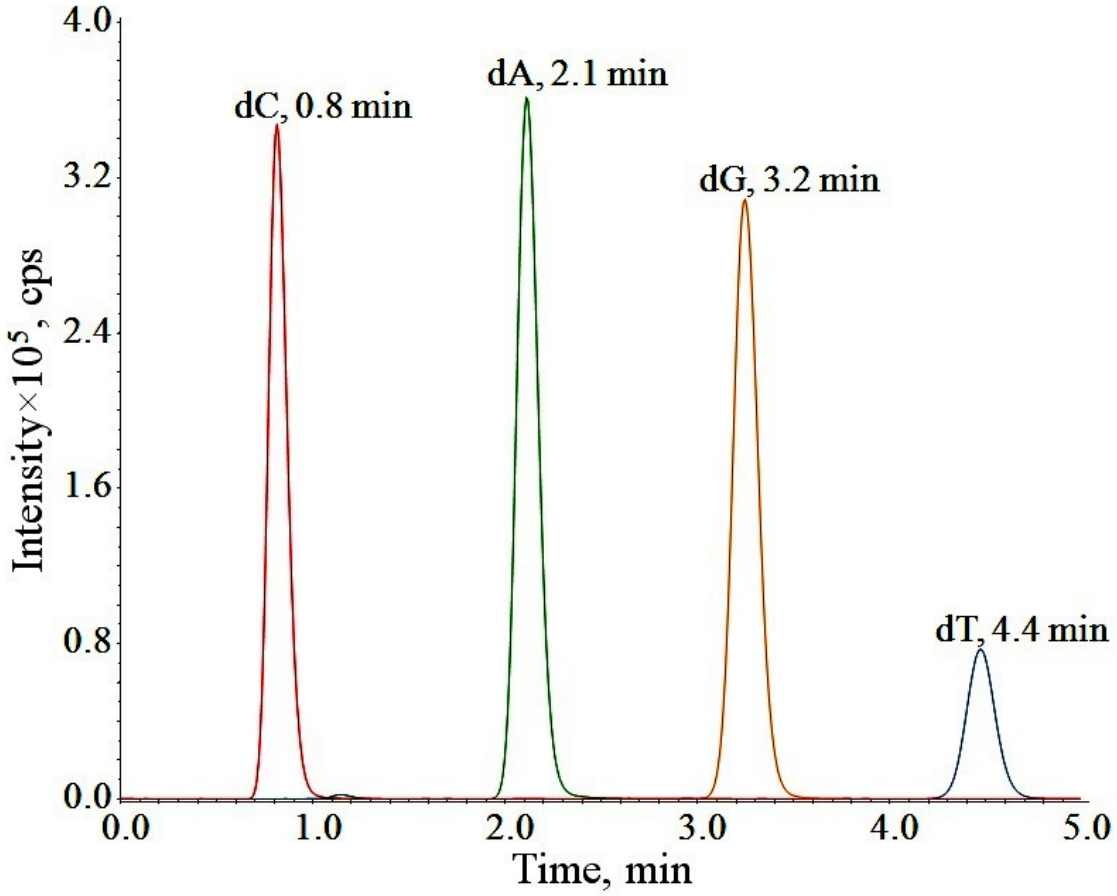

Figure 2.2, LC-MS/MS of dNs released after enzyme digestion. Column: Waters (Milford, MA) YMC-AQ® column (2.0mm×50mm, 5 μm); mobile phase: isocratic elution with 0.1% formic acid, 5% methanol, and 94.9% water (v/v/v), ambient temperature (23 ℃), at 0.3 mL/min; ESI mode: positive; MRM channels: *m/z* 252 > 136 for dA (red), *m/z* 228 > 112 for dC (green), *m/z* 268 > 152 for dG (orange), and *m/z* 243 > 127 for dT (blue); source-dependent parameters: 30 for CUR, 5000 for IS, 300 for TEM, 40 for G1, 40 for G2; compound-dependent parameters: 50 for DP, 8 for EP; MRM settings: medium for CAD, 25.0 for CE, 15.0 for CXP, 100 ms for Dewell Time.

2.4. Conclusion

In this section, a one-step enzymatic digestion protocol with a tetra-enzyme cocktail has been optimized for the release of MX-AP from DNA backbone. Comparing to the sequential digestion, this protocol possesses similar digestion efficiency, yet is much more accurate and easy to handle. The significance of each enzyme in the cocktail was evaluated, and a kinetics profile of the enzyme cocktail was obtained. Besides optimizing the digestion system, a more accurate way to calculate DNA concentrations in real samples was developed. This new method is more reliable in the concentration determination for less pure DNA samples, yet does not introduce much complication in sample processing and analysis. Our methods will not only benefit the analysis of MX-AP adducts, but also useful in the analysis of other DNA adducts with further optimizations.

2.5. References

1. E.S. Newlands, M.F. Stevens, S.R. Wedge, R.T. Wheelhouse, C. Brock. Cancer. Treat. Rev. 23 (1997) 35.

2. E. Van den Neste, S. Cardoen, F. Offner, F. Bontemps. Int. J. Oncol. 27 (2005) 1113.

3. M. Dizdaroglu. Mutat. Res. 275 (1992) 31.

4. B.M. Sutherland, P.V. Bennett, O. Sidorkina, J. Laval. Proc. Natl. Acad. Sci. USA. 97 (2000) 103.

5. M. Matsuda, H. Ogoshi. J. Biochem. 59 (1966) 230.

6. A.E. Mirsky, B. Silverman. Proc. Natl. Acad. Sci. USA. 69 (1972) 2115.

7. E. Junowicz, J.H. Spencer. Biochim. Biophys. Acta. 312 (1973) 72.

8. T. Liao. J. Biol. Chem. 250 (1975) 3831.

9. J.N. Heins, J. R. Suriano, H. Taniuchi, C.B. Anfinsen. J. Biol. Chem. 242 (1967) 1016.

10. J.J. Frank, I.A. Hawk, C.C. Levy. Biochim. Biophys. Acta. 390 (1975) 117.

11. G. Ying, L. Shi, Y. Yu, Z. Tang, J. Chen. Process Biochem. 41 (2006) 1276.

12. J.M. Falcone, H.C. Box. Biochim. Biophys. Acta. 1337 (1997) 267.

13. M. Laskowski Sr. Venom Exonuclease, The Enzymes, 3rd Ed., P. Boyer, Academic Press, NY, 1971, Vol. 4.

14. P.M. Burgers, F. Eckstein, D.H. Hunneman. J. Biol. Chem. 254 (1979) 7476.

15. G.R. Philipps, Hoppe. Seylers. Z. Physiol. Chem. 356 (1975) 1085.

16. A. Bernardi, G. Bernardi. Spleen Acid Exonuclease, The Enzymes, 3rd Ed., P. Boyer, Academic Press, NY, 1971, Vol. 4.

17. H. Weissig, A. Schildge, M.F. Hoylaerts, M. Iqbal, J.L. Millán. Biochem. J. 290 (1993) 503.

18. E.S. Harris, W.R. Bergren, L.A. Bavetta, J.W. Mehl. Proc. Soc. Exp. Biol. Med. 81 (1952) 593.

19. R. Singh, J. Sandhu, B. Kaur, T. Juren, W.P. Steward, D. Segerbäck, P.B. Farmer. Chem. Res. Toxicol. 22 (2009) 1181.

20. R.C. Le Pla, K.J. Ritchie, C.J. Henderson, C.R. Wolf, C.F. Harrington, P.B. Farmer. Chem. Res. Toxicol. 20 (2007) 1177.

21. M. Wang, N. Yu, L. Chen, P.W. Villalta, J. B. Hochalter, S.S. Hecht. Chem. Res. Toxicol. 19 (2006) 319.

22. M. Wang, G. Cheng, S.J. Sturla, Y. Shi, E.J. McIntee, P.W. Villalta, P. Upadhyaya, S.S. Hecht. Chem. Res. Toxicol. 16 (2003) 616.

23. R. Singh, F. Teichert, R.D. Verschoyle, B. Kaur, M. Vives, R.A. Sharma, W.P. Steward, A.J. Gescher, P.B. Farmer. Rapid Commun. Mass Spectrom. 23 (2009) 151.

24. K. Kawai, P.H. Chou, T. Matsuda, M. Inoue, K. Aaltonen, K. Savela, Y. Takahashi, H. Nakamura, T. Kimura, T. Watanabe, R. Sawa, K. Dobashi, Y.S. Li, H. Kasai. Chem. Res. Toxicol. 23 (2010) 630.

25. H.T. Wang, S. Zhang, Y. Hu, M.S. Tang. Chem. Res. Toxicol. 22 (2009) 511.

26. M.W. Chou, Y. Jian, L.D. Williams, Q. Xia, M. Churchwell, D.R. Doerge, P.P. Fu. Chem. Res. Toxicol. 16 (2003) 1130.

27. K. Kubo, H. Ide, S.S. Wallace, Y.W. Kow. Biochemistry. 31 (1992) 3703.

28. Y. Yamazoe, R.W. Roth, F.F. Kadlubar. Carcinogenesis. 7 (1986) 179.

29. D. Lin, K.R. Kaderlik, R.J. Turesky, D.W. Miller, J.O. Lay Jr., F.F. Kadlubar Chem. Res. Toxicol. 5 (1992) 691.

CHAPTER III

MEASUREMENT OF METHOXYAMINE (MX) ON ITS THERAPEUTIC TARGET, MX MODIFIED DNA ABASIC SITES (MX-AP), WITH LC-MS/MS

3.1. Introduction

In chemotherapy of cancers, methylating agents and anti-metabolites are often utilized because of their abilities of introducing DNA base abnormal, and thus the replication and/or repair of the cancer cell DNA can be disrupted [1, 2]. Some of the methylated bases or base analogues can be recognized and hydrolysed from DNA strand by specific DNA glycosylases [3, 4]. This enzymatic hydrolyzation process initiates an important DNA repair mechanism, BER pathways. After the removal of the abnormal

bases, AP sites are generated on the DNA strand. The non-coding, highly mutagenic AP site lesions can be recognized by AP endonuclease (APE), and then be further repaired through later steps in BER [5] (figure 3.1A). Upon complete repair, the cytotoxicity of the anti-cancer agent can be removed, and thus the drug effects will be significantly attenuated [6]. An example of BER induced drug resistance has been observed during the clinical practice with TMZ.

TMZ has been approved in glioblastoma multiforme (GBM) treatments by FDA since 2005 [7]. After been administered orally, it can be hydrolyzed spontaneously under physiological pH to its activated form, 5-(3-methyltriazen-1-yl)imidazole-4-carboxamide (MTIC), and eventually releases an active methyldiazonium cation that methylates adenine and guanine into N3-methyladenine (N3mA), N7-methylguanine (N7mG), and O^6-methylguanine (O^6mG) [8]. The high mutagenicity and cytotoxicity of these methylated bases contribute to the anti-cancer activity of the drug [9, 10]. However, the therapeutic effect of TMZ is often attenuated by drug resistance resulted from several cellular defense mechanisms: N3mA and N7mG (share over 80% of the total methylated species) can be repaired through BER [8, 10]; while O^6mG (around 5%) is often repaired by O^6-alkylguanine-DNA alkyltransferase (AGT) and DNA mis-match repair (MMR) [11, 12]. As a result, blocking drug resistance through BER can be an effective way in drug resistant reversing [6]. MX was introduced as an anti-cancer agent under this circumstance.

Being reactive to the ring-open form of the AP sites, MX was originally utilized as AP site quantification agent, and was considered as a tool in the studies of BER pathways [13]. By forming stable adducts with the AP sites, however, MX is also able to invalidate the recognition of APE toward the AP sites, and thus results a halt in the repair process [14, 15] (figure 3.1B). Since MX blocks the activity of APE by modifying AP sites chemically, instead of introducing inhibition to APE itself, it is the first drug of its kind [16]. Studies have shown that MX is able to potentiate the drug effects of at least two methylating agents [*i.e.*, TMZ and 1,3-bis-(2-chloroethyl)-1-nitrosourea (BCNU)] and one anti-metabolite (*i.e.*, fludarabine), both *in vitro* and *in vivo* [16, 14, 4]. The combined therapy of MX plus TMZ on patients with advanced solid tumors has entered into phase I clinical trial [17].

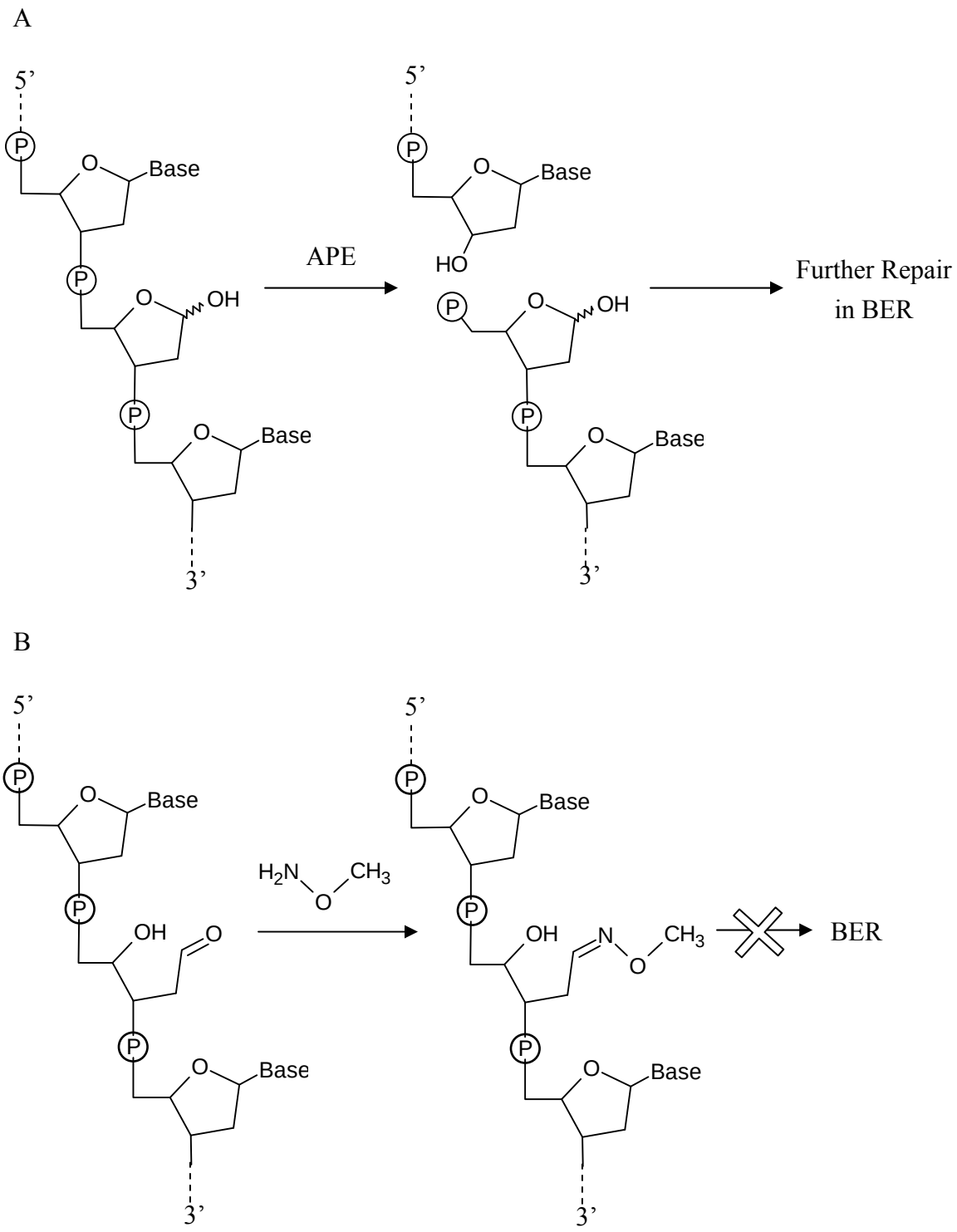

Figure 3.1, Normal AP site recognition by APE (A) and invalidated BER through AP site blockage with MX (B).

Although a LC-MS/MS method for the quantification of free MX from plasma samples has been developed by our group and has been applied to the pharmacokinetic studies of the drug [18], to evaluate the drug effect of MX, an analytical method must be developed for the analysis of MX-AP as it is the end point of drug action. In this work, we utilized a tetra-enzyme cocktail to release the MX-AP from the DNA backbone as MX-dR. The enzymatic digestion product was simply processed by protein precipitation and analyzed by a newly developed LC-MS/MS method. By utilizing MX-R as the IS, and a set of calibrators prepared by spiking DNA 11-mer with known amount of MX-AP adduct into blank CT-DNA, a calibration curve for MX-AP was established, and the method accuracy and precision were evaluated through a set of quality control calibrators. The method developed was then applied to the MX-AP analysis on cellular DNA of T98G cells treated with TMZ combined with MX. A dose-effect and a time-effect profile were obtained after the analysis. DNA was also extracted from the lymphocytes of a patient with solid tumor enrolled in the Phase I clinical study of TMZ plus MX drug combination. Analysis of the MX-AP sites with the method we developed illustrated a clear time-effect relationship in the patient. This method has already demonstrated its significance in the drug effect studies of MX, and may provide dosimetric guidelines to the future clinical trials.

3.2. Material and methods

3.2.1. Chemicals and solutions

MX·HCl, 2'-deoxyribose, ribose, ammonium formate, formic acid, isopropanol, acetonitrile, BisTris, CT-DNA, *O*-(4-Nitrobenzyl) hydroxylamine, ethanol, sodium citrate, DNase I from bovine pancreas, NP1 from *Penicillium citrinum*, bovine intestinal ALP, and Tris EDTA buffer were obtained from Sigma-Aldrich (St. Louis, MO). Triethylamine, NaH_2PO_4, NaCl, $ZnCl_2$, PBS, water saturated phenol, and chloroform were purchased from Fisher Scientific (Fair Lawn, NJ). Tris base and 10% SDS were from Bio-Rad Laboratories (Hercules, CA). DMEM medium and L-glutamine were from Mediatech (Manassas, VA). RNase and protease K were from Invitrogen (Carlsbad, CA). DNA 11-mers 5'-GCCGT-U-AGGTA-3' and 5'-AGGTAGCCGT-U-3' were synthesized by Integrated DNA Technologies (Coralville, IA). Methanol was purchased from Pharmco-AAPER (Brookfield, CT). 1,1,1,3,3,3-Hexafluoro-2-propanol was obtained from Oakwood Products (West Columbia, SC). Uracil DNA glycosylase (with 10× enzyme buffer) was from New England Biolabs (Ipswich, MA). Acetic acid was from Mallinckrodt Baker (Phillipsburg, NJ). Hydrochloric acid was from EMD Chemicals (Gibbstown, NJ). Snake venom PDE I was obtained from Worthington Biochemical Corporation (Lakewood, NJ). Fetal bovine serum was purchased from Hyclone

Laboratories (Logan, UT). TMZ was from Ochem (Des Plaines, IL). Deionized water was prepared by the Barnstead NANOpure® water purification system (Thermo Scientific, Waltham, MA, USA).

3.2.2. Synthesis of MX-dR and MX-R

MX·HCl powder was dissolved in deionized water to a concentration of 1.0 M. 2'-Deoxyribose and ribose powders were dissolved in deionized to make 1.0 M solutions, respectively. Then each concentrated solution was diluted with deionized water to a concentration of 10 mM. To synthesize MX-dR, 10 µL of MX·HCl solution (1.0 M), 10 µL of deoxyribose solution (10 mM) and 80 µL of deionized water were pipetted together into a 0.5 mL microcentrifuge tube. Then the tube was kept in 70 ℃ for 2 h. For the synthesis of MX-R, the IS, the 1 M MX·HCl solution was diluted with deionized water to 10 mM. Then, 10 µL of MX·HCl solution (10 mM), 10 µL of ribose solution (1.0 M) and 80 µL of deionized water were pipetted together into a 0.5 mL microcentrifuge tube. Then the tube was kept in 70 ℃ again for 2 h. Both reactions were stopped by 100 × dilution with deionized water. Then, the reaction products were kept in -4 ℃ till use.

3.2.3. LC-MS/MS and LC-MS instrumentations

The instrument system included a Shimadzu HPLC system (Kyoto, Japan) composed of a solvent reservoir, a degasser (DGU-20A3), a binary pump (LC-20AD), a flow controller (CBM-20A), and an autosampler (SIL-20ACHT), together with an AB SCIEX 5500 QTRAP® 5500 mass spectrometer (Foster City, CA) controlled by Analyst software (version 1.5.1).

LC-MS/MS of MX-dR and the IS

Chromatographic separation was carried out on a Thermo (West Palm Beach, FL) Hypercarb™ column (2.1×50 mm, 5 μM) at ambient temperature (23 ℃) with a flow rate of 0.4 mL/min. A two-solvent gradient, 5 mM ammonium formate (NH_4Fc, pH 3.5) (A) and 5 mM NH_4Fc (pH 3.5) in 67% methanol and 33% isopropanol (v/v) (B), was utilized for complete separation of MX-dR from the matrix interferences. At the beginning of the LC, 100% A was held for 1.0 min. Then the content of A was dropped quickly from 100% to 40% within 1.0 to 1.1 min. Next, the mobile phase was held at 40% A till 5.9 min, followed by returning to 100% A at 6.0 min. Before each run, there was an equilibration set as 5 min. The column eluent was diverted to the waste before 2.49 min, and then to the mass spectrometer between 2.50 min and 3.10 min. At 3.11 min the flow was diverted to the waste again till the end of the run.

The mass spectrometer was operated at the positive-electrospray-ionization (ESI^+) mode. It was tuned by flow injection of a mixture of MX-dR (100 ng/mL) and MX-R (100 ng/mL) in the mobile phase (60% B) at a flow rate of 0.4 mL/min. The source-

dependent parameters were as follows: curtain gas™ (CUR), 20; ionspray voltage (IS), 5500; temperature (TEM), 300; gas 1 (G1), 60.0; gas 2 (G2), 60.0. The compound-dependent parameters were as follows: Declustering Potential (DP), 50.0; Entrance Potential (EP), 8.00. Detection of MX-dR and MX-R was based on MRM with the conditions set as follows: Collision Gas (CAD), low; Collision Energy (CE), 10.0; Collision Cell Exit Potential (CXP), 11.0; Dewell Time, 100 ms. Two MRM channels: *m/z* 164 > 117, and *m/z* 180 > 102 were utilized to monitor MX-dR and MX-R, respectively.

LC-MS of the oligonucleotides

The chromatography separation of the oligonucleotides was carried out on an Xterra MSC18® column (2.0×50 mm, 3.5 μm, Waters, Milford, MA) by adjusting an existing method [19]. Isocratic separation was performed at ambient temperature (23 ℃) at a flow rate of 0.2 mL/min with a mobile phase containing 86% 200 mM 1,1,1,3,3,3-Hexafluoro-2-propanol [HFIP, adjusted to pH 7.0 with N,N,N-Triethylamine (TEA)] and 14% methanol (v/v). The column eluent was diverted to the waste before 2.00 min, and then to the mass spectrometer at 2.00 min.

Negative-electrospray-ionization (ESI^-) mode MS was operated with the source-dependent parameters as the following: CUR, 20; IS, -4500; TEM, 400; G1, 40; G2, 40. The compound-dependent parameters were as follows: DP, -100; EP, -10. DNA 11-mers

5’-GCCGT-U-AGGTA-3’ and 5’-AGGTAGCCGT-U-3’, 5’-GCCGT-AP-AGGTA-3’, as well as 5’-GCCGT-(MX-AP)-AGGTA-3’ were monitored with the Q1 M1 scan mode (selected reaction monitoring or SIR) in channel *m/z* 670.5 (M-5H), *m/z* 651.8 (M-5H), and *m/z* 657.5 (M-5H), respectively. The Dewell Time was set as 100 ms for each channel.

The DNA 11-mers were diluted with deionized water to 1 μg/mL. For each analysis, 2 μL of sample was injected onto the column.

3.2.4. Sample extraction

Briefly speaking, the samples were mixed with excessive amount of acetonitrile (20 × volumes), and vortexed for 2 min. Then, the mixtures were centrifuged at 15,000 × g at 4 ℃ for 10 min. Same volume of the supernatant as the acetonitrile added in was taken out from each sample and evaporated to dryness at 20 ℃ for 60 min in a TurboVap® LV Evaporator (Zymark, Hopkinton, MA) under a pressurized stream of nitrogen gas (10 psi). Then, the residues were reconstituted in deionized water right before LC-MS/MS analysis.

For the calibrators except for the double blank, 46.6 μL of IS spiked digestion product [including 40 μL of DNA, 2.6 μL of enzyme cocktail, and 4 μL of the IS solution

(1.00×10^4 times diluted with deionized water from the reaction product mentioned in section 3.2.2)], 932 μL of acetonitrile was added. After vortex and centrifugation, 932 μL of the supernatant was taken out and evaporated to dryness. Each residual was finally reconstituted in 39.8 μL of deionized water.

For the double blank, 45.6 μL of the digestion product [40 μL of DNA, 2.6 μL of enzyme cocktail, and 4 μL of deionized water were mixed together completely; 1 μL of the mixture was then taken out for DNA concentration normalization (section 2.3.4)], 912 μL of acetonitrile was added. After vortex and centrifugation, 912 μL of the supernatant was taken out and evaporated to dryness. The residual was finally reconstituted in 37.3 μL of deionized water.

For all the real samples, 16.5 μL of the IS spiked digestion product [15 μL of DNA, 0.98 μL of enzyme cocktail, and 1.5 μL IS solution (1.00×10^4 times diluted with deionized water from the reaction product mentioned in section 3.2.2) were mixed together completely; 1 μL of the mixture was then taken out for DNA concentration normalization (section 2.3.4)], 330 μL of acetonitrile was added. After vortex and centrifugation, 330 μL of the supernatant was taken out and evaporated to dryness. Each residual was reconstituted in 13.5 μL of deionized water before.

3.2.5. Synthesis and purification of DNA oligomer with known amount of MX-AP sites

To synthesize the DNA oligomer containing known amount of MX-AP sites, 200 μg of DNA 11-mer (with a uracil incorporated at the 6th position on each oligomer molecule) was dissolved in 92.9 μL of uracil DNA glycosylase (UDG) buffer (1 ×, pH 8.0, containing 20 mM Tris-HCl, 1 mM DTT and 0.1 mM EDTA). Then, 7.1 μL of UDG solution [5000 unit/mL enzyme in a pH 7.4 buffer solution containing 10 mM Tris-HCl, 50 mM KCl, 1 mM DTT, 0.1 mM EDTA, and 50% glycerol (v/v)] was added to remove the uracil (1.7 nmol oligomer per unit enzyme), and generate DNA 11-mer with an AP site at the 6th position (AP-oligo). The digestion system was kept in 37 ℃ water bath for 1 h with slight agitation for complete the enzymatic reaction. After the incubation, 100 μL of the resulted AP-oligo (1.00 mg/mL) was reacted with equal volume of 60 mM MX solution (dissolved in 90 mM of BisTris, pH 7.0). In order to complete the reaction between AP sites and MX, and to obtain DNA 11-mer with one MX-AP adduct at the 6th position (MX-oligo), the system was kept in 37 ℃ water bath for 2 h. The resulted MX-oligo (1.00 mg/mL) was kept at 4 ℃ before purification.

The MX-oligo obtained was purified with a solid phase extraction (SPE) procedure. Oasis® HLB cartridge (3 cc, 60 mg, Waters, Milford, MA, USA) was activated with 3 mL of acetonitrile, and then balanced with 3 mL of 0.1 M triethylammonium acetate buffer (TEAAc), pH 7.0. 100 μL of MX-oligo (1.00 mg/mL) was diluted with 900 μL of deionized water, and was added onto the SPE cartridge. After the sample had passed through, the cartridge was washed with 3 mL of 0.1 M TEAAC (pH 7.0). Finally, the MX-oligo was eluted with 2 mL of 0.1 M TEAAC (pH 11.0) in 10%

acetonitrile and 90% water (v/v) [20]. The cartridge eluent was dried on the TurboVap® LV evaporator under a pressurized stream of nitrogen gas (10 psi) at 25 ℃ for 4 h. The residue was reconstituted in 100 μL of deionized water and kept in -20 ℃ till use.

Another DNA 11-mer with a uracil incorporated at the 11th position (5'-AGGTAGCCGT-U-3') was processed exactly the same way (incubated with UDG, reacted with MX, purified with SPE, and reconstituted in deionized water to 1 mg/mL) to serve as a negative control (U-end-oligo).

3.2.6. Preparation of MX-AP DNA calibrators

MX-oligo after purification (1.00 mg/mL) was diluted with 1.00 mg/mL blank CT-DNA solution (in 5 mM BisTris, pH 7.0) for 4.00×10^3, 8.00×10^3, 1.60×10^4, 3.20×10^4, 6.40×10^4, 1.28×10^5, and 2.56×10^5 times. The resulted MX-AP DNA calibrators were 22.7, 11.4, 5.70, 2.85, 1.43, 0.715, and 0.358 MX-AP adducts/10^6 bases, respectively. Two blank samples, a single blank (1.00 mg/mL U-end-oligo diluted with 1.00 mg/mL CT-DNA for 4.00×10^3 times, with the addition of the IS solution after enzyme digestion) and a double blank (1.00 mg/mL U-end-oligo diluted with 1.00 mg/mL CT-DNA for 4.00×10^3 times, without the addition of the IS solution after enzyme digestion), were prepared at the same time. For the accuracy and precision studies, three concentrations of

MX-AP calibrators (*i.e.*, 22.7, 2.85, and 0.358 adducts/10^6 bases) were prepared in quintuplicate. The IS solution was added after the DNA hydrolysis.

3.2.7. Enzymatic release of MX-AP

An enzyme cocktail was prepared by mixing 10 μL DNase I, 15 μL NP1, 40 μL PDE I, and 0.5 μL of ALP. For each 40 μL of MX-AP DNA, 2.6 μL of the enzyme cocktail was added and mixed well with the DNA sample. The incubation was then kept at 37 ℃ for 17 h. The amount of the enzyme cocktail was adjusted proportionally to the amounts of DNA in the real samples.

3.2.8. Cell culture and treatment

T98G (a human brain fibroblast cell line) cells obtained from American Type Culture Collection (ATCC, Rockville, MD, USA) were cultured in DMEM medium supplemented with 10% (v/v) fetal bovine serum and 2 mM of L-glutamine at 37 ℃ in a humidified 5% CO_2 incubator.

In the dose-response study, each 5×10^6 cells, the dosages of TMZ were chosen as 0.750, 1.13, and 1.50 mM. At each dosage of TMZ, the concentration of MX varied as

5.00, 10.0, 15.0, 20.0, and 25.0 mM. The treatment was kept at 37 ℃ in a humidified 5% CO_2 incubator for 24 h. In the time-response study, each 5×10^6 cells were treated with 0.750 mM of TMZ plus 25.0 mM MX for 6, 12, 24, 48, and 72 h at 37 ℃ in the humidified 5% CO_2 incubator. The pre-treatment control was obtained by incubating 5×10^6 cells in the same incubator for 24 h without drug administration. The treatment was stopped by removal of culture media, and the cells were washed three times with 5 mL PBS (1×, pH 7.4). After washing, another 5 mL of PBS (1×, pH 7.4) solution was added into each culture dish. The cells were lifted by a cell scraper (Costar, Corning, NY) and transferred to a clean 15 mL centrifuge tube. Then, the cells were recovered from the suspension by centrifugation (350 × g at 4 ℃ for 10 min). After centrifugation, the cell pellets collected were stored in -20 ℃ till DNA extraction.

3.2.9. Lymphocytes separation

Peripheral blood samples were collected into heparinized Vacutainer® tubes (BD, Franklin Lakes, NJ) from the patient who had signed written informed consent at the University Hospital Case Medical Center (Cleveland, OH). At the time of blood drawing, the patient was administered with 350 mg TMZ plus 35 mg of MX. Blood was drawn at 0, 2, 4, and 24 h; and the blood samples were fractioned by Ficoll-Paque method [21]. Briefly, 10 mL heparinized blood was layered on the top of 12 mL Ficoll-Paque Plus

reagent (GE Healthcare Bio-Sciences, Piscataway, NJ, USA) in a 50 mL sterile polypropylene centrifuge tube (RNase/DNase free); then the tube was centrifuged at 4 ℃ and 300 × g for 30 min. Cells at the interface were collected and transferred into a clean 15 mL centrifuge tube, and washed twice with 10 mL PBS (1×, pH 7.4). For each wash step, the cells were gently vortexed with the PBS for 1 min, and then centrifuged down at 4 ℃ and 300 × g for 10 min. After wash, the cell pellets were frozen at -20 ℃ till DNA extraction. The time between blood sample collection and DNA extraction was within 1 month.

3.2.10. DNA extraction

For each 15 mL centrifuge tube containing the T98G cell pellet or the lymphocytes from the patient, 2 mL of TE buffer (containing 10 mM Tris and 1 mM EDTA, pH 8.0) was added. A short vortex was performed to ensure homogenous suspension. Next, 0.24 mL of 10% SDS solution was added and mixed with the cell suspension gently by inverting the centrifuge tubes slowly for several times. After complete mixing, 20 μL of RNase (20 mg/mL dissolved in deionized water) was added and was incubated with the sample at 37 ℃ for 1 h. Then, 25 μL of protease K (20 mg/mL dissolved in deionized water) was added and was incubated with the sample at 37 ℃ for another 1 h. Then, the samples were extracted twice with phenol followed by two

times extraction with chloroform. For the extraction with phenol, 2 mL of water saturated phenol was added into each tube and vortexed with the sample for 1 min. The samples were then centrifuged at 1500 × g and 4 ℃ for 30 min. Then the aqueous (upper) layer was carefully transferred to a clean 15 mL centrifuge tube. For the extraction with chloroform, the aqueous phase of each sample was transferred to a Phase Lock Gel tube (5 Prime, Gaithersburg, MD), and 2 mL of chloroform was added into the tube. Again, the samples were vortexed for 1 min, and centrifuged at 1500 × g and 4 ℃ for 15 min. After extraction with phenol and chloroform, the aqueous phase (*ca.* 2 mL) was transferred to a clean 15 mL centrifuge tube and mixed with 10 mL pre-chilled ethanol (-20 ℃). DNA was precipitated at -20 ℃ for overnight, and then recovered by centrifugation (1500 × g at 4 ℃ for 15 min). Next, the DNA pellet in each tube was dissolved in 200 μL deionized water and transferred to a 1.5 mL centrifuge tube. In each tube, 1 mL of pre-chilled ethanol (-20 ℃) was added. By inverting the tube for several times, the DNA solution was mixed with ethanol completely. Then, DNA was precipitated at -20 ℃ for 1 h. After recovered the DNA pellet through centrifugation (10000 × g at 4 ℃ for 15 min), the sample in each tube was washed with 1 mL pre-cooled 70% ethanol (4 ℃) for once, and centrifuged at 10000 × g and 4 ℃ for 5 min. The 1.5 mL centrifuge tubes containing DNA were left uncapped in a fume hood for 1 h. After drying, the DNA pellets were reconstituted with 5 mM BisTris buffer (pH 7.0) to a concentration of 1 mg/mL (based on UV absorption at 260 nm). Finally, all samples were incubated in a

boiling water bath for 15 min to remove the remaining protease K activity. The DNA samples were stored at 4 ℃ before analysis.

3.2.11. MX-AP concentration normalization

For the real samples, the concentrations of MX-AP calculated from the calibration equation were normalized according to the amount of dNs released after digestion:

After enzyme digestion and IS addition, yet prior to the sample extraction, 1 μL of the digestion product was taken out from each real sample and the double blank calibrator. Each of 1 μL the digestion product was than diluted with 1999 μL of deionized water. Next, the diluted digestion samples were injected into the LC-MS/MS system following the methods described in the legend of figure 2.2 in section 2.3.4. The percentile of a specific dN in a real sample was determined with equation 2.2.

Each sample, including the positive control, was injected and analyzed for 3 times, and the mean dN% values were obtained by taking the average of the dN% obtained from each analysis. The normalized concentration of MX-AP in each real sample was then calculated by equation 3.1:

$$[MX-AP]_{norm.} = [MX-AP]_{cal.}/[(dA\% + dC\% + dG\% + dT\%)/4] \quad (3.1)$$

Here $[MX\text{-}AP]_{cal.}$ means the calculated concentration of MX-AP obtained from the calibration equation; while $[MX\text{-}AP]_{norm.}$ indicates the normalized MX-AP concentration. Both concentrations were in the unit of adducts/10^6 bases.

3.3. Results and discussions

3.3.1. Characterization of MX-dR and the IS with mass spectrometry

Since MX-AP is bound to DNA strand, to realize the quantification, a tetra-enzyme system was utilized to release MX-AP as MX-dR (figure 3.2). By carrying out this enzymatic digestion, the quantification of MX-AP bound to DNA was converted to the quantification of the free small molecule, MX-dR. To achieve highly accurate and repeatable results, another small molecule, MX-R was synthesized as the IS. After reaction, the two post-reaction mixtures were diluted with 5 mM NH_4Fc for 100 times, respectively, and infused into the mass spectrometer by a syringe pump at a flow rate of 5 μL/min. As both MX-dR and the IS are more easily to form protonated species through ESI, ESI^+ mode was utilized. As shown in figure 3.3, MX-dR and the IS produced molecular ions at *m/z* 164 $\{[MX\text{-}dR+H]^+\}$ and *m/z* 180 $\{[MX\text{-}R+H]^+\}$, respectively. To achieve higher specificity in the quantification, the molecular ions were further dissociated with CID. From the resulted fragmentation pattern, two predominant

fragments were observed at *m/z* 117 for MX-dR and *m/z* 102 for the IS, respectively. Therefore, the mass transition pairs *m/z* 164>117 for MX-dR and *m/z* 180>102 for the IS were utilized in the quantification work with MRM mode.

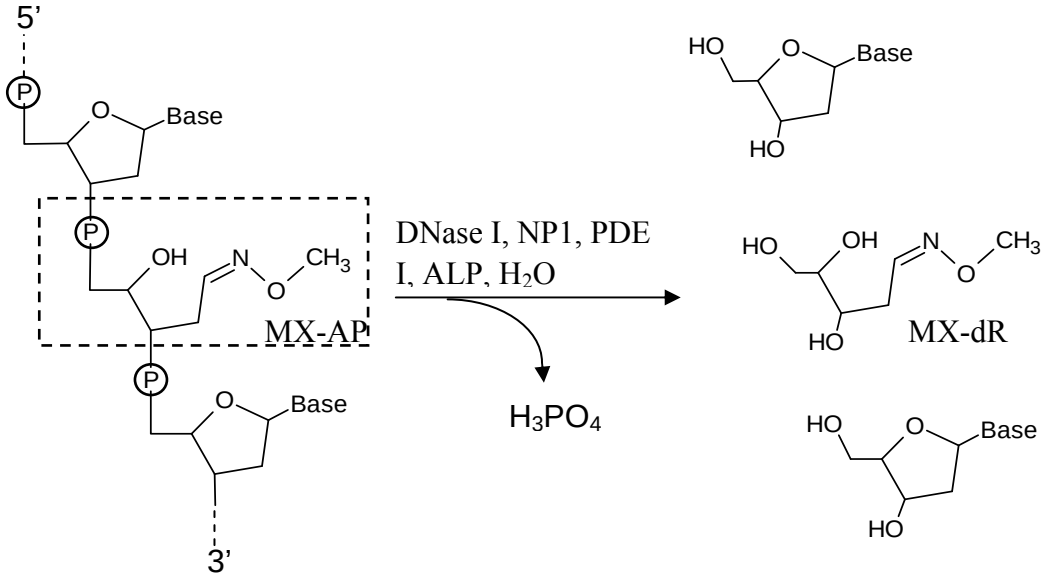

Figure 3.2, Enzymatic release of MX-AP from the DNA backbone as MX-dR.

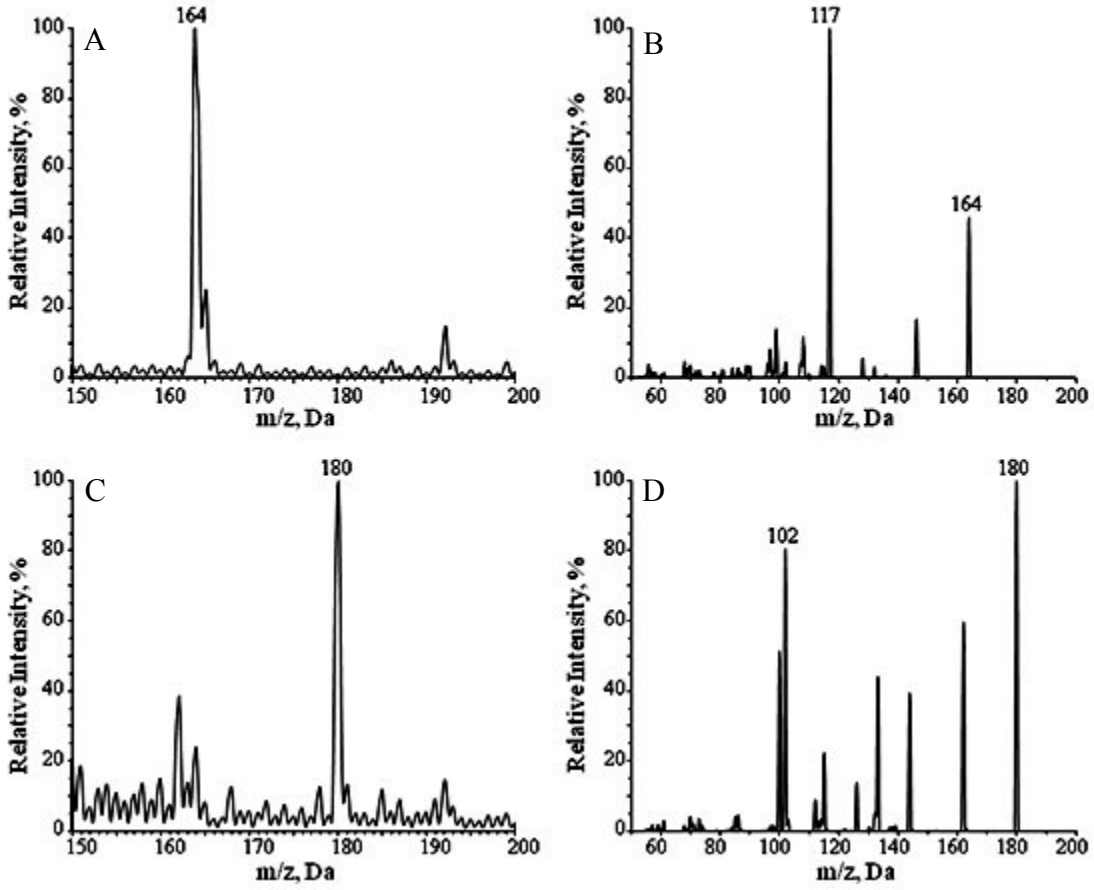

Figure 3.3, Mass spectra of MX-dR and MX-R: (A) full scan and (B) fragmentation mass spectra of MX-dR; and (C) full scan and (D) fragmentation mass spectra of MX-R.

3.3.2. Digested DNA sample extraction

As the quantification was carried out toward the MX-dR in the enzyme digested DNA samples, several major interferences were expected: buffer salts (*i.e.*, 4.69 mM BisTris, 145 μM NaCl, and 14.1 μM $ZnCl_2$), proteins (*i.e.*, protein impurities existing in the DNA samples and enzymes utilized in the digestion), and the dNs (with a total concentration of around 3 mM). To avoid signal suppression and ion source contamination caused by these interferences, the analyte must be effectively separated from these interferences through on-line and/or off-line procedures.

Two off-line extraction methods were tried in order to remove the matrix interferences:

A LLE method with a mixture of ethyl acetate and isopropanol (95:5, v/v) was tried. This method was effective in removing NaCl and $ZnCl_2$. It was also able to remove over 90% BisTris. However, it failed to eliminate the dNs effectively.

An SPE method with a cation exchange cartridge, the Oasis® MCX cartridge, was utilized under the intention of retaining all the dNs on the cartridge, yet collecting MX-dR from the cartridge pass-trough. To retain dA, dC, and dG, moderate acidic pH (*i.e.*, pH 4) had to be utilized in sample loading. Under the same pH, however, dT was

predominantly negatively charged, and could not be retained on the cartridge. Besides, extra steps were still needed to separate the analyte from the buffer salts.

As a result, the samples were simply processed by one-step acetonitrile precipitation to remove the proteins. Removal of the buffer salts and the dNs was left as a task in the LC method development.

3.3.3. LC separation of the analyte from the matrix interferences

Several columns (*i.e.*, an YMC ODS-AQ® column, an Xterra MSC18® column, and a Hypercarb™ column) were tried to obtain the separation between MX-dR and the other interference compounds.

The YMC ODS-AQ® column was tried due to its capability of retaining highly polar compounds, and its compatibility with highly aqueous mobile phases. However, even when the percentage of the organic component (*i.e.*, methanol) was dropped below 2%, no significant retention was observed for MX-dR.

As MX-AP adduct can also be converted to MX-deoxyribose 5'-phosphate (MX-dRp) in the enzymatic releasing of MX-AP through eliminating ALP from the enzyme cocktail, ion-pairing chromatography with TEA was considered. In this test, the Xterra MSC18® column was utilized. By adjust the pH and the organic percentage of the mobile

phase, MX-dRp could be retained on the column for up to 3 column volumes without causing significant tailing. However, all the 2'-deoxyribonucleotide monophosphates (dNMPs) released after enzyme cutting could not be separated from the analyte effectively.

In the work of Antonio *et al.*, several sugar and sugar phosphates were separated on a porous graphitic carbon (PGC) column, the Hypercarb^{TM} column [22]. Because the graphite surface possesses a large amount of delocalized π-electrons, it is easy to induce electronic interaction with the analytes carrying polarizable or polarized groups [23]. And thus, the columns can provide strong retention to highly polar compounds. Another advantage of the PGC columns lies in their pH stability: they are stable throughout the pH range.

As the structure of MX-dR is similar to those of the sugars, separation between the analyte and the matrix interferences was tried on this column. Isocratic elusion with a mixture of NH_4Fc and organic solvents (*i.e.*, methanol, acetonitrile, isopropanol, methanol/acetonitrile, or methanol/isopropanol) was able to retain MX-dR for at least 2 column volumes and achieve single symmetrical peak at the same time. Some of the conditions were also able to separate the analyte effectively from all the dNs and the inorganic salts. However, the separation between BisTris and MX-dR was always not enough due to the column's slightly retention to BisTris. Better separation between MX-dR and BisTris can be achieved through utilizing lower percentage of weaker organic

solvents, such as methanol, but the peak of MX-dR started to split. Besides, the retention times of the dNs were increased significantly (over 60 min for dA and dG). Based on these reasons, a gradient elusion with the conditions described in section 3.2.3 was finally adopted. With this LC method, MX-dR was able to be retained on the column for 2.8 min, while all the dNs were eluted out after 3.2 min (figure 3.4). The BisTris was eluted out at 0.6 min. By applying the same LC condition, the IS was eluted out at 2.7 min.

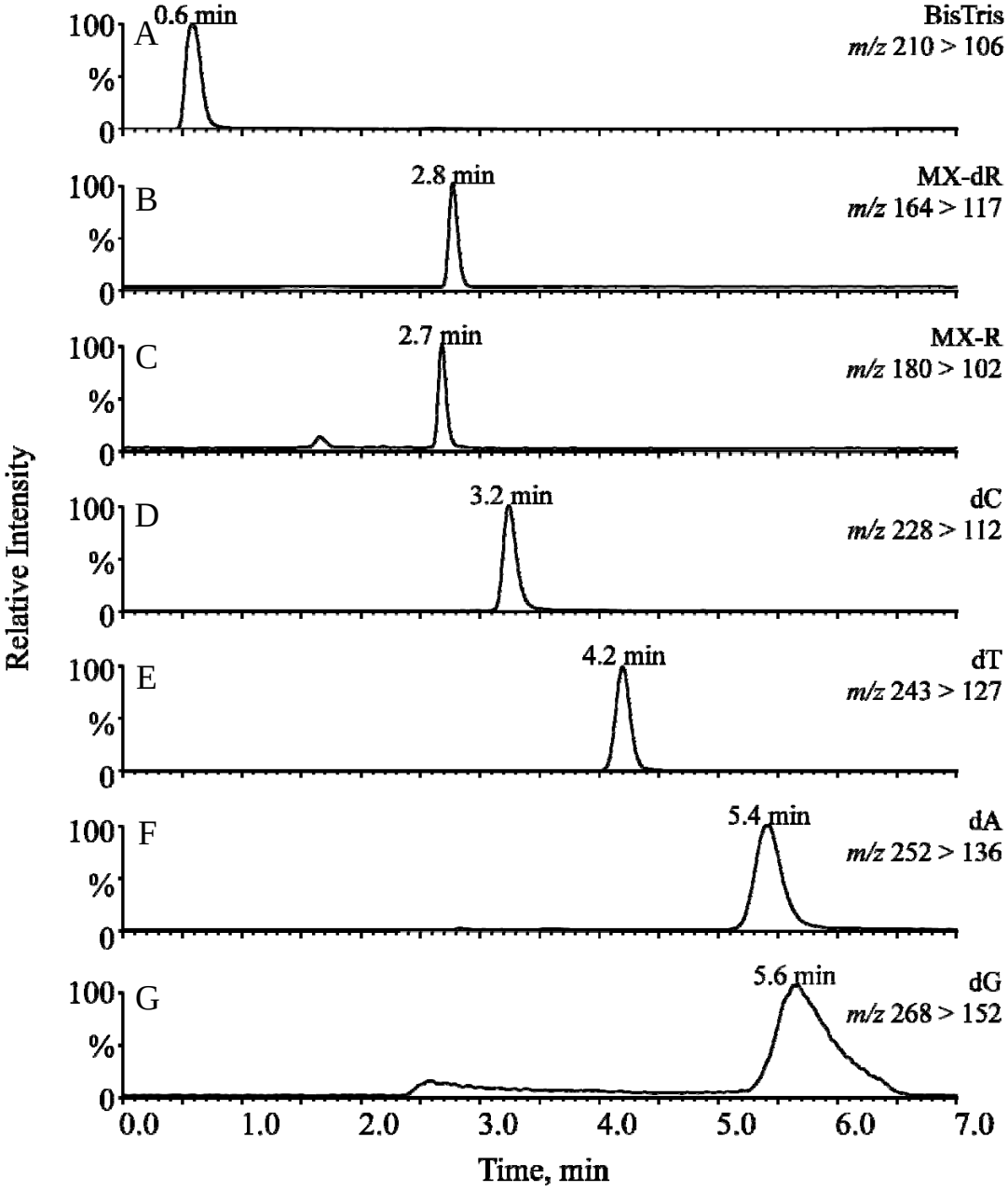

Figure 3.4. Representative MRM chromatograms of MX-dR, MX-R (IS), and other matrix interferences. (A) BisTris (*m/z* 210 > 106), (B) MX-dR (*m/z* 164 > 117), (C) MX-R (*m/z* 180 > 102), (D) dC (*m/z* 228 > 112), (E) dT (*m/z* 243 > 127), (F) dA (*m/z* 252 > 136), and (G) dG (*m/z* 268 > 152).

3.3.4. MX-AP DNA standard preparation

Since the quantification of MX-AP was realized through quantification of MX-dR released after enzyme digestion, DNA spiked with synthesized MX-dR would not be reliable in accurate quantification due to its invalidity in reflecting the digestion efficiency. Neither would the MX-AP DNA synthesized according to the protocol described in section 2.2.2 be reliable standards due to the uncertain amount of MX-AP sites it carries from batch to batch. Based on these considerations, a single strand DNA 11-mer with one MX-AP adduct located in the middle [*i.e.*, 5'-GCCGT-(MX-AP)-AGGTA, the MX-oligo] was synthesized by modifying an existing protocol for AP-oligo synthesis [24]. Spiking the MX-oligo into blank CT-DNA resulted MX-AP DNA calibrators carrying all the necessary information required by the accurate quantification.

To monitor the synthesis process of MX-oligo, the starting material and product of each step of reaction were analyzed with the LC-MS method described in section 3.2.3 (figure 3.5). As the remaining reactant was less than 1% of the original amount after each step of reaction, both steps were considered as complete. The U-mid-oligo was converted to equal amount of MX-oligo.

To avoid high quantification background caused by the reaction between the excessive MX in the synthesis product and the AP sites generated through spontaneous hydrolysis during the enzyme digestion, the MX-oligo was purified on an Oasis® HLB

SPE cartridge with a protocol adjusted from a published method [20]. By comparing the peak area of MX-oligo from the reaction product before and after purification, the recovery was determined as 94.2±1.6%.

As UDG is unable to remove uracil from the end of a DNA strand, UDG digestion on the U-end-oligo is not effective in producing AP-oligo (figure 3.5). Further reaction with MX was not able to generate MX-oligo efficiently as well. Thus, the U-end-oligo was processed parallel with the U-mid-oligo as a negative control of the studies. In another word, the U-mid-oligo is able to reflect any background caused by excessive MX remaining in the purified oligomer products, or the background caused by MX-AP adducts formed from the reaction between MX and the AP sites generated spontaneously during the oligomer synthesis.

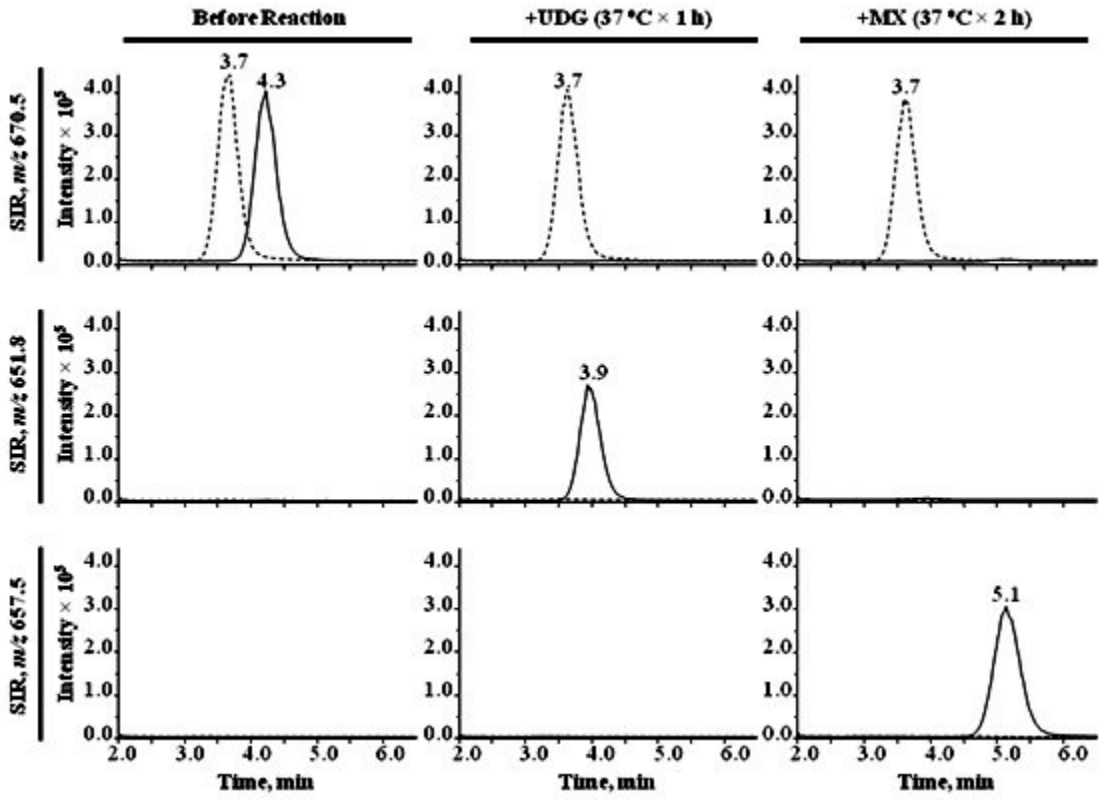

Figure 3.5, MX-oligo synthesis. Solid lines: the chromatograms obtained from the experiments with U-mid-oligo as the starting material; dash lines: the chromatograms obtained from the experiments with U-end-oligo as the starting material.

3.3.5. Method performance

To evaluate the performance of the developed methods in quantitative studies, a calibration curve was established with a linear calibration range of 0.358- 22.7 MX-AP adducts/10^6 bases. The curve was weighted by the reciprocal of MX-AP concentration, 1/x. The calibration equation has been shown in table 3.1, and the linearity, represented by correlation coefficient R^2, was 0.999 ± 0.000. The accuracy and inter-assay precision of each point on the calibration curve ranged from 93.6-115% and 0.73-4.53%, respectively (table 3.1).

The accuracy, intra-assay precision, and inter-assay precision of the analysis were determined through the quintuplicate calibrators at three concentration levels (low, medium, and high). All data were summarized in table 3.2. The accuracy ranged from 86.7- 98.2%; while the intra- and inter- assay precision varied from 1.02-5.25% and 3.14-3.78%, respectively.

Here the accuracy was calculated by the relative deviation between a calculated concentration and the nominal concentration; while the precision was calculated by percent standard deviation.

Table 3.1, Calibration equation of MX-AP.

Actual [MX-AP], adducts/10^6 bases	**Measured [MX-AP], adducts/10^6 bases**	**Accuracy (%)**	**Inter-assay Precision (%)**
0.358	0.409	114	4.53
0.715	0.664	92.9	3.32
1.43	1.37	95.8	0.730
2.85	2.73	95.8	2.78
5.70	5.58	97.9	2.84
11.4	11.2	98.3	2.36
22.7	23.1	102	1.30

Calibration equation: $Y = (0.26 \pm 0.01)\ X + (0.024 \pm 0.005)$, $R^2 = 0.999\ (\pm 0.000)$

Each datum point was based on three separate measurements toward the same set of samples.

Table 3.2, Accuracy, intra- and inter-assay precision.

	Low	**Medium**	**High**
Accuracy (%) n=5	86.7	96.5	98.2
Intra-assay Precision (%) n=5	5.25	1.02	3.97
Inter-assay Precision (%) n=3	3.78	3.14	3.60

The concentrations of MX-AP in the calibrators of low, medium and high concentrations were 0.358, 2.85, and 22.7 adducts/10^6 bases respectively.

3.3.6. Analysis of TMZ plus MX treated T98G cells

In the cellular DNA analysis in this section and section 3.3.7, the MX-AP concentration of every real sample was normalized with the method described in section 2.12. The reason of carrying out this normalization procedure lies in its advantages in more accurate quantification.

T98G cells treated with TMZ plus MX with different dosages and time spans were analyzed with the developed methods. A dose-effect profile (figure 3.6 A) and a time-effect profile (figure 3.6 B) were obtained afterward.

From the dose-effect profile, a clear relationship between the dosage of TMZ plus MX and the concentration of MX-AP can be observed. For each dosage level of TMZ, the concentration of MX-AP was elevated with the increase of the MX dosage. Meanwhile, when the dosage of TMZ was increased, the profile of response was lifted systematically. These results are consistent with our hypothesis: higher concentration of MX blocks more AP sites; while higher concentration of TMZ generates more AP sites systematically.

From the time-effect profile, when the treatment time increased from 6 h to longer, the concentration of MX-AP decreased slightly at the beginning, and then reaches a relatively steady state after 24 h treatment.

3.3.7. Analysis DNA samples from TMZ plus MX treated patient

The DNA samples from the patient with solid tumor enrolling in the phase I clinical trial of TMZ plus MX drug combination were analyzed. The time-response profile has been illustrated in figure 3.6 C. Determined from the profile, the concentration of MX-AP quickly reaches to the maximum after 4 h treatment, and then decreased gradually below 0.500 MX-AP adducts/10^6 bases after 24 h. The quick response of the patient to the treatment was consistent with our *in vitro* result. The clearance rate of MX-AP adducts, however, was much higher in the patient comparing to the cultured cells. The reason for the difference is still under investigation.

In fact, DNA samples from 4 patient enrolled in the phase I clinical studies were analyzed with our method, and only this one showed detectable signals for MX-AP. The PK profile of the patient indicated a significantly lower blood concentration of free MX. This may indicate extremely high MX incorporation into the patient's DNA. However, during the drug effect analysis, the amounts of MX-AP detected from the real samples were much lower comparing to the expectation.

Under physiological conditions, DNA bases can be dissociated from the DNA strand through spontaneous hydrolysis at rate of 2 bases/10^6 bases in every 24 h. Under the treatment of TMZ, although the amount of AP site generated after treatment has not been evaluated, it should be much higher than the AP sites generated by spontaneous

hydrolysis. Assume that addition of MX will lead to 1 MX-AP adduct/10^6 bases after 24 h treatment; at the same time, the white blood cell count in of the patient is 5×10^6 cells/mL blood. As the blood drawn from each time point was around 5 mL and the extracted DNA samples were typically dissolved in 15 μL of BisTris buffer before digestion, a calculation on the total amount of MX-AP adduct in the patient DNA samples can be roughly estimated as the following:

$$[MX-AP], mole/L$$

$$= 5mL \times (5\times10^6\ cell/mL) \times (6\times10^9\ bases/cell) \times (1$$

$$\times 10^{-6}\ MX-AP/base) \div (6.02\times10^{23}\ MX-AP/mole) \div (1.5\times10^{-5}\ L) = 16.6\ nM$$

Since the total concentration of the dNs in a digested DNA sample is around 3.2 mM, if convert the detection limit of MX-AP from standards to mole concentration:

$$[MX-AP], mole/L = (0.358\times10^{-6}\ MX-AP/base) \times 3.2\ mM = 1.15\ nM$$

Based on the calculation, the MX-AP signal should be detectable in the patient DNA. However, due to the patients enrolled in the clinical trial were with solid tumor, the white blood cell count in these patient may be much lower than healthy donors. Meanwhile, as the cellular DNA was extracted in a relatively inefficient way, the recovery of the DNA may well below 100%. Last but not the least, the DNA extracted from the real samples can be easily contaminated with histon, SDS, and protease K. All three kinds of impurities may greatly inhibit the releasing efficiency of the enzyme

cocktail on the MX-AP adducts. In another word, before applying the developed method into the analysis of patient DNA samples, further optimizations must be carried out. The optimization can be done in two aspects. First, the DNA extraction and purification method can be further optimized. DNA extraction kit can be utilized for higher recovery and purity, as well as more reproducible results from sample to sample. Second, the enzyme digestion conditions can be further optimized. If necessary, different enzymatic system can be experimented.

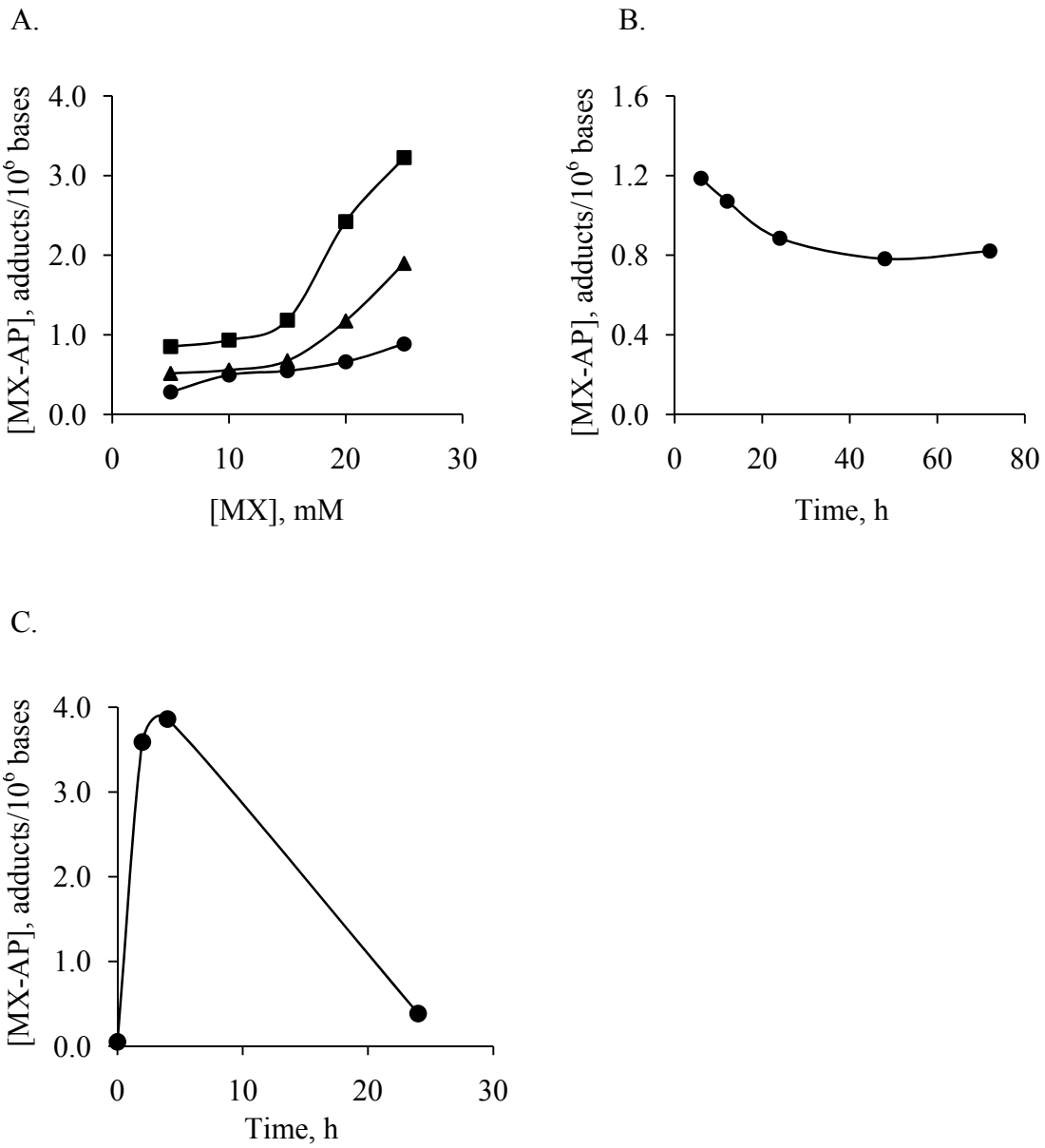

Figure 3.6, MX drug effect studies. (A) The dose-effect profile obtained from TMZ plus MX treated T98G cells: (■) 1.50 mM TMZ; (▲) 1.13 mM TMZ; (●) 0.750 mM TMZ. (B) The time-effect profile obtained from TMZ (0.750 mM) plus MX (25 mM) treated T98G cells. (C) The time-effect profile obtained from the clinical patient.

3.4. Conclusion

A tetra-enzyme cocktail containing DNase I, NP1, PDE I and ALP has been utilized for the quantitative releasing of MX-AP from the DNA backbone as MX-dR. A protein precipitation procedure was utilized in the sample preparation to remove protein interferences in the sample matrix. LC separation was realized on a Hypercarb^{TM} column for further separation of MX-dR and the IS from all the other interferences existing in the sample matrix. The MX-AP calibrators were prepared by spiking DNA 11-mers with one MX-AP site on each 11-mer into blank CT-DNA. A calibration curve ranged from 0.358-22.7 MX-AP adducts/10^6 bases were established, and the accuracy and precision were evaluated through a set of quality control calibrators. The feasibility of the method was tested by drug effect studies both *in vitro* (*i.e.*, with the TMZ plus MX treated T98G cells) and *in vivo* (*i.e.*, with the lymphocytes of the clinical patient treated with TMZ plus MX in a phase I clinical trial). The method we developed provided direct information on drug effect of MX, and thus will assist in providing dosimetric guidance in future clinical trials.

3.5. References

1. P.D. Lawley, D.H. Phillips. Mut. Res. 355 (1996) 13.

2. E. Van den Neste, S. Cardoen, F. Offner, F. Bontemps. Int. J. Oncol. 27 (2005) 1113.

3. J.W. Cardinal, G.P. Margison, K.J. Mynett, A.P. Yates, D.P. Cameron, R.H. Elder. Mol. Cell Biol. 21 (2001) 5605.

4. A.D. Bulgar, M. Snell, J.R. Donze, E.B. Kirkland, L. Li, S. Yang, Y. Xu, S.L. Gerson, L. Liu. Leukemia. 24 (2010) 1795.

5. E. Seeberg, L. Eide, M. Bjørås. Trends Biochem. Sci. 20 (1995) 391.

6. M.R. Middleton, G.P. Margison. Lancet Oncol. 4 (2003) 37.

7. National Cancer Institute, Cancer Drug Information, FDA Approval for Temozolomide, 2005, available at http://www.cancer.gov/cancertopics/druginfo/fda-temozolomide/.

8. E.S. Newlands, M.F. Stevens, S.R. Wedge, R.T. Wheelhouse, C. Brock. Cancer Treat Rev. 23 (1997) 35.

9. G. Mitra, G.T. Pauly, R. Kumar, G.K. Pei, S.H. Hughes, R.C. Moschel, M. Barbacid. Proc. Natl. Acad. Sci. USA. 86 (1989) 8650.

10. G. Dianov, T. Lindahl. Curr. Biol. 4 (1994) 1069.

11. S.R. Wedge, J.K. Porteus, B.L. May, E.S. Newlands. Br. J. Cancer. 73 (1996) 482.

12. P. Karran, P. Macpherson, S. Ceccotti, E. Dogliotti, S. Griffin, M. Bignami. J. Biol. Chem. 268 (1993) 15878.

13. M. Liuzzi, M. Talpaert-Borlé. J. Biol. Chem. 260 (1985) 5252.

14. L. Liu, P. Taverna, C.M. Whitacre, S. Chatterjee, S.L. Gerson. Clin. Cancer Res. 5 (1999) 2908.

15. L. Liu, Y. Nakatsuru, S.L. Gerson. Clin. Cancer Res. 8 (2002) 2985.

16. L. Liu, L. Yan, J.R. Donze, S.L. Gerson. Mol. Cancer Ther. 2 (2003) 1061.

17. National Institute of Health, Methoxyamine and Temozolomide in Treating Patients with Advanced Solid Tumors, 2009, available at http://clinicaltrials.gov/ct2/show/NCT00892385.

18. S. Yang, L. Liu, S.L. Gerson, Y. Xu. J. Chromatogr. B. 795 (2003) 295.

19. A. Apffel, J.A. Chakel, S. Fischer, K. Lichtenwalter, W.S. Hancock. J. Chromatogr. A. 777 (1997) 3.

20. M. Gilar, E.S.P. Bouvier. J. Chromatogr. A. 890 (2000) 167.

21. E. de Rock, N. Taylor. J. Immunol. Methods. 17 (1977) 373.

22. C. Antonio, T. Larson, A. Gilday, I. Graham, E. Bergström, J. Thomas-Oates. J. Chromatogr. A. 1172 (2007) 170.

23. P. Ross, J.H. Knox. Adv. Chromatogr. 37 (1997) 121.

24. K.P. Roberts, J.A. Sobrino, J. Payton, L.B. Mason, R.J. Turesky. Chem. Res. Toxicol. 19 (2006) 300.

CHAPTER IV

DRUG EFFECT ANALYSIS OF FLUDARABINE (F-ARA-A) BY MEASURING THE DRUG INCORPORATION IN DNA WITH LC-MS/MS

4.1. Introduction

Fludarabine (9-β-D-arabino-furanosyl-2-fluoradenine or F-ara-A) is an adenosine analogue mainly utilized in the treatment of hematological malignencies, such as non-Hodgkin's lymphoma, B-cell chronic lymphocytic leukemia (CLL) and acute myeloid leukemia (AML) [1-3]. The monophosphorylated F-ara-A (9-β-D-arabino-furanosyl-2-fluoradenine monophosphate, or F-ara-AMP) is the major form of the drug utilized in clinical purposes due to its improved solubility, and thus bioavailability in aqueous

environment [4]. The clinical application of F-ara-AMP has been approved by FDA, and the drug is now commercially available under the brand name of Fludara® (used for intravenous injection) or Oforta® (used for oral administration).

A brief functioning mechanism of F-ara-AMP after administration can be summarized as the following: first, the drug is dephosphorylated by serum phosphatase to F-ara-A shortly after being administrated intravenously; then, the dephosphorylated drug can be transported into the cells through nucleoside-specific membrane transport carrier (NT); after uptake, F-ara-A is first re-phosphorylated by deoxycytidine kinase to F-ara-AMP and gets activated; next, F-ara-AMP is further phosphorylated, under the successive actions of nucleoside monophosphate- and diphosphate-kinases, to F-ara-ADP and then F-ara-ATP; finally, the triphosphorylated form of the drug can be incorporated into the DNA strand, halting DNA strand elongation through inhibiting multi enzymes involved in DNA synthesis; meanwhile, both the di- and tri-phosphorylated forms of the drug can inhibit ribonucleotide reductase (RR), causing deoxyribonucleotide poor imbalance and affecting DNA repair and synthesis [5,6].

As an FDA approved chemotherapy agent, the pharmacology properties of F-ara-A have been studied intensively during the past years. However, the drug effect of F-ara-A has never been quantified on a molecular level. Besides, some details about the drug's functioning mechanisms are still not fully understood. To be more specific, although the drug has been generally accepted as a chain terminator due to its inhibition on enzymes involved in DNA synthesis, argument on F-ara-A's incorporation into the middle of the

DNA strands has also been raised. Quantifying F-ara-A incorporated in cellular DNA is not only meaningful in providing drug effect data on the molecular level, but may also be essential in drug mechanism elucidation. Once the amount of the free 3'-end of DNA is quantified, by comparing the data with the quantity of the total incorporated F-ara-A, the number of F-ara-A incorporated in the middle of the strand can be determined.

In this work, the incorporated drug was first released by the tera-enzyme system described in Chapter II from the DNA backbone as free F-ara-A. Then, an LC-MS/MS method was developed in order to analyze the released F-ara-A from the digestion matrix. An *in vitro* drug effect study was carried out afterward on HL60 cells. Cellular DNA extracted from HL60 cells treated with different dosage of F-ara-AMP was analyzed, and a semi-quantitative dose-effect profile was established with the unvalidated method.

4.2. Material and methods

4.2.1. Chemicals and solutions

Formic acid, acetonitrile, BisTris, deoxyribonuclease I from bovine pancreas, nuclease P1from *Penicillium citrinum*, bovine alkaline phosphatase, and Tris EDTA buffer were obtained from Sigma-Aldrich (St. Louis, MO). NaCl, $ZnCl_2$, PBS, water saturated phenol, and chloroform were purchased from Fisher Scientific (Fair Lawn, NJ).

The 10% SDS were from Bio-Rad Laboratories (Hercules, CA). RPMI 1640 medium and L-glutamine were from Mediatech (Manassas, VA). RNase and protease K were from Invitrogen (Carlsbad, CA). Methanol was purchased from Pharmco-AAPER (Brookfield, CT). Snake venom Phosphodiesterase I was obtained from Worthington Biochemical Corporation (Lakewood, NJ). Fetal bovine serum was purchased from Hyclone Laboratories (Logan, UT). Fludarabine 5'-monophosphate (F-ara-AMP) was from Ochem (Des Plaines, IL). Deionized water was prepared by the Barnstead NANOpure® water purification system (Thermo Scientific, Waltham, MA, USA).

4.2.2. Preparation of F-ara-A

F-ara-AMP stock solution (25 mg/mL in 1×PBS) was diluted with 5 mM BisTris (pH 7.0) to 3.2 mM. 1 mL of this diluted solution was mixed with 0.5 μL of ALP (12.5 units) at 37 ℃ for 6 h. The reaction was stopped by addition of equal volume of acetonitrile. The reaction product was kept at 4 ℃ till use.

4.2.3. LC-MS/MS instrumentation

The instrument system included a Shimadzu HPLC system (Kyoto, Japan) composed of a solvent reservoir, a degasser (DGU-20A3), a binary pump (LC-20AD), a

flow controller (CBM-20A), and an autosampler (SIL-20ACHT), together with an AB SCIEX 5500 QTRAP® 5500 mass spectrometer (Foster City, CA) controlled by Analyst software (version 1.5.1).

For the LC-MS/MS of F-ara-A, a Waters (Milford, MA) YMC-AQ® column (2.0mm×50mm, 5 μm) was utilized. An isocratic elution with a mobile phase containing 0.1% formic acid, 14.5% methanol, and 85.4% water (v/v/v) was utilized at ambient temperature (23 ℃) at 0.2 m/min. The column eluent was diverted to the mass spectrometer after 2.5 min. The ESI-MS was operated under positive-electrospray-ionization (ESI^+) mode. The source-dependent parameters were as follows: CUR, 40; IS, 5000; TEM, 300; G1, 40; G2, 40. The compound-dependent parameters were as follows: DP, 50; EP, 5. Detection of the F-ara-A was achieved on MRM with the mass transition of 286 > 154 *m/z*. The related MRM conditions were set as follows: CAD, medium; CE, 30.0; CXP, 13.0; Dewell Time, 100 ms.

4.2.4. Cell culture and treatment

HL60 (a human AML cell line) cells obtained from ATCC (Rockville, MD, USA) were cultured in RPMI 1640 medium supplemented with 10% (v/v) fetal bovine serum and 2 mM of L-glutamine at 37 ℃ in a humidified 5% CO_2 incubator.

For each 5×10^6 cells, the dosages of F-ara-AMP added into the culture media were 0.0, 5.0, 10, 20, or 40 μM. Cells were treated for 24 h at 37 ℃ in a humidified 5% CO_2 incubator. The treatment was stopped by removal of culture media through centrifugation at 350 × g at 4 ℃ for 10 min, and the cells were washed three times with 5 mL PBS (1×, pH 7.4). For each wash step, the cells were resuspended in PBS, and then centrifuged down at 350 × g at 4 ℃ for 10 min. After centrifugation, the cell pellets collected were stored in -20 ℃ till DNA extraction.

4.2.5. Cellular DNA extraction

For each 15 mL centrifuge tube containing the HL60 cell pellet, 2 mL of TE buffer (containing 10 mM Tris and 1 mM EDTA, pH 8.0) was added. A short vortex was performed to ensure homogenous suspension. Next, 0.24 mL of 10% SDS solution was added and mixed with the cell suspension gently by inverting the centrifuge tubes slowly for several times. After complete mixing, 20 μL of RNase (20 mg/mL dissolved in deionized water) was added and was incubated with the sample at 37 ℃ for 1 h. Then, 25 μL of protease K (20 mg/mL dissolved in deionized water) was added and was incubated with the sample at 37 ℃ for another 1 h. Then, the samples were extracted twice with phenol followed by two times extraction with chloroform. For the extraction with phenol, 2 mL of water saturated phenol was added into each tube and vortexed with the sample

for 1 min. The samples were then centrifuged at 1500 × g and 4 ℃ for 30 min. Then the aqueous (upper) layer was carefully transferred to a clean 15 mL centrifuge tube. For the extraction with chloroform, the aqueous phase of each sample was transferred to a Phase Lock Gel tube (5 Prime, Gaithersburg, MD), and 2 mL of chloroform was added into the tube. Again, the samples were vortexed for 1 min, and centrifuged at 1500 × g and 4 ℃ for 15 min. After extraction with phenol and chloroform, the aqueous phase (*ca.* 2 mL) was transferred to a clean 15 mL centrifuge tube and mixed with 10 mL pre-chilled ethanol (-20 ℃). DNA was precipitated at -20 ℃ for overnight, and then recovered by centrifugation (1500 × g at 4 ℃ for 15 min). Next, the DNA pellet in each tube was dissolved in 200 μL deionized water and transferred to a 1.5 mL centrifuge tube. In each tube, 1 mL of pre-chilled ethanol (-20 ℃) was added. By inverting the tube for several times, the DNA solution was mixed with ethanol completely. Then, DNA was precipitated at -20 ℃ for 1 h. After recovered the DNA pellet through centrifugation (10000 × g at 4 ℃ for 15 min), the sample in each tube was washed with 1 mL pre-cooled 70% ethanol (4 ℃) for once, and centrifuged at 10000 × g and 4 ℃ for 5 min. The 1.5 mL centrifuge tubes containing DNA were left uncapped in a fume hood for 1 h. After drying, the DNA pellets were reconstituted with 5 mM BisTris buffer (pH 7.0) to a concentration of 0.5 mg/mL (based on UV absorption at 260 nm). Finally, all samples were incubated in a boiling water bath for 15 min to remove the remaining protease K activity. The DNA samples were stored at 4 ℃ before analysis.

4.2.6. Enzymatic hydrolysis of DNA

The enzyme working solutions were prepared as those described in section 2.2.3. An enzyme cocktail was prepared by mixing 10 μL DNase I, 15 μL NP1, 40 μL PDE I, and 0.5 μL of ALP together. For each 40 μL of DNA sample, 2.6 μL of the enzyme cocktail was added and mixed well with the DNA sample. The incubation was then kept at 37 ℃ for 17 h.

4.3. Results

4.3.1. MS characterization of F-ara-A

The F-ara-A obtained from ALP digested F-ara-AMP (section 4.2.2) was diluted with the mobile phase containing 0.1% formic acid, 14.5% methanol, and 85.4% water (v/v/v), and then infused into the mass spectrometer by a syringe pump at a flow rate of 5 μL/min. As F-ara-A tends to be protonized under the pH of the mobile phase, ESI^+ mode was utilized. As shown in figure 4.1, F-ara-A produced molecular ions at *m/z* 286 {$[F\text{-}ara\text{-}A+H]^+$}. To achieve higher specificity in the quantification, the molecular ions were further dissociated with CID. From the resulted fragmentation pattern, a predominant

fragment was observed at *m/z* 154. Thus the mass transition 286 > 154 has been utilized in the compound monitoring.

4.3.2. LC method development

As it has occurred in the analysis of MX-dR, after enzyme digestion, large amount of dNs were released. Together with the interferences caused by the buffer salts existing in the digestion system, it is necessary to develop a method, so that the analyte, F-ara-A, can be separated from the matrix interferences. With the method we developed, we were able to retain F-ara-A on the column for 2.9 min (figure 4.2 B). All the buffer salts were not retained to the column under the LC conditions we developed, and were eluted out before 1.0 min. With the same condition, BisTris, dC, dA, dG, and dT were eluted out before 2.5 min (figure 4.2 A).

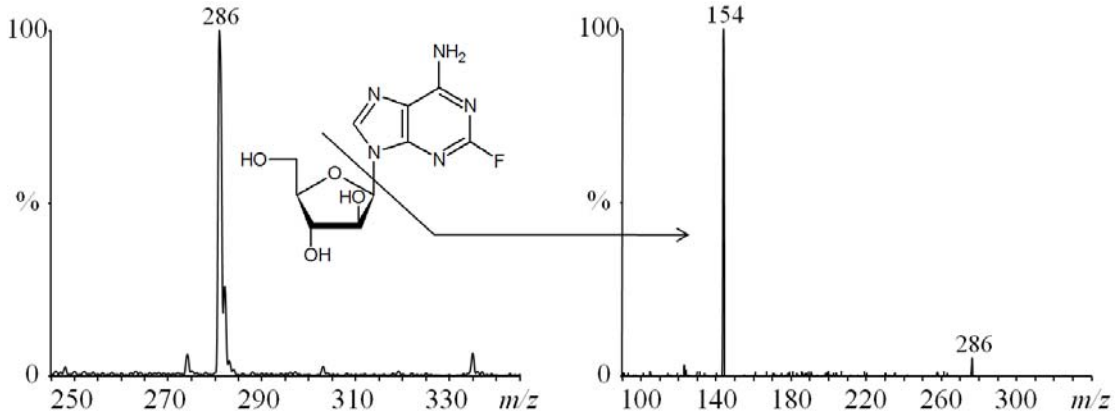

Figure 4.1, Mass spectra of F-ara-A. (A) Full scan spectrum; (B) fragmentation spectrum of F-ara-A after CID.

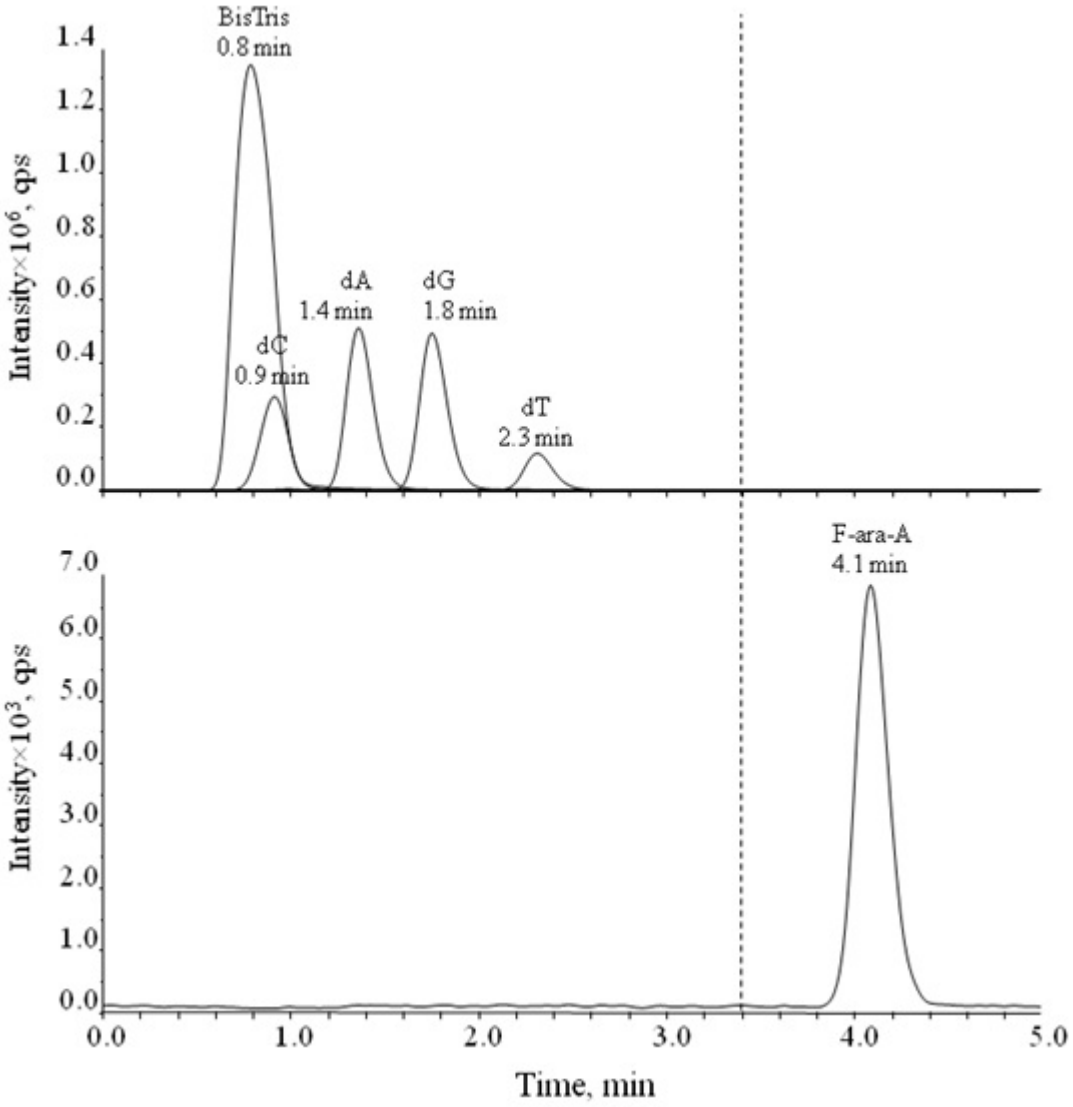

Figure 4.2, Representative MRM chromatograms of F-ara-A (B) and other matrix interferences (A).

4.3.3. Drug effect analysis of F-ara-A on HL60 cells

In the HL60 cellular DNA analysis, the peak area of every sample was normalized with equation 4.1. Here the dN% of the sample with the highest peak areas for the dNs was assigned as 100%. The dN% of the other samples were then determined with the method described in section 2.3.4.

$$A_{norm.} = A_{meas.}/[(dA\% + dC\% + dG\% + dT\%)/4] \quad (4.1)$$

In this equation, $A_{norm.}$ indicates the normalized peak area of F-ara-A; while $A_{meas.}$ indicates the actual peak area obtained from experiments.

After data analysis, a dose-effect profile of F-ara-AMP has been illustrated in figure 4.3. From the profile, a clear relationship between the dosage of F-ara-AMP and the incorporated drug can be observed. The drug incorporation first increase with the treatment dosage, and then reached to a relatively stable level after the dosage of the drug exceeds 10 μM.

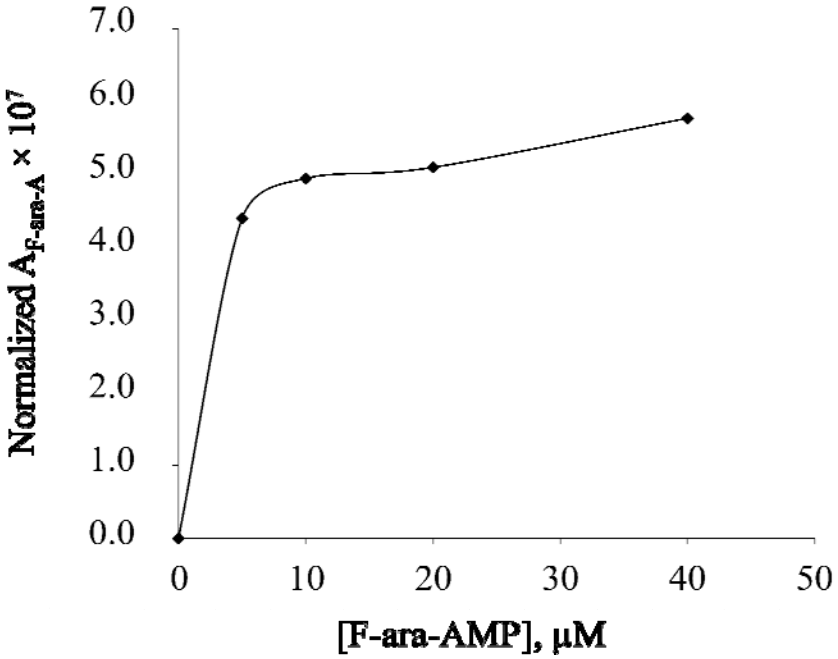

Figure 4.3, A dose-effect profile of F-ara-AMP on HL60 cells. The Y axis represents the peak area of F-ara-A released from the cellular DNA (normalized according to the amounts of dNs released from the samples).

4.4. Conclusion

A tetra-enzyme cocktail containing DNase I, NP1, PDE I and ALP was utilized in the releasing of incorporated F-ara-A from the DNA backbone as free small molecules. A protein precipitation procedure was utilized in the sample preparation to remove protein interferences in the sample matrix. LC separation was realized on an YMC-AQ® column for further separation of F-ara-A from all the other interferences existing in the sample matrix. The method has been applied to an *in vitro* drug effect study involving analysis of F-ara-A incorporation after the HL60 cells were treated with F-ara-AMP. The developed method, although still a semi-quantitative one, has provided direct information on the drug effect evaluation. With further validation, the method can become a quantitative one, and assist in providing dosimetric guidance in clinical trials and practice.

4.5. References

1. V.R. Anderson, C.M. Perry. Drugs. 67 (2007) 1633.

2. A.M. Tsimberidou, M.J. Keating. Cancer. 115 (2009) 2824.

3. G.H. Jackson. Hematol. J. 5 Suppl 1 (2004) S62.

4. V. Gandhi, W. Plunkett. Clin. Pharmacokinet. 41 (2002) 93.

5. W. Plunkett, P. Huang, V. Gandi. Semin. Oncol. 5 Suppl 8 (1990) 3.

6. V.I. Avramis, S. Wiersma, M.D. Krailo, L.V. Ramilo-Torno, A. Sharpe, W. Liu-Mares, R. Kowck, G.H. Reaman, J.K. Sato. Clin. Cancer Res. 4 (1998) 45.

CHAPTER V

DETERMINATION OF 2-FLUOROADENINE REMOVED FROM FLUDARABINE (F-ARA-A) INCORPORATED IN DNA WITH LC-MS/MS

5.1. Introduction

2-Fluoroadenine (F-Ade, figure 3-1A) has long been known as a toxic metabolite of fludarabine phosphate (9-β-D-arabino-furanosyl-2-fluoradenine monophosphate or F-ara-A, figure 3-1B) [1], which is used as therapeutic agent for treatments of hematological malignancies such as CLL, AML, and non-Hodgkins lymphomas [2, 3]. Metabolic studies of F-ara-A in animals found that F-Ade was present in plasma, urine, and cerebrospinal fluid [4-6]. As F-Ade is a potent cytotoxic compound yet lacks of

therapeutic benefit [7], investigations of biological origin of F-Ade were attempted [8-10]. After failing to identify the enzyme responsible for generation of F-Ade in mammalian cells [8, 9], it was suggested that F-Ade might be released by bacterial purine nucleoside phosphorylase because the bacteria were systemically available by the enterohepatic circulation [10].

Our recent study reveals that uracil-DNA glycosylase (UDG) is most likely accountable for the releasing of F-Ade [11]. Since it has been well accepted that F-ara-A exerts its therapeutic effect through the incorporation of its triphosphorylated metabolite, F-ara-ATP, into elongating DNA strand [12], it is hypothesized that the F-Ade moiety of the F-ara-A incorporated DNA is recognized by UDG as an abnormal base, which triggers DNA base excision repair (BER) pathways [11, 13]. To prove this mechanism, a series of experiments were carried out [11], yet the most direct proof would be the detection of F-Ade from the UDG digested DNA samples where F-ara-A was incorporated by either chemical synthesis or dosing cells with F-ara-A.

There were two methods reported for analysis of metabolites of F-ara-A in biological matrices [14, 15]. In the method by Struck *et al*, ^{3}H-labeled fludarabine monophosphate was used and the amount of F-Ade was measured by the radioactivity in the corresponding HPLC fraction [14]; whereas in the method by Kemena *et al*, F-Ade was first derivatized with chloroacetaldehyde to form a fluorescent product which was then detected by HPLC with fluorescent detection [15]. Both methods involved laborious sample preparations and neither had been validated for F-Ade quantification.

In this paper, we report a simple LC-MS/MS method for the direct determination of F-Ade from F-ara-A incorporated DNA 40-mer and from cells treated with F-ara-A. In this method, 2-Chloroadenine (Cl-Ade) was chosen as the IS (figure 5.1 C). A solid phase extraction (SPE) protocol was adopted for sample preparation, and a reversed-phase liquid chromatographic method with tandem mass spectrometric detection (LC-MS/MS) was developed for quantitative determination of F-Ade. The method was validated following the US FDA guidance for bioanalytical method [16]. The method has been used for determination of F-Ade in DNA samples from UDG digested synthetic DNA 40-mer with F-ara-A incorporated in position 19 of the sense strand, and cell lysate of F-ara-A treated human promyelocytic leukemia cell line HL60, as well as cell lysates of F-ara-A treated lymphocytes of chronic lymphcytic leukemia patients and healthy donors. The data obtained not only confirm the feasibility of the analytical method, but also support the hypothesis of UDG-initiated base excision repair of F-ara-A incorporated DNA. This method is useful for quantifying F-Ade in cell lysate and for studying tumor resistance of fludarabine phosphate by BER pathways.

A

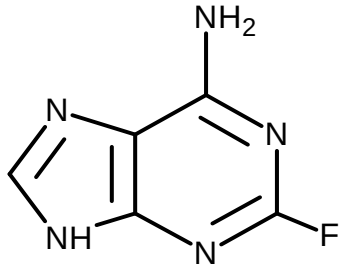

2-Floroadenine (F-Ade)
MW = 153

B

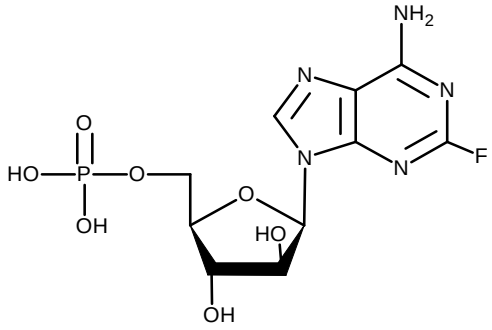

Fludarabine phosphate (F-ara-AMP)
MW = 365

C

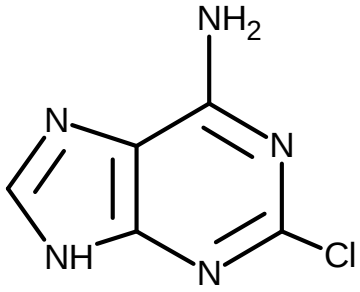

2-Chloroadenine (Cl-Ade, IS)
MW = 169

Figure 5.1, The chemical structures of 2-fluoroadenine (A), fludarabine phosphate (B), and the IS, 2-chloroadenine (C).

5.2. Material and methods

5.2.1. Chemicals and solutions

Sterile lyophilized fludarabine phosphate (for intravenous use) was obtained from Berlex Laboratories (Richmond, CA, USA). F-Ade, dithiothreitol (DTT), bovine serum albumin, glycerol, formic acid, and HPLC-grade methanol were from Sigma-Aldrich (St. Louis, MO, USA). Cl-Ade was from Waterstone Technology (Carmel, IN, USA). EDTA disodium salt and tris (hydroxymethyl) aminomethane were from Bio-Rad (Hercules, CA, USA). Sodium chloride, potassium chloride, sodium phosphate (dibasic), and phosphate buffer saline (PBS, 1 ×, pH 7.4) were from Fisher Scientific (Fair Lawn, NJ, USA). Hydrochloric acid was from Pharmco (Brookfield, CT, USA). Sodium phosphate (monobasic) was from J.T. Baker Chemical (Phillipsburg, NJ, USA). 5'-hexachloro-fluorescein phosphoramidite (HEX) labeled DNA 17-mer (*i.e.*, 5'-[HEX] GTA AAA CGA CGG CCA GT-3'), DNA 21-mer (*i.e.*, 5'-ATT CGA GCT CGG TAC CCG GGG-3'), and DNA 40-mer (*i.e.*, 5'-C CCC GGG TAC CGA GCT CGA ATT CAC TGG CCG TCG TTT TAC-3') were from Operon Biotechnologies (Huntsville, AL, USA). Deoxyguanosine triphosphate (dGTP) was from Roche Applied Science (Indianapolis, IN, USA). F-ara-ATP was from Sierra Bioresearch (Tucson, AZ, USA). DNA polymerase was from Travigen (Gaithersburg, MD, USA). T4 DNA ligase was from Invitrogen

(Carlband, CA, USA). RPMI 1640 medium and fetal bovine serum were from HyClone (Logan, UT, USA). L-glutamine was from Cellgro (Manassas, VA, USA). Uracil-DNA glycosylase (UDG, 5 U/μL) in a buffer containing 10 mM Tris-HCl, 50 mM KCl, 1 mM DTT, 0.1 mM EDTA, and 50% glycerol at pH 7.0, and 10 × UDG buffer (200 mM Tris-HCl, 10 mM EDTA, 10 mM DTT, pH 8.0) were from New England BioLabs (Ipswich, MA, USA). Fludarabine phosphate stock solution was prepared by dissolving the lyophilized solid cake in RPMI 1640 medium to a concentration of 25 mM. Working solutions of fludarabine phosphate (10.0, 40.0 and 50.0 μM) were prepared freshly by serial dilution of the stock solution with RPMI 1640 medium. Deionized water was prepared by the Barnstead NANOpure® water purification system (Thermo Scientific, Waltham, MA, USA).

5.2.2. LC-MS/MS instrumentation

The LC-MS/MS system included an Agilent 1100 HPLC system (Agilent, Santa Clara, CA, USA) and a Micromass Quattro II triple quadrupole tandem mass spectrometer (Micromass, Wythenshawe, Manchester, UK), which was controlled by Micromass MassLynx software (version 3.3). The system consisted of a solvent reservoir, a degasser, a binary pump, an autosampler, an inert in-line filter (0.5 μm pore) (Upchurch Scientific, Oak Harbor, WA, USA), a Waters YMC-ODS AQ® column (2.0×50 mm, 5

μm particle size with 120 Å pore size), a two-position 6-port switching valve (Alltech, Deerfield, IL, USA), and an electrospray ionization tandem mass spectrometer (ESI-MS/MS).

The LC separation was carried out by isocratic elution with a mobile phase containing 20% methanol, 0.1% formic acid and 79.9% deionized water (v/v/v) at a flow rate of 0.15 mL/min and a room temperature of 23 ℃. For each analysis, 20-μL sample was injected to the system. By controlling the switching valve, eluate within the time window of 2.5-5 min was diverted to the ESI-MS/MS detector.

The ESI-MS/MS was operated under positive-electrospray-ionization (ESI^+) mode. The ionization conditions were tuned by infusion of a mixture of F-Ade (10.0 μg/mL) and IS (10.0 μg/mL) in the mobile phase at a flow rate of 3 μL/min with a syringe pump (Harvard Apparatus, South Natick, MA, USA). The optimized conditions were as follows: drying gas, 300 L/h; nebulizer gas, 15 L/h; capillary voltage, 3.5 kV; HV lens, 0.5 kV; cone voltage, 35 V; skimmer voltage, 1.5 V; RF lens, 0.2 V; ion source temperature, 90 ℃; ion energy, -0.2 V. Analyte quantification was carried out by the multiple-reaction-monitoring (MRM) mode with mass transitions of m/z 154 > 134 for F-Ade and m/z 170 > 134 for the IS. The optimized parameters of MRM were as follows: argon collision gas, 2.0-2.5 μbar; collision energy, 18 eV for F-Ade and 23 eV for the IS; dwell time, 0.4 sec; inter-scan delay, 0.05 sec; low- and high-mass resolution, 15 for both quadrupoles 1 and 3; and multiplier voltage, 650 V.

5.2.3. Synthesis of F-ara-A incorporated DNA 40-mer

DNA 40-mer with an F-ara-A incorporated at position 19 of the sense strand was synthesized using the procedure described by Yang *et al.* [17] with modifications as follows: (a) three single-stranded DNA oligomers {i.e., 5'-[HEX] GTA AAA CGA CGG CCA GT-3' (17-mer), 5'-ATT CGA GCT CGG TAC CCG GGG-3' (21-mer), and 5'-C CCC GGG TAC CGA GCT CGA ATT CAC TGG CCG TCG TTT TAC-3' (40-mer)} at 100 pmol each annealed together in a 100-μL buffer solution (containing 10 mM Tris-HCl, 50 mM KCl, and 1 mm EDTA; pH 7.6) at 95 ℃ for 5 min, followed by a cooling down period at room temperature for 1 h. This annealing step produced a double-stranded DNA oligomer with fluorescent labels on both ends, and a gap of two nucleotides at the 18^{th} and the 19^{th} positions on the sense strand 5'-[HEX] GTA AAA CGA CGG CCA GT_ _AT TCG AGC TCG GTA CCC GGG G-3' which complemented the anti-sense strand 3'-CAT TTT GCT GCC GGT CAC TTA AGC TCG AGC CAT GGG CCC C-5'; (b) 20 μL of the resulted DNA oligomer was incubated at 37 ℃ for 1 hr with 2.5 nmol dGTP (500 μM, 5 μL), 2.5 nmol of F-ara-ATP (500 μM, 5 μL), 10 U of DNA polymerase 5 U/μL, 2 μL), 5 μL of 10 × polymerization buffer (containing 0.500 M Tris-Cl at pH 8.8, 0.100 M $MgCl_2$, 1.00 M KCl, 10.0 mM DTT, and 10.0% glycerol), and 13 μL of water. This reaction step extended the sense strand of the 17-mer with dGMP on the 18th position and F-ara-A on the 19^{th} position; (c) the extended oligomer was then precipitated from the reaction buffer using ice-cold solution containing 25 μL of 7.5 M

ammonium acetate and 250 μL of ethanol and kept at -80 ℃ for 1 h, then, recovered by centrifugation at 16100 × g and 4 ℃ for 10 minutes. The resulted pellet was washed with 100 μL of 70% ice-cold ethanol twice, and dried at room temperature for 20 min; (d) the recovered extended oligomer was further incubated with 25 U of T4 DNA ligase in a 50 μL reaction buffer consisting 50 mM Tris-HCl (pH 7.6), 10 mM $MgCl_2$, 1 mM ATP, 1 mM DTT at 14 ℃ for 18 h. This ligation step resulted in an intact double-stranded DNA 40-mer with an F-ara-A incorporated at the 19^{th} position of the sense strand (*i.e.*, sense strand 5'- [HEX] GTA AAA CGA CGG CCA GTG FAT TCG AGC TCG GTA CCC GGG G-3', and anti-sense strand 3'-CAT TTT GCT GCC GGT CAC TTA AGC TCG AGC CAT GGG CCC C-5'); (e) the synthesized DNA 40-mer was electrophoresed through a polyacrylamide (19%)-urea (7 M) gels and visualized by using a Typhoon 9200 fluorescent Imager (Amersham BioScience, Piscarawat, NJ, USA). After electrophoresis, the band of the 40-mer was cut out and purified with Qiaex II Gel Extraction Kit (Qiagen, Valencia, CA, USA) following the instruction provided by the manufacturer; (f) the purified DNA 40-mer was suspended in 20 μL buffer containing 10 mM Tris-HCl, 50 mM NaCl, and 1 mM EDTA at pH 8.0 to give an approximate concentration of 1 μM; (g) repeated (a) to (f) to give 500 μL of F-ara-A incorporated DNA 40-mer solution.

5.2.4. Removal of F-Ade from F-ara-A incorporated DNA 40-mer by UDG

In this part of the experiment, 500 μL of F-ara-A incorporated DNA 40-mer solution (*ca*. 1 μM) was mixed with 60 μL of 10 × UDG buffer and 40 μL (or 200 U) of UDG. The excision of F-Ade from the DNA 40-mer by UDG took place at 37 ℃ overnight (12 h). After reaction the reaction mixture was heated at 95 ℃ for 5 min to deactivate UDG; then, centrifuged at 16100 × g for 5 min. The supernate was stored at -20 ℃ before the LC-MS/MS analysis.

5.2.5. Cell isolation and culture

Peripheral blood samples were collected into heparinized Vacutainer® tubes from CLL patients and healthy donors who had signed written informed consent at the University Hospital Case Medical Center (Cleveland, OH, USA). The CLL patients were mixed-sex with median age of fifty-eight, and had absolute lymphocytes counts of typical CLL patients (11-365 × 10^3 counts/mL). At the time of blood drawing, they were not on therapy. In this work, heparinized blood was fractioned by Ficoll-Paque method [18]. Briefly, 10-mL heparinized blood was layered on the top of 12-mL Ficoll-Paque Plus reagent (GE Healthcare Bio-Sciences, Piscataway, NJ, USA) in a 50-mL sterile polypropylene centrifuge tube (RNase/DNase free); then the tube was centrifuged at room temperature and 300 × g for 30 min. Cells at the interface were collected, washed twice with PBS (1×, pH 7.4) solution, and resuspended at a density of 1 × 10^6 cell

counts/mL in a pre-warmed culture medium [*i.e.*, RPMI 1640 medium supplemented with 10 % (v/v) fetal bovine serum and 2 mM L-glutamine].

The isolated lymphocytes from CLL patients, and human promyelocytic leukemia HL60 cells obtained from American Type Culture Collection (Rockville, MD, USA) were cultured in the culture medium at 37 ℃ in a humidified 5% CO_2 incubator.

5.2.6. Cell treatment

The human promyelocytic leukemia HL60 cells (5×10^6 each) were treated with 40 μM of fludarabine phosphate for 0 (pre-dosing), 3, 6, and 24 hrs. The lymphocytic cells (5×10^6 each) collected from CLL patients were treated with 10 and 50 μM of fludarabine phosphate for 0 (pre-dosing), 6 and 24 hrs. At the indicated time points, cells were harvested by centrifugation at 4 ℃ and 300 × g for 10 min. Cell pellets were washed twice with 1 mL each of PBS (1×, pH 7.4). The cell pellets collected were resuspended in deionized water in a concentration of 10^7 cells/mL and lysated by a Branson Sonifier 450 (VWR Scientific, Batavia, IL, USA) with 2 sonication cycles at 15 impulses per cycle. The duty cycle of the sonicator was set at 30 and output control was set at 3. After sonication, the cell lysate was immersed in boiling water bath for 5 min; then, centrifuged at 16100 × g for 5 min. The supernate was stored at -20 ℃ before the LC-MS/MS analysis.

5.2.7. Preparation of F-Ade calibrators and QCs

F-Ade stock solution (1.00 mg/mL) and Cl-Ade (IS) stock solution (1.00 mg/mL) were prepared individually by dissolving proper amount of solid compound in known volume of 1.0 M and 10 M HCl, respectively. F-Ade standard solutions (10.0, 16.5, 20.0, 40.0, 44.4, 49.4, 80.0, 148, 160, 320, 400, 444, 640, 1.28×10^3, 1.33×10^3, 3.60×10^3, and 4.00×10^3 ng/mL) and the IS solution (100 and 200 ng/mL) were prepared by serial dilution of their corresponding stock solutions with 0.1 M phosphate buffer at pH 8.0.

F-Ade calibrators (1.67, 3.33, 6.67, 13.3, 26.7, 53.3, 107, and 213 ng/mL) in UDG digestion matrix for the measurement of F-Ade from the F-ara-A incorporated DNA 40-mer were prepared individually by mixing 50-μL buffer containing 100 mM Tris-HCl, 500 mM NaCl, and 10 mM EDTA at pH 8.0; 60 μL of 10× UDG buffer; 40 μL of UDG mimic solution containing 10 mM Tris-HCl, 50 mM KCl, 1 mM DTT, 0.1 mM EDTA, 0.2 mg/mL BSA, and 50% glycerol at pH 7.0; 100 μL of F-Ade standard solution (at 6× of the corresponding calibrator concentration) and 350 μL of deionized water.

F-Ade calibrators (0.825, 2.47, 7.40, 22.2, 66.5, and 200 ng/10^6 cells) and F-Ade QCs (2.22, 20.0, and 180 ng/10^6 cells) in cell lysate for the measurements of F-Ade from cells after F-ara-A treatment were prepared individually by mixing 100-μL HL60 cell lysate of the untreated cell control (10^7 cells/mL), and 50-μL F-Ade standard solution (for calibrators at 16.5, 49.4, 148, 444, 1.33×10^3, and 4.00×10^3 ng/mL, respectively; for QCs at 44.4, 400, and 3.60×10^3 ng/mL, respectively).

5.2.8. SPE of cell lysates and UDG-digested DNA

Oasis® HLB cartridges (3 cc, 60 mg, Waters, Milford, MA, USA) were used for analyte extraction. Prior to sample extraction, the cartridges were equilibrated with 3.0 mL of methanol and 3.0 mL of 10 mM phosphate buffer (pH 8.0), sequentially. For the F-Ade calibrators in UDG reaction buffer and the supernate of UDG digested F-ara-A incorporated DNA 40-mer, 600 μL of each calibrator or supernate sample was mixed with 100 μL of IS solution (100 ng/mL) and 700 μL of 10 mM phosphate buffer (pH 8.0) before loading to the cartridge. For the F-Ade calibrators in cell lysate and cell samples after F-ara-A treatment, 150 μL of each calibrator or cell sample was mixed with 50 μL of IS solution (200 ng/mL) and 1000 μL of 10 mM phosphate buffer (pH 8.0) before loading to the cartridge. After loading samples, the cartridges were washed with 4.0 mL of deionized water; then, the analytes were eluted with 2.0 mL of 10% formic acid in methanol (v/v). The eluates were then evaporated to dryness at 60 ℃ for 60 min in a TurboVap® LV Evaporator (Zymark, Hopkinton, MA, USA) under a pressurized stream of nitrogen gas (25 psi). Each residual was reconstituted in 100 μL of deionized water before the LC-MS/MS analyses.

5.2.9. Construction of calibration curves

The calibration curve of F-Ade in UDG digestion matrix was established using a blank (*i.e.*, matrix without F-Ade and IS), a zero (*i.e.*, matrix with IS at 16.7 ng/mL) and eight non-zero calibrators (F-Ade at1.67, 3.33, 6.67, 13.3, 26.7, 53.3, 107 and 213 ng/mL; IS at 16.7 ng/mL). The calibration curve of F-Ade in cell lysate was established using a blank, one zero and six non-zero calibrators (F-Ade at 0.825, 2.47, 7.40, 22.2, 66.5 and 200 ng/10^6 cells; IS at 10.0 ng/10^6 cells). Peak-area ratios of F-Ade (*m/z* 154 > 134) to the IS (*m/z* 170 > 134) were plotted against F-Ade concentrations for linear regression equations with weighting factor of 1/x and passing zero.

5.2.10. Matrix effect and recovery

For the matrix effect study, aliquots of 500 µL UDG digestion matrix or 100 µL HL60 cell lysate were first extracted with the established SPE protocol; then, F-Ade and IS standard solutions were spiked in the extracted matrix to make standard solutions containing F-Ade at 1.67, 16.7, 167 ng/mL and IS at 16.7 ng/mL in the extracted UDG digestion matrix; and F-Ade at 2.22, 20.0 and 180 ng/10^6 cells and IS at 10.0 ng/10^6 cells in the extracted HL60 cell lysate. The peak area ratios of F-Ade to IS in these spike-after-extraction (SAE) standards $(A/A')_{matrix}$ were compared with those of the corresponding standard solutions in 0.1 M phosphate buffer at pH 8.0 $(A/A')_{buffer}$. The matrix effect

(either suppression or enhancement) on analytical signal of F-Ade was calculated by the IS normalized matrix factor (MF_{IS}) (equation 5.1):

$$MF_{IS} = \frac{(A/A')_{matrix}}{(A/A')_{solvent}} \tag{5.1}$$

Here, unless otherwise specified, A represents the peak area of the analyte; while A' indicates the peak area of the IS. (A/A') indicates the peak area ratio of the analyte over the IS. Thus, $(A/A')_{matrix}$ indicates the peak area ratio in the post-extraction matrix; while $(A/A')_{solvent}$ indicates that in the pure solvent [19].

For the recovery study, standard solutions containing F-Ade at 1.67, 16.7 and 167 ng/mL and IS at 16.7 ng/mL in the UDG digestion matrix; F-Ade at 2.22, 20.0 and 180 ng/10^6 cells and IS at 10.0 ng//10^6 cells in HL60 cell lysate were prepared, and analyzed. The peak area ratios of F-Ade to IS in sample matrix $(A/A')_{extraction}$ were compared with those of the corresponding SAE standards $(A/A')_{matrix}$ for the calculation of IS normalized recovery RC_{IS} (equation 5.2).

$$RC_{IS} = \frac{(A/A')_{extraction}}{(A/A')_{matrix}} \times 100\% \tag{5.2}$$

Here $(A/A')_{extraction}$ represent the peak area ratio in extracted plasma samples.

5.2.11. Stability

The stability of F-Ade in HL60 cell lysate was evaluated at two different concentrations (2.22 and 180 ng/10^6 cells). These stability controls were prepared in the similar way of the QCs except the IS was added right before the solid phase extraction. All experiments were run in triplicate and the results were compared with freshly prepared stability controls.

In the short-term stability study, the stability controls were kept at the room temperature (23 ℃) for 4 h prior to analysis. For the freeze and thaw stability study, the stability controls were undergone 3 freeze-and-thaw cycles; and in each cycle, the stability controls were frozen at −20 ℃ for at least 24 h and thawed at room temperature unassisted. For the long-term stability study, the stability controls were stored at -20 ℃ for 30 days prior to analysis.

5.3. Results

5.3.1. Synthesis of F-ara-A incorporated DNA 40-mer

Use the anti-sense strand 3'-CAT TTT GCT GCC GGT CAC TTA AGC TCG AGC CAT GGG CCC C-5' as template, the extension of the green fluorescent labeled 17-mer oligonucleotide, 5'-[HEX] GTA AAA CGA CGG CCA GT-3' to the 19-mer oligonucleotide with F-ara-A at position 19 of the sense strand 5'-[HEX] GTA AAA

CGA CGG CCA GTG F-3', and the ligation of the 19-mer with the 21-mer 5'-ATT CGA GCT CGG TAC CCG GGG-3' to produce the sense strand of 40-mer 5'-[HEX] GTA AAA CGA CGG CCA GTG FAT TCG AGC TCG GTA CCC GGG G-3' can be illustrated by figure 5.2 A, and visualized in figure 5.2 B and C. The F-ara-A incorporated double-stranded DNA 40-mer has a mismatch base pair (F-ara-A:T) at position 19, which can be repaired by UDG enzyme to give off F-Ade as a free base and a double-stranded oligonucleotide 40-mer containing an arabinose abasic site (ara-AP) at its 19^{th} position.

A

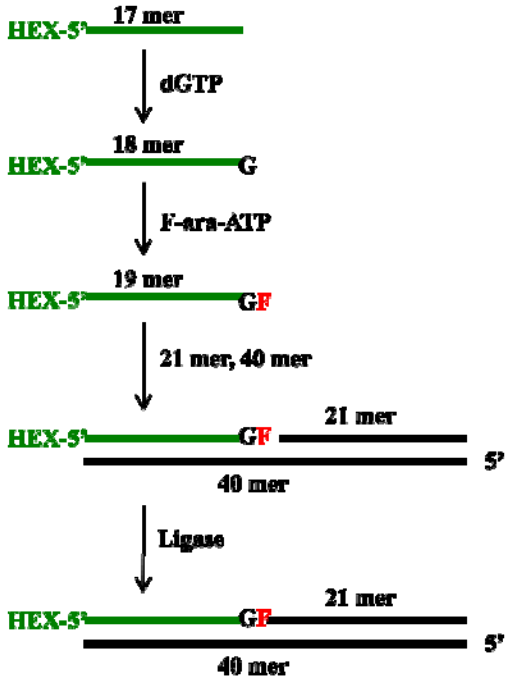

B

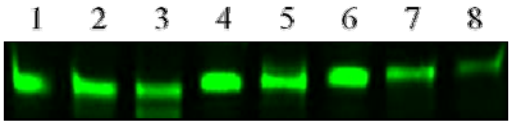

Lane 1: 17 mer (control)
Lane 2: 17 mer + FTP =17 mer
Lane 3: 17 mer + dATP = 17mer
Lane 4: 18 mer (control)
Lane 5: 17 mer + dGTP = 18 mer
Lane 6: 19 mer (control)
Lane 7: 17 mer + dGTP + FTP = 19 mer
Lane 8: 17 mer + dGTP + dATP =19 mer

C

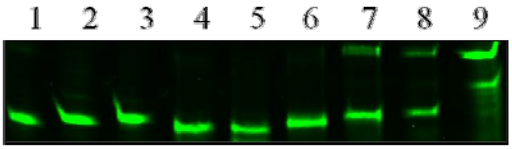

Lane 1: 17 mer (control)
Lane 2: 18 mer (control)
Lane 3: 19 mer (control)
Lane 4: 17 mer + FTP = 17mer
Lane 5: 17 mer + dATP =17mer
Lane 6: 17 mer + dGTP = 18mer
Lane 7: 17 mer + dGTP + FTP ligation =40mer
Lane 8: 17 mer + dGTP + dATP ligation =40mer
Lane 9: 40 mer (control)

Figure 5.2, Synthesis of F-ara-A incorporated DNA 40-mer. Schematic illustration of incorporation of F-ara-A in DNA oligomers (A); confirmation of F-ara-A incorporated DNA 19-mer (Lane 7) (B) and DNA 40-mer (Lane 7) (C).

5.3.2. LC-MS/MS method for the measurement of F-Ade

F-Ade and Cl-Ade (IS) are basic compounds which can be protonated in acidic solution and detected by positive electrospray ionization tandem mass spectrometer. As shown in figure 5.3 A and C, F-Ade and the IS produced molecular ions $[F\text{-}Ade + H]^+$ at *m/z* 154 and $[IS+H]^+$ at *m/z* 170, respectively. These molecular ions could further undergo collision induced dissociation (CID) by argon gas and produce product ion spectra (figures 5.3 B and D). The predominant product ions of F-Ade and IS are both at m/z 134 which may due to the loss of HF from F-Ade and HCl from Cl-Ade. Therefore, mass transition pairs of *m/z* 154 > 134 for F-Ade and *m/z* 170 > 134 for IS were chosen for quantification by multiple-reaction-monitoring (MRM) mode.

The representative chromatograms for separation of F-Ade and IS in UDG digestion matrix and HL-60 cell lysate were shown in figure 5.4. Baseline resolution of F-Ade and IS were achieved using Waters YMC-ODS AQ® column (2.0 × 50 mm, 5 μm) with a mobile phase containing 20% methanol, 0.1% formic acid and 79.9% deionized water (v/v/v) at a flow rate of 0.15 mL/min. The retention times of F-Ade and the IS were 3.0 an 4.0 min, respectively.

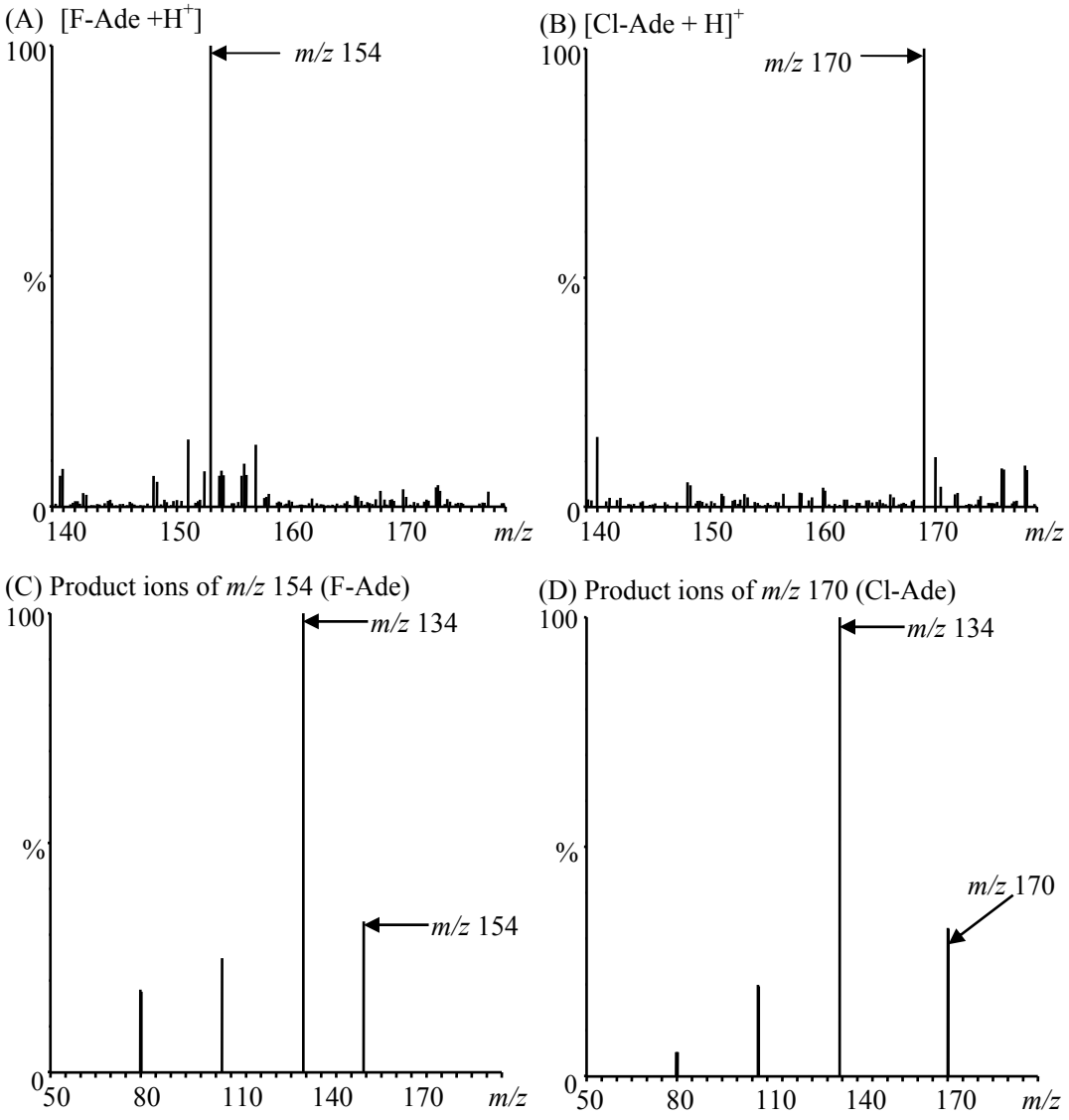

Figure 5.3, The mass spectra of F-Ade and Cl-Ade (IS).

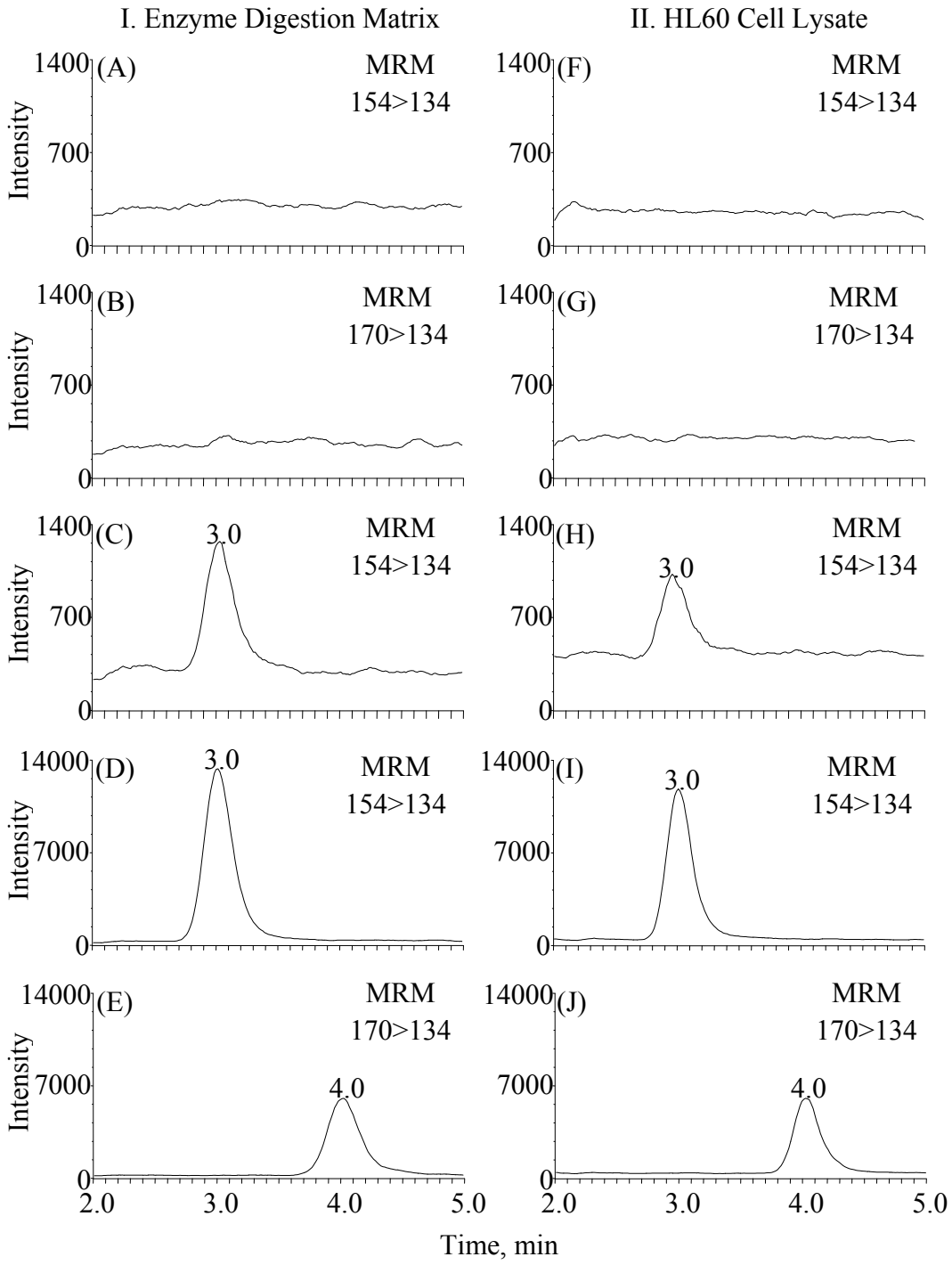

Figure 5.4, Representative MRM chromatograms of F-Ade and IS. Column I (in UDG digestion matrix): (A) Blank 1 (no F-Ade), (B) Blank 2 (no IS), (C) F-Ade at 1.67 ng/mL (LLOQ, S/N = 25.6), (D) F-Ade at 26.7 ng/mL, and (E) IS at 16.7 ng/mL; and Column II

(in HL60 cell lysate): (F) Blank 1 (no F-Ade), (G) Blank 2 (no IS), (H) IS at 0.825 ng/10^6 cells (LLOQ, S/N = 14.7), (I) F-Ade at 22.2 ng/10^6 cells, and (J) IS at 10.0 ng/10^6 cells.

5.3.3. Analytical method validation

Matrix effect and recovery

Table 5.1 summarized the data from the matrix effect and recovery studies. As shown in the table, over the concentration range studies, the IS normalized matrix factors (MF_{IS}) were 0.977-1.00 in the UDG digestion matrix and 0.878-0.921 in the HL60 cell lysate, whereas the IS normalized recovery (R_{IS}) were 90-101% in the UDG digestion matrix, and 84-104% in the HL60 cell lysate.

Calibration equations and lower limit of quantification (LLOQ)

The internal calibration curves of F-Ade were established in both UDG digestion matrix (1.67-213 ng/mL) and HL60 cell lysate (0.823-200 ng/10^6 cells) and the data were summarized in table 5.2. With the weighing factor of 1/X, the linear calibration equations were derived as $Y_1 = 0.075 (\pm 0.002) X_1$, $R_1^2 = 0.999 (\pm 0.001)$ in the UDG digestion matrix, and $Y_2 = 0.079 (\pm 0.001) X_2$, $R_2^2 = 0.999 (\pm 0.000)$ in the HL60 cell lysate. The LLOQs of the calibration curves defined by the lowest F-Ade calibrators were 1.67 ng/mL in UDG digestion matrix and 0.823 ng/10^6 cells in HL60 cell lysate.

Table 5.1, Recovery and matrix effect data.

Matrix	**Concentration level (ng/mL)**	**Recovery ± S.D. (%)**	**$MF_{I.S.}$ ± S.D.**
Enzyme Digestion Matrix	1.67	89.5 ± 2.6	1.00 ± 0.05
	16.7	95.3 ± 2.1	0.989 ± 0.041
	167	101 ± 0	0.977 ± 0.028
Matrix	**Concentration level (ng/10^6 cells)**	**Recovery ± S.D. (%)**	**$MF_{I.S.}$ ± S.D.**
HL60 Cell Lysate	2.22	84.3 ± 6.8	0.912 ± 0.026
	20.0	101 ± 3	0.878 ± 0.033
	180	104 ± 3	0.921 ± 0.006

Three measurements were performed for each datum point. S.D. here and in table 2 and 4 represents standard deviation.

Table 5.2, Calibration equations of F-Ade in enzyme digestion matrix and HL60 cell lysate.

Biological matrices	**$[F\text{-}Ade]_{actual}$ ng/mL**	**$[F\text{-}Ade]_{measured}$ ng/mL**	**S.D.**	**Accuracy (%)**	**Precision (%)**
Enzyme digestion matrix	1.67	1.76	0.08	5.39	4.55
	3.33	3.38	0.07	1.40	1.97
	6.67	7.2	0.1	7.45	1.62
	13.3	14.3	0.4	7.63	2.71
	26.7	28	2	3.37	7.03
	53.3	54	2	1.79	4.14
	107	108	3	0.984	2.57
	213	209	2	-2.14	0.857
Biological matrices	**$[F\text{-}Ade]_{actual}$ ng/10^6 cells**	**$[F\text{-}Ade]_{measured}$ ng/10^6 cells**	**S.D.**	**Accuracy (%)**	**Precision (%)**
HL60 cell lysate	0.823	0.84	0.09	1.82	10.6
	2.47	2.47	0.07	-0.202	2.74
	7.41	7.7	0.1	4.04	1.58
	22.2	23.7	0.5	6.97	2.27
	66.7	69.9	0.8	4.73	1.12
	200	195	0	-2.50	0.140

Calibration equations: Enzyme digestion matrix, $Y = 0.075 (\pm 0.002) X$, $R^2 = 0.999 (\pm 0.001)$

HL60 cell lysate, $Y = 0.079 (\pm 0.001) X$, $R^2 = 0.999 (\pm 0.000)$

Each datum point was based on three separate measurements toward the same set of samples.

Accuracy and precision

The accuracy and precision for the quantification of F-Ade in HL60 cell lysate were further evaluated with QC samples at three-concentration levels (2.22, 20.0, and 180 ng/10^6 cells). At each concentration level, five replicates of QC samples were prepared and each was analyzed by triplicate measurements. The results are summarized in table 5.3. The accuracy was determined by the percent deviation of the measured concentration from the nominal concentration, which was $\leqslant \pm 14\%$. The intra- and inter-assay precisions determined as by the percent peak area ratios of F-Ade to the IS were $\leqslant \pm 9\%$ and $\pm 7\%$, respectively.

Stability

The stabilities of F-Ade in HL60 cell lysate were tested at two concentration levels (2.22 and 180 ng/10^6 cells) with triplicate measurements, and the results expressed as recovery were summarized in table 5.4. As seen in the table, there was no significant loss of F-Ade observed under the tested conditions with recovery ranged from 86% to 104%. Therefore, F-Ade stock solutions and cell lysate samples were kept at −20 ℃ for this work, and the analyses of F-Ade samples were done within a 4 h timeframe.

Table 5.3, Accuracy, intra- and inter-assay precision of F-Ade in HL60 cell lysate.

	LQC	**MQC**	**HQC**
Accuracy (%) n=5	-14.3	-1.47	2.45
Intra-assay Precision (%) n=5	8.58	1.89	0.97
Inter-assay Precision (%) n=3	7.12	2.88	2.64

The concentrations of F-Ade in the LQC, MQC and HQC were 2.22, 20.0, 180 ng/10^6 cells respectively in the HL60 cell lysate. The concentration of the I.S. was 10.0 ng/10^6 cells.

Table 5.4, Stability of F-Ade in HL60 cell lysate under various test conditions.

Storage Conditions	**[F-Ade] added ng/10^6 cells**	**Recovery ± S.D. (%)**
Room Temperature, 4 hr	2.22	99 ± 1
	180	99 ± 1
Freeze-thaw, 3 cycles, -20 ℃	2.22	104 ± 7
	180	102 ± 6
Long-term, 30 days, -20 ℃	2.22	91 ± 1
	180	86 ± 1

Each datum point was based on triplicate measurements.

5.3.4. Determination of F-Ade in F-ara-A incorporated DNA 40-mer and cells treated with F-ara-A

The validated LC-MS/MS method was applied to the determination of F-Ade in UDG digested F-ara-A incorporated DNA 40-mer, or cells (*i.e.*, human promyelocytic leukemia HL60, lymphocytes of CLL patients) treated with F-ara-A at various dosages and durations. As shown in table 5.5, UDG digested F-ara-A incorporated DNA 40-mer gave a concentration of F-Ade at 28.5 ng/mL; HL60 cells treated with 40 μM F-ara-A at 3, 6 and 24 h gave concentrations of F-Ade at 0.363, 0.622, and 1.22 ng/10^6 cells; lymphocytic cells of CCL patients treated with 10 μM, or 50 μM F-ara-A at 6 and 24 h gave concentrations of F-Ade at 0.165 and 0.333 ng/10^6 cells, or 0.861 and 1.73 ng/10^6 cells. Since the actual concentrations of F-Ade in several cell samples treated with F-ara-A were below the LLOQ of the LC-MS/MS method, these samples were enriched 9 times together with the concentration QCs (0.247, 2.22, and 20.0 ng/10^6 cells) by solid phase extraction prior to their analyses by LC-MS/MS (table 5.5).

Table 5.5, F-Ade concentrations measured from QCs, UDG digested F-ara-A incorporated DNA 40-mer, HL60 cells, and lymphocytic cells of CLL patients.

Samples	$[F\text{-}Ade]_{measured}$ ng/10^6 cells	Concentration Factor	$[F\text{-}Ade]_{actual}$ ng/10^6 cells	Accuracy (%)
QC1 (0.247 ng/10^6 cells, n = 5)	2.21	9	0.246	99.6
QC2 (2.22 ng/10^6 cells, n = 5)	21.5	9	2.39	108
QC3 (20.0 ng/10^6 cells, n = 5)	154	9	17.1	85.4
UDG digested F-ara-A incorporated DNA 40-mer	28.5 (ng/mL)	1	28.5 (ng/mL)	N/A
HL60 untreated	0.00	1	0.00	N/A
HL60 treated with F-ara-A (40 μM, 3 h)	3.27	9	0.363	N/A
HL60 treated with F-ara-A (40 μM, 6 h)	5.60	9	0.622	N/A
HL60 treated with F-ara-A (40 μM, 24 h)	1.22	1	1.22	N/A
CLL lymphocytes untreated	0.00	1	0.00	N/A
CLL lymphocytes treated with F-ara-A (10 μM, 6 h), n = 3	1.49	9	0.165	N/A
CLL lymphocytes treated with F-ara-A (10 μM, 24 h), n = 3	3.00	9	0.333	N/A
CLL lymphocytes treated with F-ara-A (50 μM, 6 h), n = 3	0.861	1	0.861	N/A
CLL lymphocytes treated with F-ara-A (50 μM, 24 h), n = 3	1.73	1	1.73	N/A

5.4. Discussion

5.4.1. F-ara-A incorporated DNA is a target for BER pathways

F-ara-A is a chemotherapy agent that is widely used in the treatment of hematological malignancies. The primary action of F-ara-A is its incorporation into DNA during replication. The incorporated F-ara-A is a poor substrate for DNA replication enzymes (*i.e.*, DNA polymerase alpha, ribonucleotide reductase and DNA primase), thus inhibiting further DNA synthesis [12, 20, 21]. F-ara-A produces higher response rates in CLL patients comparing to some alkylating agents (*e.g.*, chlorambucil) alsong, and thus it is highly effective in CLL treatments [22]. However, the therapeutic effect of F-ara-A is often transient, and most patients experience relapse of the disease. In our previous studies [11], we hypothesized that F-ara-A resistance by patients may due to the recognition of F-ara-A nucleotide by DNA glycosylases as abnormal nucleobase and trigger the DNA BER pathways. Co-administration of F-ara-A and methoxyamine (MX, an investigational chemotherapeutic agent that blocks BER through forming stable adducts with abasic sites generated during BER) enhanced the fludarabine induced apoptotic cell death in HL60 and Jurkat cells. In an in vivo study with nude mice carrying HL60 and U937 xenografts, co-administration of F-ara-A with MX also significantly

reduced the tumor sizes and resulted growth delay to the tumors comparing to the treatments with F-ara-A along [11].

5.4.2. UDG is a DNA glycosylase having activity on F-ara-A:T mismatches

In addition to its incorporation in DNA and the inhibition on DNA replication enzymes, fludarabine-induced inhibition of ribonucleotide reductase results in the depletion and imbalance of deoxynucleotide pools that are required for DNA repair and synthesis. This imbalance may subsequently favor the incorporation of F-ara-A itself, and other mismatched nucleotides such as uridine, into the newly synthesized DNA strand. These mismatched DNA base pairs would activate BER [11].

Actually, another experiment involving UDG digestion to the F-ara-A incorporated DNA has already strongly supported our hypothesis with indirect evidence [11]. In this experiment, DNA 40-mer with F-ara-A incorporated at the 19^{th} position was digested with UDG followed by apurinic/apyrimidinic endonuclease (APE). According to the basic mechanisms of BER, removal of F-Ade by UDG will generate an apurinic (AP) site on the DNA strand and this AP site can be recognized by APE. Then, the APE will cleave at the 5' end of the AP site and introduce a strand break on the DNA strand [23]. Based on this mechanism, we should expect a DNA fragment with 18 bases after digesting the F-ara-A incorporated DNA 40-mer with UDG plus APE. In our experiments,

after electrophoresis on a denature gel, a single strand DNA 18-mer was observed from the digestion product and thus proved the actions of both enzymes. This result can well support our hypothesis, however, recovery of F-Ade from the UDG digested F-ara-A incorporated 40-mer DNA directly confirmed the releasing activity of UDG on the F-Ade. By quantifying the F-Ade moiety released by UDG, we are even able to analyze the repair speed and efficiency quantitatively.

As an effective therapeutic agent for hematological malignances, fludarabine and its metabolites are under intensive investigation. Our hypothesis of UDG-initiated BER of F-ara-A incorporated DNA, once fully proved, will not only illustrate a possible source of this toxic metabolite, but also discover a new drug resistance mechanism and thus provide a new target for drug effect enhancement.

5.4.3. LC-MS/MS method provides unequivocal identification and quantification of F-Ade

LC-MS/MS excels in F-Ade identification and quantification because of the direct and accurate results it is able to provide. As this technique identifies F-Ade by its molecular weight (through the *m/z* ratio) and structure (through the fragmentation pattern), the specificity of the detection is higher than most of the indirect identification methods. The validated method, on the other hand, enables the quantification to be more

reproducible, and thus allows the results from different experiments to be more comparable.

5.4.4. F-Ade concentrations in cells treated with F-ara-A correlate with dose and time

When we applied our method to the analysis of HL60 cells treated with fludarabine for different time spans. From the data obtained we were able to see a clear relationship between treatment time and the concentration of F-Ade in the cell lysate: with the increase of the treatment time, the concentration of F-Ade also increased. Although this phenomenon is not adequate to prove that the releasing of F-Ade is caused by UDG, it at least provided a possible origin of F-Ade other than bacterial enzymes. As the cells were cultured in a sterilized environment, lysed immediately after harvest and stored on ice or dry ice before analysis, there is little chance for the samples to get contaminated by bacterial enzymes.

Moreover, in another set of experiments carried out by Bulgar *et al.* [11], a colon cancer cell line DLD1 with $UDG^{+/+}$ and $UDG^{-/-}$ were treated with 10 or 50 μM of fludarabine for 24 h. F-Ade concentrations in the treated cell samples were evaluated with the method described in this paper. Although without fully validating our method in DLD1 cell lysate, the semi-quantitative results still clearly indicated that at both treatment doses, $UDG^{+/+}$ cells released significant higher ($p < 0.05$) amount of F-Ade

comparing to $UDG^{-/-}$ cells. This may indicate that the F-Ade detected from HL60 lysate is, at least partially, released by UDG.

By applying our method to the F-Ade quantification from CLL patient and healthy donor cells treated with fludarabine, we again observed a clear relationship between F-Ade concentration and treatment time/dose. Besides, data summarized in table 5 indicated that when treated with higher dose (*i.e.*, 50 μM) for longer time (*i.e.*, 24 h), CLL patient lymphocytic cells showed averagely higher F-Ade signals than the lymphocytic cells obtained from the healthy donors. This result is consistent with the results obtained from another set of experiments performed by Bulgar *et al.*, indicating higher UDG activity in CLL patient cells than the healthy donor cells [11].

5.4.5. Identification of an unknown substance existing in the same MRM channel with F-Ade, yet with different retention time

During the process of analyzing cell samples, we observed that in some samples, the signal obtained from MRM channel *m/z* 154>134 shifted around 0.7 min in retention time comparing to the chromatography peaks detected from cell lysates spiked with F-Ade standard solutions. Although differed from the standard peak significantly in retention time, the shifted peak, however, was positively related to fludarabine treatment dose and time. To further identify the shifted peak, MS2 function on the mass

spectrometer was utilized to give a full scan of the fragmentation pattern of the shifted peak after CID (figure 5.5 B). A fragmentation scan under exactly the same conditions was carried out to the F-Ade standard spiked in blank cell lysate (figure 5.5 A). Highly similar spectra were obtained for both peaks in spite of the differences in retention time. The results indicated that the species coming out in the shifted peak may share a high similarity with F-Ade structural wise and most likely to be an isomer of F-Ade with the fluorine transferred to another position. Further investigation is still under going for better understanding of the identity of this shifted peak.

5.5. Conclusion

An LC-MS/MS method for quantitative determination of F-Ade in DNA enzyme digest matrix and cell lysates has been developed and validated. This method employed an internal standard (*i.e.*, Cl-Ade) for calibration, a SPE protocol (*i.e.*, Oasis® HLB cartridge, 3cc) for sample preparation, a reverse-phase LC column (*i.e.*, YMC-ODS AQ®, 2.0 x 50 mm) for analyte separation, and a tandem mass spectrometer for analyte quantification. The feasibility of the method for the quantification of F-Ade in UDG digested F-ara-A incorporated DNA 40-mer solution, and cells (*i.e.*, HL60 cells, lymphocytic cells of CCL patients and healthy donors) treated with F-ara-A has been established. This method provided supporting evidence that UDG is a major DNA

glycosylase for repairing F-ara-A:T mispair. It may be useful not only for the quantitative measurement of action of fludarabine phosphate, but also for the assessment of efficiency of DNA base excision repair.

A

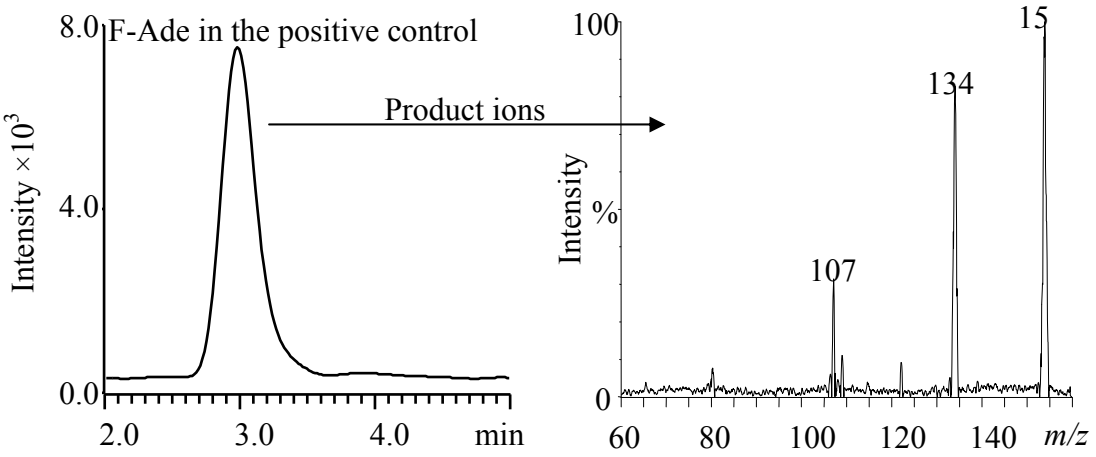

B

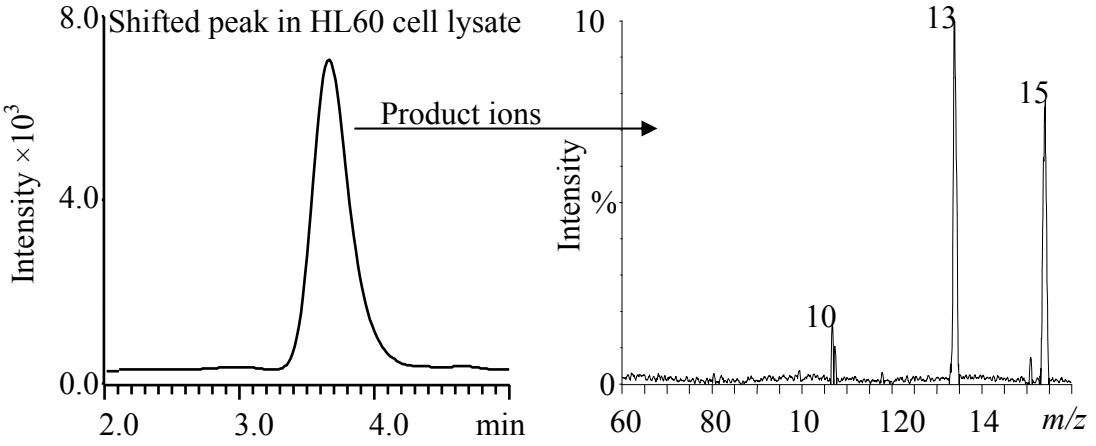

Figure 5.5, Identification of the shifted peak. (A) Chromatogram and fragmentation spectrum of F-Ade (retention time 3.0 min) from cell lysate spiked with F-Ade; (B) chromatogram and fragmentation spectrum of the unknown species (retention time 3.7 min) from a F-ara-AMP treated cell sample.

5.6. References

1. D.L. Hill, S. Straight, P.W. Allan. J Protozool. 17 (1970) 619.

2. V. Gandhi, W. Plunkett. Clin Pharmacokinet. 41 (2002) 93.

3. E. Månsson, T. Spasokoukotskaja, J. Sällström, S. Eriksson, F. Albertioni. Cancer Res. 59 (1999) 5956.

4. R.F. Struck, A.T. Shortnacy, M.C. Kirk, M.C. Thorpe, R.W. Brockman, D.L. Hill, S.M. El Dareer, J.A. Montgomery. Biochem Pharmacol. 31 (1982) 1975.

5. V.I. Avramis, W. Plunkett. Cancer Drug Del. 1 (1983) 1.

6. P.E. Noker, G.F. Duncan, S.M. El Dareer, D.L. Hill. Cancer Treat Rep. 67 (1983) 445.

7. L.L. Bennett H.P. Jr, Schnebli, M.H. Vail, P.W. Allan, J.A. Montgomery. Mol Pharmacol. 2 (1966) 432.

8. V.I. Avramis, W. Plunkett. Biochem Biophys Res Comm. 113 (1983) 35.

9. E.L. White, S.C. Shaddix, R.W. Brockman, L.L. Bennett. Jr. Cancer Res. 42 (1982) 2260.

10. P. Huang, W. Plunkett. Biochem Pharmacol. 36 (1987) 2945.

11. A.D. Bulgar, M. Snell, J.R. Donze, E.B. Kirkland, L. Li, S. Yang, Y. Xu, S.L. Gerson, L. Liu. Leukemia. 24 (2010) 1795.

12. P. Huang, S. Chubb, W. Plunkett. J Biol Chem. 265 (1990) 16617.

13. P. Fortini, E. Parlanti, O.M. Sidorkina, J. Laval, E. Dogliotti. J Biol Chem. 274 (1999) 15230.

14. R.F. Struck, A.T. Shortnacy, M.C. Kirk, M.C. Thorpe, R.W. Brockman, D.L. Hill, S.M. El Dareer, J.A. Montgomery. Biochem Pharmacol. 31 (1982) 1975.

15. A. Kemena, M. Fernandez, J. Bauman, M. Keating, W. Plunkett. Clin Chim Acta. 200 (1991) 95.

16. U.S. Food and Drug Administration (FDA) & Center for Drug Evaluation and Research (CDER), Guidance for Industry: Bioanalytical Method Validation, available at http://www.fda.gov/cder/guidance/4252fnl.htm, 2001.

17. S.W. Yang, P. Huang, W. Plunkett, F. Becker, J.Y.H. Chan. J. Biol. Chem. 267 (1992) 2345

18. E. de Rock, N. Taylor. J Immunol Methods. 17 (1977) 373.

19. E.R. Badman, Z. Liang, S. Bansal, J. Gibbons. Users Meeting, ASMS, Denver, CO, June 1, 2008.

20. V.A. Rao, W. Plunkett. Clin. Cancer. Res. 9 (2003) 3204.

21. H. Iwasaki, P. Huang, M.J. Keating, W. Plunkett. Blood. 90 (1997) 270.

22. K.R. Rai, B.L. Peterson, F.R. Appelbaum, J. Kolitz, L. Elias, L. Shepherd, J. Hines, G.A. Threatte, R.A. Larson, B.D. Cheson, C.A. Schiffer. N. Engl. J. Med. 343 (2000) 1750.

23. T.K. Hazra, A. Das, S. Das, S. Choudhury, Y.W. Kow, R. Roy. DNA Repair (Amst). 6 (2007) 470.

CHAPTER VI

QUANTITATIVE DETERMINATION OF 6BT WITH LC-MS/MS, A PHARMACOKINETIC STUDY IN MICE, AND AN IN VITRO DRUG MECHANISM STUDY

6.1. Introduction

6BT is an adenosine analogue (figure 1.1 C) that has been originally used in the property studies of adenosine aminohydrolase [1]. In the later 1990s, 6BT was discovered to be potentially useful in the treatment of toxoplasmosis [2,3] caused by *Toxoplasma gondii*, an intracellular parasite that infects humans and many other warm-blooded animals, due to its specific entry into the parasite [4,5]. Recently, 6BT was identified

through a small molecule library screen as a promising differentiation-inducing agent for leukemic cells as less toxic and more efficacious treatment for acute myeloid leukemia (AML) [6].

According to statistics data reported by American Society of Clinical Oncology in 2008, AML is the most common form of acute leukemia in the United States. It is most often observed in elderly population over age 65 [7,8]. The general accepted molecular pathogenesis of AML is a combination of differentiation arrest together with the uncontrolled proliferation of the myeloblasts [9]. The standard chemotherapy agents represented by adriamycin and cytarabine work through introducing high cytotoxicity and nonselectively killing of highly proliferative cells [8]. In spite of the fact that up to 75% of the patients can achieve complete remission (CR), the prognosis of the patients remains poor. The average 5-year survival rate of the patients after treatments is as low as 21% [7]. Unlike the traditional chemotherapeutics, the treatment of acute promyelocytic leukemia, a rare subtype of AML that only share around 5% of the total AML cases, utilizes a differentiation-inducing agent, all-trans retinoic acid (ATRA). With the treatment that induces the terminal differentiation of the myeloblasts, the 5-year disease free survival rate of the patients can reach to 74% [10]. Due to its high therapeutic specificity, ATRA can be effectively used in combination with low dose chemotherapeutic agents without introducing extra toxicity significantly [11]. This differentiation approach is especially meaningful for elderly patients, to whom the traditional chemotherapeutics are often too toxic to tolerate. However, ATRA is only

useful for acute promyelocytic leukemia patients. To search for efficacious differentiation-inducing agents for the treatment of other AML subtypes, a cell-based compound-library screen has been carried out by Wald *et al.* [6]. In their research, 6BT has been identified as a promising differentiation-inducing agent that not only displays high differentiation-inducing activity to myeloid leukemia cell lines (*i.e.*, HL-60 and OCI-AML3), but also to the primary cells of AML patients. More interestingly, 6BT induces cell death to a subset of AML cell lines (*i.e.*, HNT34 and MV4-11) as well. However, 6BT shows very low toxicity to non-malignant cells, such as fibroblasts, normal bone marrow, and endothelial cells. In mouse xenograft studies, 6BT significantly inhibited the xenograft tumor (HL-60 and/or MV4-11) growth and formation. A 129% increase of CD11b (a mature myeloid marker) in comparison to the untreated ones has been shown by flow cytometric analysis of the dissected tumors in 6BT treated tumors [6].

The preclinical studies of 6BT for the treatment of AML and toxoplasmosis demonstrated its high potential of being an investigational new drug, and thus further therapeutic development has been warranted. To insure the validity of the future pharmacological and toxicological studies, quantitative analytical methods for 6BT will be needed. Measurement of 6BT from biological samples will also provide useful information in drug metabolism and functioning mechanisms. Nevertheless, a recent search by SciFinder® Scholar revealed that there is no analytical method available to date for quantification of 6BT in biological matrices. Only a qualitative LC–UV method for

6BT and its analogues was reported by Rais *et al.* [12], which was not validated for quantitative measurement of 6BT and did not have the sensitivity and specificity required for pharmacokinetic study of 6BT.

Given the above considerations, we have developed a novel LC–MS/MS method for the direct analysis of 6BT in both mouse and human plasma, as well as in several types of whole cell lysates. The IS was selected as 2-amino-6-benzylthioinosine (2A6BT). Sample preparation was realized by a liquid–liquid extraction procedure, and LC was realized on an YMC ODS-AQ® column with a mobile phase consists 0.1% formic acid, 45% acetonitrile and 54.9% deionized water (v/v/v). A QqQ mass spectrometer with an ESI source was employed in the analyte detection. The method developed has been validated in both mouse and human plasma according to the FDA guidance, and has become a quantitative method [13]. Semi-quantitative analysis of 6BT from different cell lines treated with the drug also confirmed the enhanced entry of the drug into leukemia cell lines. The quantitative and semi-quantitative assessment of 6BT fills the gap of lacking analytical method for the pharmacokinetic studies.

6.2. Material and methods

6.2.1. Chemicals and solutions

6BT and the IS, 2A6BT, were kindly provided by the Developmental Therapeutics Program of the National Cancer Institute (Bethesda, MD, USA). Deionized water was collected from the Barnstead NANOpure® water purification system (Thermo Scientific, Waltham, MA, USA).Formic acid was purchased from Acros (Morris Plains, NJ, USA). Dimethylsulfoxide (DMSO), HPLC-grade acetonitrile and ethyl acetate were obtained from Sigma–Aldrich (St. Louis, MO, USA). Pooled blank mouse plasma was from Equitech-Bio (Kerrville, TX, USA). Isoflurane was obtained from Baxter Healthcare Corporation (Deerfield, IL, USA). Pooled blank human plasma was from Haemtech, Inc. (Essex Junction, VT, USA).

6BT and IS stock solutions were prepared according to the following procedure: first, the compounds were weighted out by an analytical balance and dissolved separately into acetonitrile to a concentration of 1.00 mg/mL; then, for 6BT, the stock solution was transferred into 1.5-mL microcentrifuge tubes as 100 µL per aliquot, and the IS, 25.0 µL per aliquot; afterward, the microcentrifuge tubes containing either 100 µg/tube of 6BT or 25.0 µg/tube of the IS stock solution were dried on a DNA120 SpeedVac® (ThermoSavant, Hollbrook, NY, USA) vacuum evaporator at 25 ℃ for 10 min; finally, the dried stocks were kept at −20 ℃ until use.

Each time before use, 1.00 mLof deioinized water was added in to each microcentrifuge tube to make the working solution of 6BT and IS at 100 and 25.0 µg/mL, respectively. The 6BT and the IS working solutions were freshly prepared daily right before the analysis.

The mobile phase of LC was prepared by mixing 0.1% formic acid, 45.0% acetonitrile and 54.9% deionized water (v/v/v) together.

6.2.2. LC-MS/MS instrumentation

The LC–MS/MS system was composed by an Agilent (Santa Clara, CA, USA) 1100 HPLC and a Micromass (Manchester, UK) Quattro II triple quadrupole mass spectrometer. The HPLC unit included of two binary pumps, a degasser, an autosampler, an inline filter (0.5 μm pore) (Upchurch Scientific, Oak Harbor,WA,USA), a Waters (Milford, MA, USA) YMC-AQ® column (2.0 mm×50 mm, 5mparticle size with 120Å pore size), a two-position 6-port switching valve (Alltech, Deerfield, IL, USA), and a post-column splitter (Valco, Houston, TX, USA). Micromass MassLynx software (version 3.3) was utilized for the LC–MS/MS system operation, data acquisition and processing. For each LC-MS/MS analysis, the injection volume of the sample onto the column was 20 μL. Isocratic elution was utilized in the chromatographic separation. The flow rate was set as 100 μL/min. The post-column switching valve was programmed so that only the column eluate after 2.0 min was diverted to the mass spectrometer for analysis. A post-column splitter splits the total column flow at a ratio of 1:3, so that only 1/3 of the flow entered into the mass analyzer. Positive electrospray- ionization (ESI^+) mode was adopted when operating the mass spectrometer. The mass spectrometer was

tuned by direct infusion of a solution containing 10.0 μg/mL 6BT and IS 10.0 μg/mL IS dissolved in the mobile phase. The flow rate of infusion was set at 3 μL/min with a syringe pump (Harvard Apparatus, South Natick, MA, USA). After signal optimization, a set of ionization condition parameters were obtained: drying gas 300 L/h, nebulizer 15 L/h, capillary voltage 3.5 kV, HV lens 0.5 kV, cone voltage 25 V, skimmer 1.5 V, RF lens 0.2 V, ion source temperature 40 ℃, ion energy 0.3 V. Multiple-reaction-monitoring (MRM) was utilized for analyte monitoring and quantification. The MRM parameters were set as: argon collision gas 2.0–2.5bar, collision energy 17 eV, dwell time 0.4 s, inter-scan delay 0.05 s, lowand high-mass resolution 15 (for both quadrupoles 1 and 3), and multiplier 650.

6.2.3. Standard solutions, plasma calibrators and controls, and mouse plasma samples

6BT standard solutions at the concentration of 6.00, 18.0, 20.0, 60.0, 180, 200, 600, 1.80×10^3, 2.00×10^3, and 3.20×10^3 ng/mL were prepared by serial dilution of 100 μg/mL 6BT working solution. The standard solution of the IS was diluted from the 25 μg/mL working solution to 100 ng/mL.

The calibrators (3.00, 10.0, 30.0, 100, 300, and 1.00×10^3 ng/mL) of 6BT in mouse and human plasma were obtained individually by mixing 100 μL of pooled blank plasma, together with 50.0 μL of 6BT standard solution (at twice of the concentration of the

related calibrator) and 50.0 μL of IS standard solution at 100 ng/mL. The controls of 6BT in mouse plasma (3.00, 9.00, 90.0, 900, and 1.60×10^3 ng/mL) and human plasma (3.00, 90.0 and 900 ng/mL) were prepared individually according to the same way as the calibrators.

Mouse plasma samples obtained from the preliminary pharmacokinetic study were prepared by mixing 100 μL of plasma from 6BT administered mice with 50.0 μL of deionized water and 50.0 μL of 100 ng/mL IS standard solution.

6.2.4. LLE of 6BT

Plasma calibrators, controls and animal samples were extracted with an LLE protocol: 1mL of ethyl acetate was mixed with the plasma sample in a 1.5mL microcentrifuge tube. Then, a short vortex for 1 min followed by a centrifugation at 13000×g for 10 min were applied to the samples. Next, 85% of the organic (upper) layer (*ca.* 850 μL) was transferred into a clean 1.5-mL microcentrifuge tube and dried by vacuum evaporation on the DNA 120 SpeedVac® at 25 ℃ for 30 min. The sample residue was finally reconstituted with 85 μL of deionized water.

6.2.5. Matrix effect and recovery studies

In the matrix effect study, of 100 µL pooled blank plasma mixed with 100 µL of water was extracted with the protocol described in Section 6.2.4. Afterward, a mixture of 6BT and the IS standard solutions were spiked into the post-extract matrix. The resulted samples possessed 6BT of 9.00, 90.0 and 900 ng/mL, and the IS of 50.0 ng/mL. The peak area ratios of 6BT to IS in these spike-after-extraction (SAE) standards were compared with those of the corresponding authentic pure standards.

To obtain the recovery data, 6BT plasma calibrators (9.00, 90.0 and 900 ng/mL, with the IS at 50.0 ng/mL) were analyzed. IS normalized recovery of 6BT was calculated after comparing the peak area ratios of 6BT to IS in the plasma calibrators with those of the corresponding SAE standards. The absolute recovery of the IS was obtained by comparing the peak areas of the IS in the plasma calibrators with those of the corresponding SAE standards.

6.2.6. Stability studies

Mouse and human plasma test controls (9.00 and 900 ng/mL) were prepared as described in Section 6.2.3 except the IS standard was added prior to the LLE. All experiments were run in triplicate and the results were compared with freshly prepared plasma controls. For the freeze and thaw stability study, the test controls were undergone three freeze and thaw cycles. In each cycle, the test controls were frozen for at least 24 h

at −20 ℃ and thawed at room temperature without help. The short-term temperature stability study was carried out by leaving the test controls at the room temperature (23 ℃) for 4–24 h. For the long-term stability, the test controls were stored at −20 ℃ for 30 days prior to analysis.

6.2.7. Preliminary PK study of 6BT in mice

This preliminary PK study is also a feasibility test of the developed methods. Male C57BL/6 mice from Charles River Laboratories International (Spencerville, OH, USA) were utilized in the preliminary PK study. The mice were housed randomly in a group of five. The average body weight of the mice at the time of administration was 24 g. 6BT was dissolved in 10% DMSO–PBS (1×) solution at a concentration of 0.2 mg/mL. Mice were administered through intraperitoneal injection at a single bolus of 1mg/kg. After the mice were under anesthesia with isoflurane, blood samples were collected through cardiac puncture using heparinized needle and syringe at 5, 13, 22, 35, 45, 58, 121 and 237 min post-6BT injection. For each mouse, an average of 0.4 mL of blood sample was collected. The whole blood was placed on ice immediately after collection and centrifuged at 8000 × g for 15 min within 1 h. The plasma samples harvested from the whole blood samples were stored at −20 ℃ before analysis. Predose plasma samples were obtained from mouse injected with 10% DMSO–PBS (1×) along. PK analysis was

modeled with WinNonLin® nonlinear estimation program (Version 5.2) (Pharsight Corp., Mountain View, CA, USA). PK model 5 (1 compartment 1st order, K10 = K01, 1st order elimination) was finally adopted.

6.3. Results and discussions

6.3.1. Method development

Mass spectrometric detection of 6BT and the IS

In this work, "auto-tune" function of the MassLunx was utilized for the instrument response optimization. Due to their chemical properties, 6BT and the IS can form protonated species more easily than the deprotonated species through electrospray ionization. Thus, the positive electrospray ionization mode was utilized for the identification and quantification of 6BT and the IS. Figure 6.1 A and B demonstrates the predominant molecular ions of 6BT and the IS at *m/z* 375 for $[6BT+H]^+$ and *m/z* 390 $[IS+H]^+$, respectively. With collision-induced-dissociation (CID) introduced by argon gas in the second quadrupole, these two molecular ions were further dissociated into product ions illustrated in figure 6.1 C and D, respectively. The major product ion of the protonated 6BT and the IS were shown at *m/z* 243 and *m/z* 258, respectively. As a result, the mass transition pairs *m/z* 375 > 243 for 6BT and *m/z* 390 > 258 for the IS were

adopted in the compound quantification with the multiple-reaction-monitoring (MRM) mode. To understand the fragmentation mechanisms in CID, the m/z difference of the compound before and after CID were compared. Summarized with the structural information of the compounds, the proposed fragmentation mechanism is shown in figure 6.2.

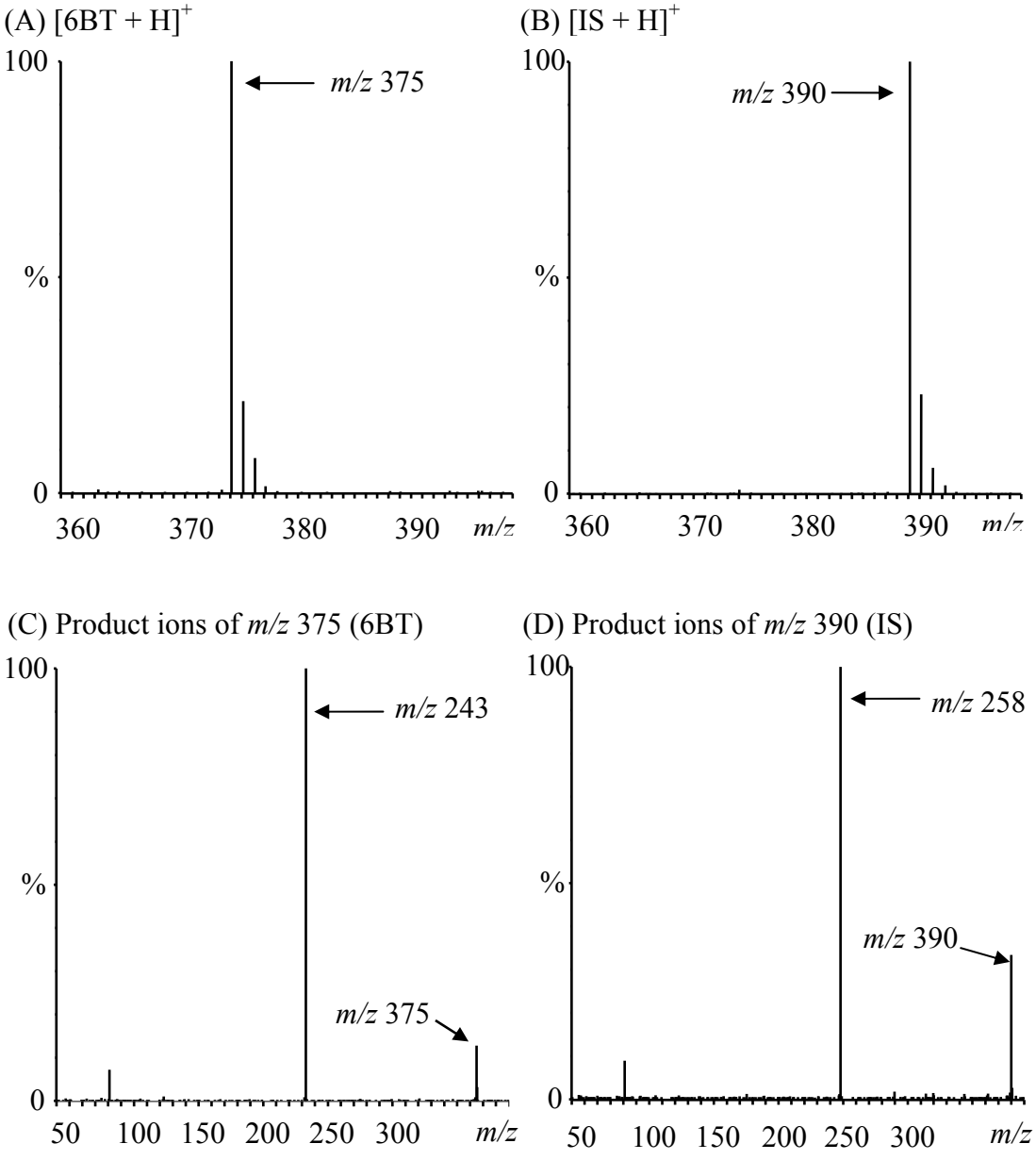

Figure 6.1, The mass spectra of 6BT and the internal standard.

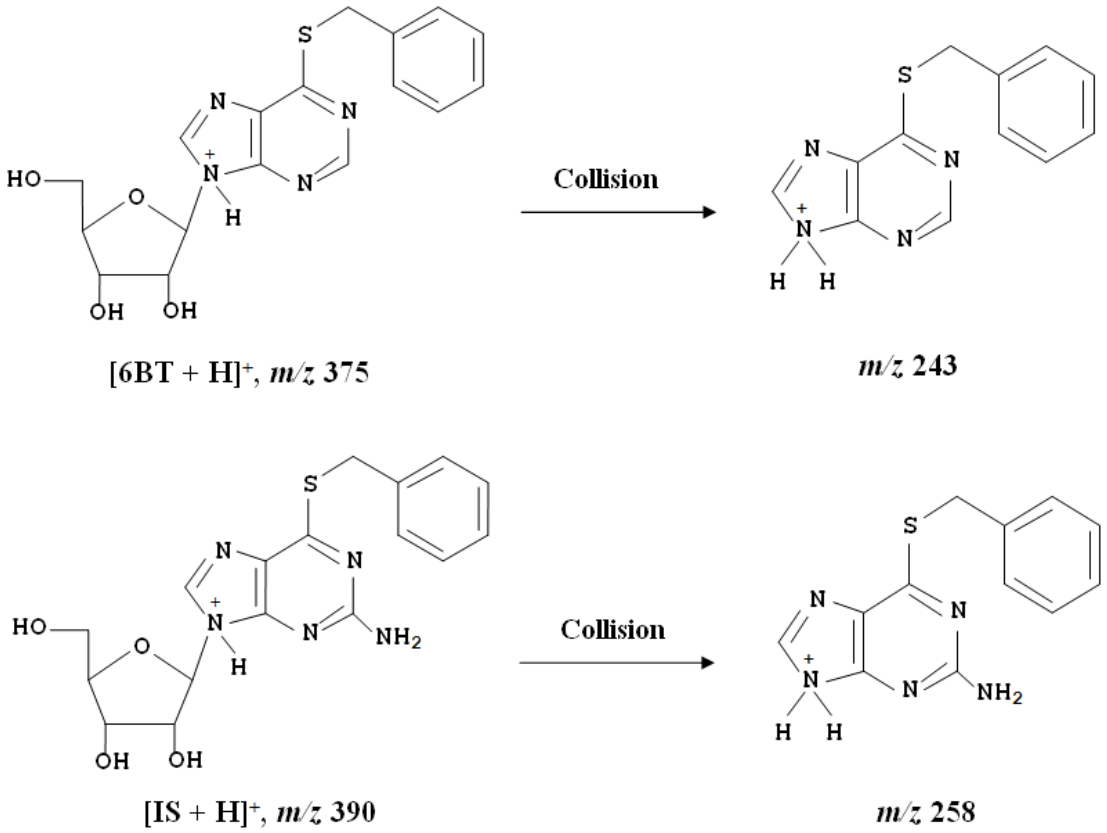

Figure 6.2, The proposed major fragments of 6BT and the IS.

LC separation of 6BT

According to a SciFinder® search, at the intended the mobile phase pH, pH 3.0, the logD values of 6BT and 2A6BT are 1.45 and 0.94, respectively. Thus, both compounds can be considered as more hydrophobic than hyerophilic. Based on this reason, two C-18 based reverse phase columns, a Phenomenex Gemini® column (2.0mm×50mm, 5 μm particle size with 110Å pore size) and a YMC ODS-AQ® column (2.0mm×50mm, 5 μm particle size with 120Å pore size) have been tried for optimized LC separation. Both columns successfully retained 6BT and the IS on the column for over 2 column volumes and were able to provide base line separation between 6BT and the IS. However, the YMC ODS-AQ® column was able to provide better peak shape comparing to the Phenomenex Gemini® column. Meanwhile, since 6BT and the IS are basic compounds, 0.1% of formic acid was added into the mobile phase in order to facilitate the protonation of the analytes, and thus enhance the sensitivity of MS detection. The increased hydrophilicity of the analyte after the addition of the formic acid also reduced the retention times of the analyte and the IS, and lead to shorter retention time and faster LC analysis.

In this work, to optimize the separation efficiency, the percentage of acetonitrile in the mobile phase was adjusted. Although a complete baseline resolution between 6BT and the IS can be achieved with a mobile phase consists of 35.0% acetonitrile, 0.1% formic acid and 64.9% deionized water (v/v/v), the total LC time was as long as 7 min at a flow rate of 0.1 mL/min. To shorten the total run time so that time can be significantly

saved in the future method application stage, the percentage of acetonitrile has been increased to 45%. This kind of adjustment resulted partial separation between 6BT and the IS with retention time of 3.9 and 3.5 min, respectively (figure 6.3). Nevertheless, it was able to reduce the total LC time to 5 min. To shorten the total running time to 5.0 min (nearly 30%) at the same flow rate. Since the two compounds were still retained on the column long enough and can be completely separated from the sample matrix, the detection sensitivity was not significantly affected. Besides, as both compounds were quantified by MRM in different MS transition, no interferences between the two compounds would take place. Therefore, the mobile phase gave shorter LC time was adopted.

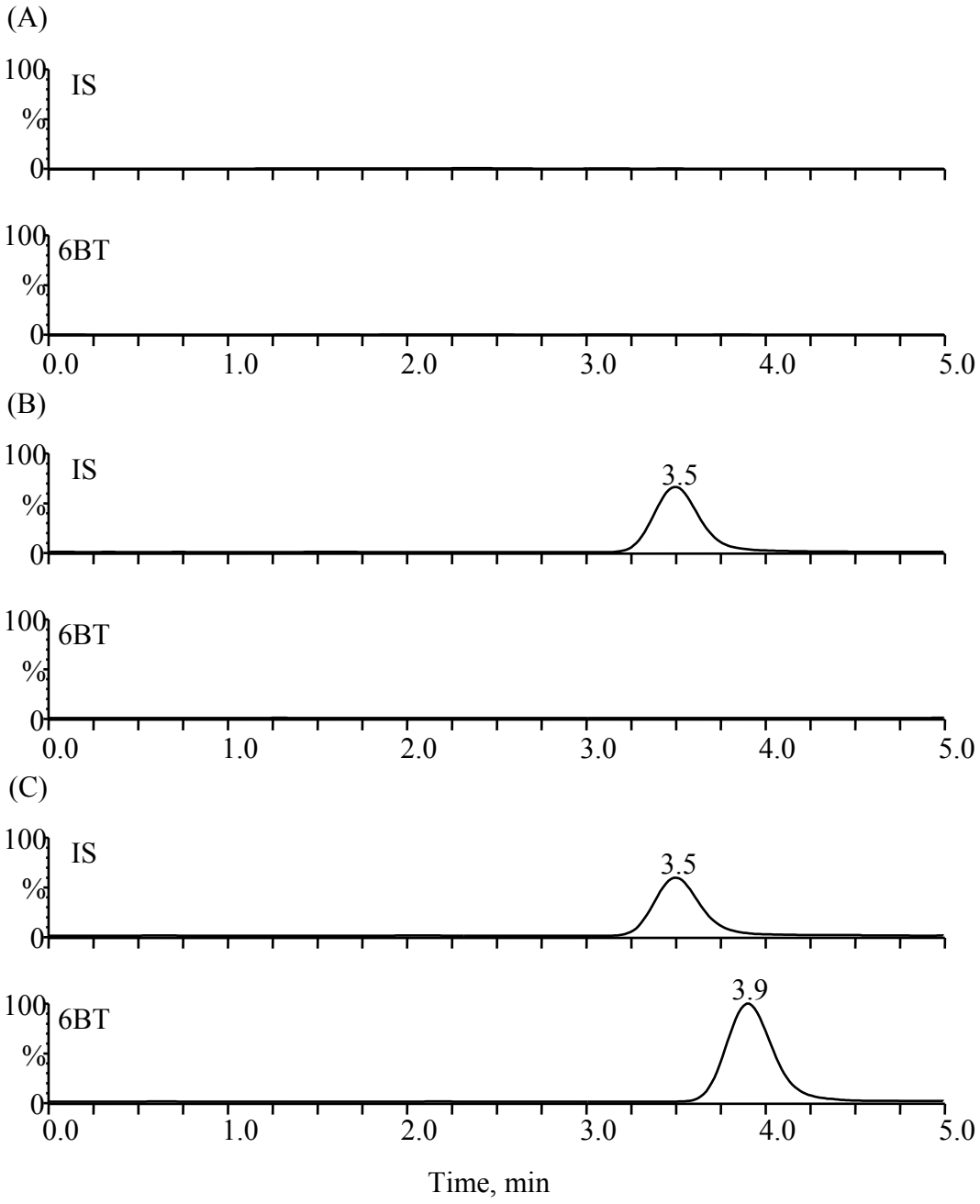

Figure 6.3, Representative MRM chromatograms of analytes in human plasma. (A) double-blank plasma (no 6BT detected); (B) 3 ng/mL 6BT in plasma (at LLOQ with a S/N of 18.3); (C) 100 ng/mL 6BT in plasma; (D) double-blank plasma (no IS detected); and (E) 50 ng/mL IS in plasma.

6.3.2. Method validation

The performance of the method developed was validated according to the FDA guidance for industry bioanalytical method validation [13].

Matrix effect and recovery studies

In the studies of matrix effect and recovery, triplicate measurements were performed at each concentration level of three different concentration levels (*i.e.*, low, medium, and high). The matrix effect was normalized by the signal of the IS (MF_{IS}), and thus was calculated with equation 5.1. As table 6.1 illustrated, the MF_{IS} in mouse and human plasma matrices varied between 1.10–1.13 and 0.97–1.04, respectively. Meanwhile, the values of MF_{IS} were quite consistent over the concentration range with a deviation of −0.03 to +0.13 from its ideal value of 1.00 (i.e., no matrix effect) and reproducible with standard deviation (SD) ⩽0.06.

To reduce the variation caused by instrument, the recovery was also studies as the IS normalized form (R_{IS}). It was calculated with equation 5.2. The summarized recovery data can be viewed in table 6.1. The values ranged from 82 to 87% for mouse plasma, and 90 to 98% for human plasma. The absolute recoveries (RC') of the IS from both kinds of plasma samples were also calculated (equation 6.1):

$$RC' = \frac{A'_{extraction}}{A'_{matrix}} \times 100\% \quad (6.1)$$

Here $A'_{extraction}$ means the peak area of the IS in the extracted plasma sample; while A'_{matrix} means the peak area of the IS in the post-extraction matrix. The values of RC' ranged from 59 to 66% in mouse plasma, and from 60 to 64% in human plasma. In spite of the low recovery of IS from both kinds of plasma samples, the results were reproducible and consistent within the calibration range.

Table 6.1, Matrix effect and recovery.

Plasma matrices	**[6BT] (ng/mL)**	**Recovery ± SD (%)**	**MF_{IS} ± SD**
Mouse	9.00	82 ± 2	1.13 ± 0.06
	90.0	83 ± 1	1.10 ± 0.05
	900	87 ± 1	1.11 ± 0.04
Human	9.00	98 ± 5	0.97 ± 0.02
	90.0	90 ± 6	1.04 ± 0.02
	900	96 ± 7	1.04 ± 0.04

Each datum point was based on triplicate measurements.

Calibration curve, accuracy, and precision of the method

The calibration curve of 6BT in both mouse and human plasma were established with six non-zero plasma calibrators. For each set of calibrator, one double-blank (with neither 6BT nor IS) plasma sample and one zero (with IS only) plasma sample were also included, The concentrations of 6BT for the non-zero calibrators were 3.00, 10.0, 30.0, 100, 300 and 1.00×10^3 ng/mL. The linear calibration curves ranged from 3.00 to 1.00×10^3 ng/mL were established by plotting A/A' in mouse and human plasma versus the concentrations of 6BT. The weighting factor for both calibration curves were utilized as 1/x (the reciprocal of 6BT concentration). Both calibration equations were given in table 6.2. When it came to the determination of the lower limits of quantification (LLOQ), the plasma calibrator with the lowest concentration, yet still fit in the calibration curve with acceptable accuracy and precision were defined as the LLOQ. The concentrations of the calibrators were back-calculated according to the calibration equation with the information of the A/A'. The accuracy and precision were calculated as they have been described in chapter I. For the analysis of mouse plasma samples, the accuracy and precision ranged from 0.2 to 5% and from 1 to 4%, respectively. For the human plasma samples, both accuracy and precision ranged from 1 to 7% (table 6.2). All values fell within the acceptable criteria (*i.e.*, $\leqslant\pm15\%$ at all concentrations except at LLOQ where $\leqslant\pm20\%$) suggested by the FDA guidance.

The precision of the method was evaluated in two aspects: the intra-and inter-assay precisions. As described in Chapter I, to determine the precisions, five replicates of

plasma control samples at low-, mid- and high-concentration levels (LQC, MQC and HQC) were prepared and analyzed. Since the LQC of mouse plasma were then same with the LLOQ for human plasma control samples, no extra LQC or LLOQ samples were prepared and analyzed. Meanwhile, as one sampling point in the preliminary pharmacokinetic study in mouse exceeded the upper limit of quantification (ULOQ), a set of dilution quality control samples (DQC) for mouse plasma were also evaluated. The intra- and inter-assay precision data were summarized in table 6.3.

The accuracies of the above studies were between −13 to 5% (table 6.3). They, again, fell well within the acceptable criteria suggested by the FDA guidance.

Table 6.2, Calibration equations of 6BT in mouse and human plasma.

Plasma Matrices	**Actual [6BT] ng/mL**	**Measured [6BT] ng/mL**	**SD**	**Accuracy (%)**	**Precision (%)**
Mouse	3.00	2.84	0.04	5	1
	10.0	9.8	0.2	2	2
	30.0	30.3	0.9	-1	3
	100	101	4	-1	4
	300	301	9	-0.3	3
	1.00×10^3	1.00×10^3	0.01×10^3	0.2	1
Human	3.00	2.78	0.09	7	3
	10.0	9.8	0.3	2	3
	30.0	29.3	0.7	2	3
	100	102	1	-1	1
	300	3.1×10^2	0.2×10^2	-4	7
	1.00×10^3	9.9×10^2	0.2×10^2	1	2

Calibration Equations: Mouse plasma $y = (0.020 \pm 0.002)\ x + (-0.007 \pm 0.002)$, $R^2 = 1.00 \pm 0.00$

Human plasma $y = (0.017 \pm 0.002)\ x + (-0.003 \pm 0.001)$, $R^2 = 0.999 \pm 0.002$

Each measured concentration was based on three measurements carried out on three different days and the S.D. values showed in the table indicated the standard deviation of each triplicate measurement. The calibration equations were based on three separate measurements carried out on three different days.

Table 6.3, Accuracy, intra- and inter-assay precisions of 6BT in human and mouse plasma.

Plasma matrices	**LQC**	**MQC**	**HQC**
Mouse			
Accuracy (%), n = 5	4	-3	3
Intra-assay precision (%), n = 5	6	4	4
Inter-assay precision (%), n = 3	5	5	3
Human			
Accuracy (%) n = 5	-13	-0.6	4
Intra-assay precision (%), n = 5	3	4	2
Inter-assay precision (%), n = 3	11	2	1

The concentrations of 6BT in the LQC, MQC and HQC of mouse plasma were 9.00, 90.0 and 900 ng/mL, respectively. For the human plasma, they were 3.00, 90.0 and 900 ng/mL, respectively. The concentration of the I.S. was 50.0 ng/mL.

Stability studies

Two concentration levels, 9.00 and 900 ng/mL, were utilized in the stability tests. Triplicate measurements were performed in each concentration level. The stability results were summarized in table 6.4. As indicated by the table, no significant loss of 6BT (recovery ranged from 97 to 108%) was observed in human plasma under the tested storage conditions. Indicated by the data, again, 6BT also remain stable in mouse plasma samples when stored at room temperature for up to 4 h and after three freeze-and-thaw cycles (recovery ranged between 88 and 106%. Long-term storage of mouse plasma samples spiked with 6BT at -20 ℃ also showed adequate recoveries after storage. Based on these experimental facts, 6BT stock solutions and the plasma samples were kept at −20 ℃ for freshness, and the analysis of mouse plasma samples was done within 4 h timeframe.

Table 6.4, Stability data of 6BT under various test conditions.

Storage Conditions	**Plasma Matrices**	**[6BT] added ng/mL**	**Recovery ± S.D. (%)**
Room Temperature, 4 hr	Mouse	9.00	88 ± 5
		900	94 ± 2
	Human	9.00	102 ± 7
		900	102 ± 2
Room Temperature, 8 hr	Mouse	9.00	68 ± 7
		900	87 ± 3
	Human	9.00	102 ± 8
		900	99 ± 1
Room Temperature, 24 hr	Mouse	9.00	19 ± 2
		900	30 ± 2
	Human	9.00	100 ± 4
		900	97 ± 1
Freeze-thaw,	Mouse	9.00	$(1.1 \pm 0.1)\times 10^2$
(3 cycles, -20 ^{o}C)		900	98 ± 8
	Human	9.00	100 ± 4
		900	103 ± 4
Long-term,	Human	9.00	108 ± 8
(30 days, -20 ^{o}C)		900	108 ± 3
Each datum point was based on triplicate measurements.			

6.3.3. Method application in a preliminary PK study in mice

A preliminary PK study of 6BT in mice was carried out with the validated LC–MS/MS method. The mouse plasma samples together with eight calibrators (*i.e.*, one double-blank, one zero and six nonzero) and three sets of quality control samples at low-, mid- and high-concentrations (*i.e.*, 9, 90, 900 ng/mL) were extracted after the addition of the IS. The PK sample with the concentration exceeding the ULOQ (*i.e.*, 1.00×10^3 ng/mL) were re-analyzed along with the DQC (1.60×10^3 ng/mL) after 1:1 dilution with blank pooled mouse plasma.

Figure 6.4 included representative mass chromatograms of mouse plasma samples obtained from the PK analysis. From the chromatograms, no sign of interference from endogenous compound in mouse plasma was observed in the pre-administered sample. The plasma concentrations of 6BT were plotted against the sampling times. The preliminary PK profile after single bolus injection was illustrated in figure 6.5. With the analysis by the WinNonLin® software, the profile fitted the best in a nonlinear one-compartment first-order pharmacokinetic model (percent relative standard deviations of 12–15%). The PK parameters were calculated accordingly as: T_{max}, 18.9 min; C_{max} 1086 ng/mL; T1/2 13.1 min; and AUC, 5.57×10^4 min ng/mL.

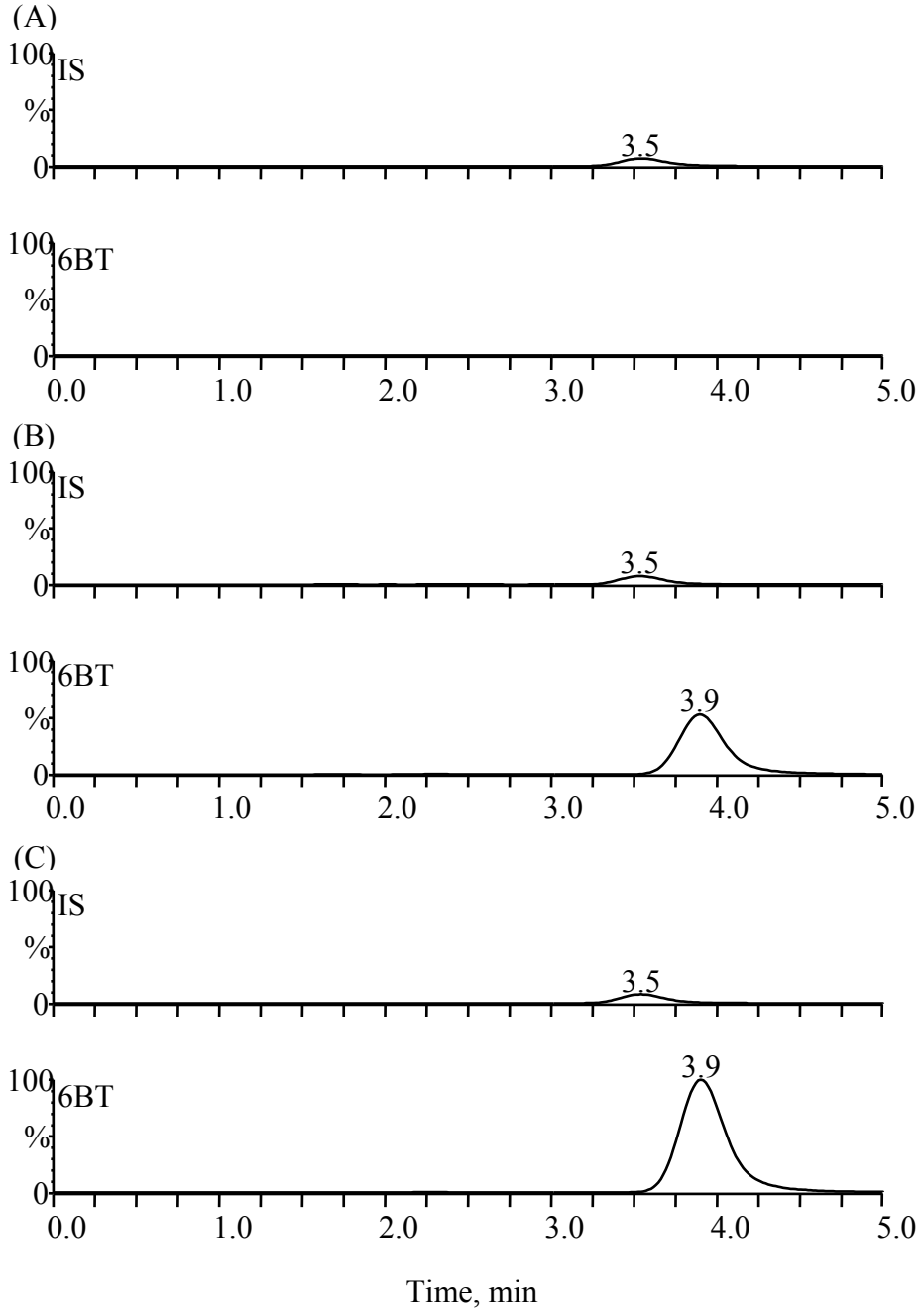

Figure 6.4, Representative MRM chromatograms of mouse plasma samples. (A) predosed mouse plasma with IS, (B) the plasma sample collected 5 min after intraperitoneal injection with IS, and (C) the plasma sample collected 13 min after intraperitoneal injection with IS.

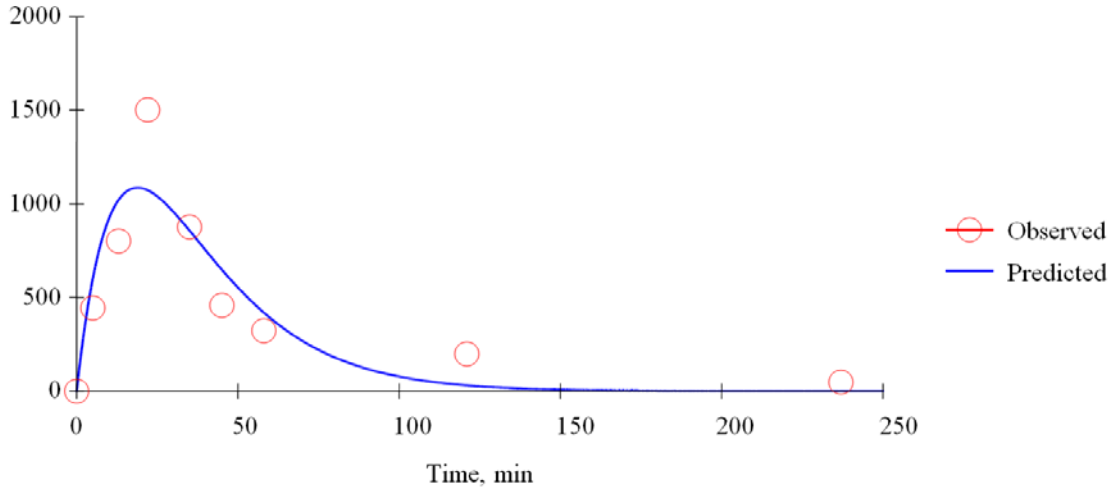

Figure 6.5, Plasma concentration-time profile of 6BT. Mice: C57BL/6, male; administration: intraperitoneal injection; dosage: 1 mg 6BT/kg mouse.

6.3.4. Enhanced 6BT uptake in leukemia cell lines

Two human AML cell lines (*i.e.*, OCI-AML3 and Nomo-1), normal human bone marrow cells, one human embryonic kidney cell line (*i.e.*, 293), a human prostatic carcinoma cell line (*i.e.*, LNCap), and a human ovarian cancer cell line (*i.e.*, SK-OV-3) were treated with 10 μM 6BT. After harvest, the cells were washed with PBS for 3 times first, and then the cell lysates were obtained by sonication. The concentration of the cell lysate samples were normalized according to their protein concentrations (determined by UV_{280}). To be more specific, when the cell lysate with the lowest protein concentration was determined, other cell lysates with higher protein concentrations were diluted with deionized water accordingly till all the samples reach to the same protein concentration level. Then, 200 μL of each sample was taken and extracted with 1.00 mL ethyl acetate. After centrifugation, 900 μL (90%) of the organic phase was recovered for each sample. After the samples were dried with vacuum evaporation, 162 μL deionized water and 18 μL of 500 ng/mL IS solution was added to each sample, making the final volume of each sample as 180 μL and the concentration of the IS in each sample as 50 ng/mL.

After analyzing the cell lysates with the developed LC-MS/MS method, the peak area ratios of 6BT and the IS (A/A') in each sample was obtained. The relative uptake of 6BT by the cells was determined through comparing the A/A' ratio of 6BT in a specific cell sample with the sample possessing the highest A/A' ratio (assigned as 1.00 for the

relative uptake). The relative uptakes of 6BT in other samples were then determined by equation 6.2:

$$Relative\ Uptake = \frac{(A/A')}{(A/A')_{max}} \tag{6.2}$$

Here, $(A/A')_{max}$ indicates the maximum peak area ratio obtained from the samples.

From table 6.5, a significant enhanced uptake of 6BT can be observed from the two AML cell lines, OCI-AML3 and Nomo-1. While the normal human bone marrow cells, the embryonic kidney cell, and the two cell lines coming from other cancer types indicated much lower drug uptake. The result explained, at least from one aspect, the mechanism of the selective cytotoxicity of 6BT to leukemia cells. This enhanced entry may due to elevated expression of certain membrane transporter. However, detailed mechanism is still under investigation.

Table 6.5, 6BT uptake in different cell lines.

Cell Lines	**Treatment Status**	**A_{6BT}**	**A_{31730}**	**A_{6BT}/A_{31730}**	**Relative Uptake**
OCI	Untreated	31	1.09×10^{3}	0.0284	0.000792
	Treated	5.03×10^{4}	1.68×10^{3}	29.9	0.835
Nomo	Untreated	29	1.30×10^{3}	0.0224	0.000624
	Treated	7.31×10^{4}	2.04×10^{3}	35.9	1.00
Normal	Untreated	131	1.43×10^{3}	0.0918	0.00256
	Treated	5.29×10^{3}	1.25×10^{3}	4.25	0.118
293	Untreated	31	1.99×10^{3}	0.0156	0.000435
	Treated	6.22×10^{3}	1.55×10^{3}	4.01	0.112
LNCap	Untreated	11	1.35×10^{3}	0.00812	0.000227
	Treated	1.50×10^{4}	2.04×10^{3}	7.34	0.205
SK-OV-3	Untreated	14	2.01×10^{3}	0.00697	0.000194
	Treated	81	1.53×10^{3}	0.0528	0.00147

6.3.5. On-line SPE extraction of 6BT with a boronic acid cartridge

Besides the LLE combined with LC-MS/MS method developed above, an on-line SPE combined with MS/MS analysis method was also developed for 6BT. The on-line SPE method was based on the specific reversible interaction between the *cis*-hydroxyl groups of 6BT and boronic acid. Under basic conditions, phenylboronic acid is able to condense the *cis*-hydroxyl moieties of sugar in aqueous solution and form stable cyclic ester (figure 6.6). In this work, an SPE cartridge (2.0 × 20 mm) was packed in our lab with silica based NuGEL^{TM} Phenyl Boronic Acid (particle size 50 μm, Biotech Support Group, Monmouth JCT, NJ) as the packing material. As binding between 6BT and the phenylboronic group takes place most efficiently under basic pH, a mobile phase containing 5 mM of NH_4HCO_3 buffer at pH 8.4 was utilized as the loading buffer. The analyte was eluted out from the cartridges with 45% acetonitrile plus 54.9% water with 0.1% formic acid, the mobile phase utilized in the LC-MS/MS method. The flow rate was set as 0.1 mL/min, and the MS/MS parameters were the same as those described in section 6.2.2. The instrumentation of the on-line extraction was set up as it has been illustrated in figure 1.4.

Two minutes after the injection of 6BT standard solution (100 ng/mL), the switcher was switched from the loading position to the elution position. At 4.5 min after injection, the switcher was switched back to the loading position, and the cartridge was re-equilibrated for next injection. From figure 6.7, a sharp and symmetrical

chromatography peak of 6BT can be observed at 2.3 min. The result indicated the effective extraction of 6BT with this self-packed cartridge. As the process is simple and time saving in sample preparation, it has great potential to provide fast and low cost methods in future 6BT analysis from biological samples.

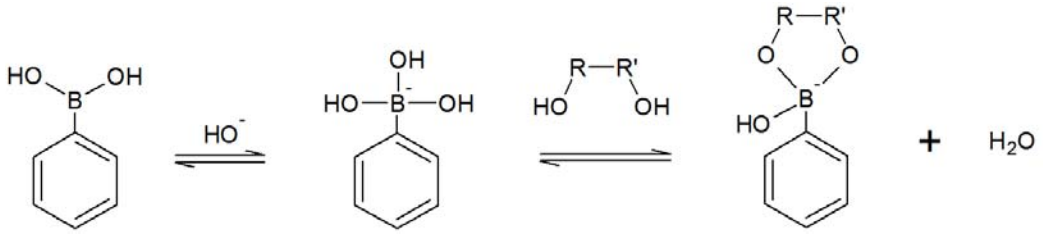

Figure 6.6, Reaction between the phenyl boronic acid and a molecule carrying *cis*-hydroxyl groups.

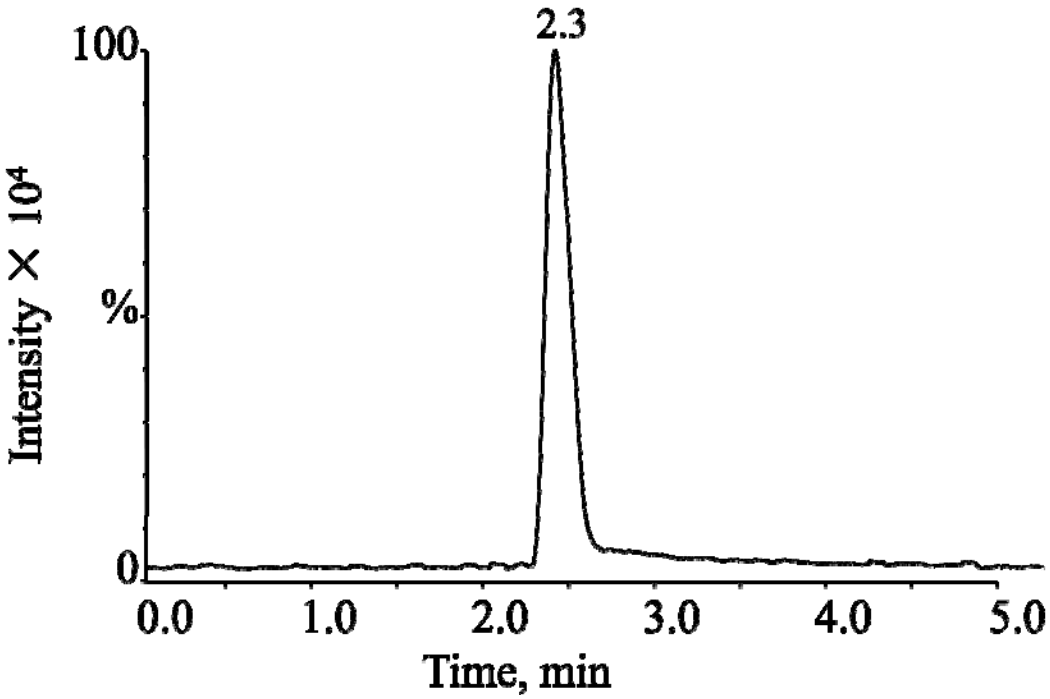

Figure 6.7, Representative MRM chromatogram for the on-line SPE of 6BT.

6.4. Conclusions

Based on all the experimental data obtained, a quantitative LC–MS/MS method for the assessment of 6BT in mouse and human plasma has been developed. Briefly speaking, the analytes in plasma were extracted by ethyl acetate, separated by Waters YMC ODS-AQ® column, and then analyzed through the tandem mass spectrometry. Method validation has been performed in mouse and human plasma by referring to the FDA guidance. The linear range of the method is from 3.00 to 1.00×10^3 ng/mL in both mouse and human plasma. The method was also successfully applied to a preliminary PK study of 6BT in mice. Due to its high accuracy, precision, and sensitivity, it will facilitate the therapeutic development of not only 6BT but its analogues in human. Meanwhile, semi-quantitative analysis of 6BT from cells treated with 6BT confirmed the enhanced uptake of 6BT by leukemia cell lines, and provided insight in drug functioning mechanism elucidation.

6.5. References

1. B.M. Chassy, R.J. Suhadolnik, J Biol Chem. 242 (1967) 3655.

2. M.H. Iltzsch, S.S. Uber, K.O. Tankersley, M.H. el Kouni, Biochem. Pharmacol. 49 (1995) 1501.

3. M.H. el Kouni, V. Guarcello, O.N. Al Safarjalani, F.N. Naguib, Antimicrob. Agents. Chemother. 43 (1999) 2437.

4. J.P. Dubey, C.P. Beattie. Toxoplasmosis of animals and man, CRC Press, Boca Raton, FL, 1988, p. 1.

5. P.D. Walzer, R.M. Genta (Eds.), Parasitic infections in the compromised host, Marcel Dekker, New York, NY, 1989, p. 179.

6. D.N. Wald, H.M. Vermaat, S. Zang, A. Lavik, Z. Kang, G. Peleg, S.L. Gerson, K.D. Bunting, M.L. Agarwal, B.L. Roth, W. Tse, Cancer Res. 68 (2008) 4369.

7. American Society of Clinical Oncology, Leukemia - Acute Myeloid: overview, available at http://www.cancer.net/patient/Cancer+Types/Leukemia+-+Acute+Myeloid+-+AML.

8. E. Estey, H. Döhner, Lancet. 368 (2006) 1894.

9. B. Steffen, C. Müller-Tidow, J. Schwäble, W.E. Berdel, H. Serve, Crit Rev Oncol Hematol. 56 (2005) 195.

10. Z.Y. Wang, Z. Chen, Blood. 111(2008):2505.

11. M.S. Tallmann, Ann Hematol. 83 (2004) S81.

12. R.H. Rais, O.N. Al Safarjalani, V. Yadav, V. Guarcello, M. Kirk, C.K. Chu, F.N. Naguib, M.H. el Kouni, Biochem. Pharmacol. 69(2005) 1409.

13. U.S. Food and Drug Administration (FDA) & Center for Drug Evaluation and Research (CDER), Guidance for Industry: Bioanalytical Method Validation, available at http://www.fda.gov/cder/guidance/4252fnl.htm, 2001.

14. E.R. Badman, Z. Liang, S. Bansal, J. Gibbons, Applied Biosystems Users Meeting, ASMS, Denver, CO, June 1, 2008.